N P

JOURNAL OF FOOD PROCESS ENGINEERING

D.R. HELDMAN
and
R.P. SINGH
COEDITORS

FOOD & NUTRITION PRESS, INC.

VOLUME 9, NUMBER 1

QUARTERLY

JOURNAL OF FOOD PROCESS ENGINEERING

All articles for publication and inquiries regarding publications should be sent to either DR. D.R. HELDMAN, COEDITOR, *Journal of Food Process Engineering,* National Food Processors Association, 1401 New York Ave., N.W., Washington, D.C. 20005 USA; or DR. R.P. SINGH, COEDITOR, *Journal of Food Process Engineering,* University of California, Davis, Department of Agricultural Engineering, Davis, CA 95616 USA.

All subscriptions and inquiries regarding subscription should be sent to Food & Nutrition Press, Inc., 155 Post Road East, P.O. Box 71, Westport, Connecticut 06881 USA.

One volume of four issues will be published annually. The price for Volume 9 is $75.00 which includes postage to U.S., Canada, and Mexico. Subscriptions to other countries are $89.00 per year via surface mail, and $97.00 per year via airmail.

Subscriptions for individuals for their own personal use are $55.00 for Volume 9 which includes postage to U.S., Canada, and Mexico. Personal subscriptions to other countries are $69.00 per year via surface mail, and $77.00 per year via airmail. Subscriptions for individuals should be sent to the publisher and marked for personal use.

The *Journal of Food Process Engineering* (ISSN 0145-8876) is published quarterly (March, June, September and December) by Food & Nutrition Press, Inc.—Office of Publication is 155 Post Road East, P.O. Box 71, Westport, Connecticut 06881 USA. (Current issue is March 1987.)

Second class postage paid at Westport, CT 06881.

POSTMASTER: Send address changes to Food & Nutrition Press, Inc., 155 Post Road East, P.O. Box 71, Westport, CT 06881.

JOURNAL OF FOOD PROCESS ENGINEERING

JOURNAL OF FOOD PROCESS ENGINEERING

Journal of
FOOD PROCESS ENGINEERING

VOLUME 9
NUMBER 1

Coeditors: D. R. HELDMAN
R.P. SINGH

FOOD & NUTRITION PRESS, INC.
WESTPORT, CONNECTICUT 06881 USA

Food & Nutrition Press, Inc.
Westport, Connecticut USA

ISSN 0145-8876

Printed in the United States of America

CONTENTS

SCRAPED SURFACE HEAT EXCHANGERS

A literature survey of flow patterns, mixing effects, residence time distribution, heat transfer and power requirements.

MAGNUS HÄRRÖD

SIK — The Swedish Food Institute
Box 5401
S-402 29 GÖTEBORG
Sweden

Accepted for Publication September 24, 1986

ABSTRACT

In this literature survey flow patterns, mixing effects, heat transfer and power required for rotation in scraped surface heat exchangers (SSHE) are thoroughly discussed, with the emphasis on assumptions and results, while the principal design of different SSHEs are only briefly discussed.

The flow patterns control the desired radial mixing and the undesired axial mixing. The flow in a SSHE can be regarded as the sum of an axial flow and a rotational flow. The axial flow is laminar and the rotational flow is laminar or vortical.

With laminar flow the radial mixing is poor, which causes poor heat transfer and allows the axial flow profile to control the residence time distribution. The precise onset of vortical flow in a SSHE is hard to predict. The vortical flow makes the radial mixing very efficient, giving good heat transfer and perhaps plug flow behavior. However, vortical flow also causes axial mixing which reduces the apparent heat transfer coefficient and increases the residence time distribution.

The power required to rotate the shaft and blades is mainly determined by the design of the blades.

BACKGROUND

Cooking of high-viscosity products in the food industry is primarily done in kettles, where the possibilities to control and optimize the heat treatment process generally are very limited. The increased demand for effi-

Journal of Food Process Engineering 9 (1986) 1-62.

cient and labor-saving processes in the food industry favors the application of continuous cooking with heat exchangers. For heating of high-viscosity products with or without particles, the scraped surface heat exchanger — the SSHE — is the most suitable heat exchanger.

The story of SSHEs began in 1928 when Vogt patented an ice cream freezer. Today SSHEs are frequently used in the food industry and the chemical industry for heating and cooling of high-viscosity products. They are also used as crystallizers and chemical reactors (Härrröd 1982). To a very great extent SSHEs have replaced kettles in the production of fruit sauces and marmalades. In these processes heating is directly followed by cooling. Production of rice porridge, pea soup and other soups has recently started on an industrial scale. These processes also include some time of cooking before cooling. There is now great interest within the industry in aseptic processing and packaging of high-viscosity products with and without particles.

The final quality of the products can be improved if the processes can be modelled and optimized. Successful modelling of a process pre-requires knowledge of: (1) Flow and temperature patterns in the processing equipment, e.g. SSHEs and holding tubes, and (2) Kinetics for the important reactions.

This literature survey is one part of a basic investigation into the performance of SSHEs for high-viscosity products without particles.

Continuous Processes — SSHEs

For processes in which both desired and undesired reactions are controlled by time and temperature, the ideal continuous process can be modelled using the plug flow model with perfect radial mixing and no axial mixing. Each molecule spends an equally long time at each temperature level during the process, and all reactions proceed to the same degree for all molecules.

Non-ideal processes have complex flow and mixing situations, in which molecules spend different lengths of time at different temperatures during the process and the reactions proceed to a varying degree for different molecules.

To be able to understand and predict the performance of SSHEs, it is necessary to have knowledge of the mixing effects for the various flow patterns in SSHEs and to know how the mixing effects control the time and temperature conditions for the molecules during the process.

Methods Used to Describe Continuous Processes

Two different approaches have been used to model the complex situation in a SSHE. In the first approach the process may be regarded as a black box. Performed experiments can be summarized with dimensional analysis to dimensionless equations. In the second approach assumptions can be made and the process modelled with equations and then the model can be compared with experimental results. With this analytical approach the final result can also be described by dimensionless equations.

The black box method, together with dimensional analysis, usually describes the actual experiments satisfactorily. However, this method gives little basic understanding of the process. In a comparison between a theoretical model and experimental results, the assumptions can be discussed and improved upon and this may lead to a more fundamental understanding of the process.

Aims

(1) To describe, on the basis of the literature, when different flow patterns occur, particularly Taylor vortex flow and whether plug flow behavior occur in SSHEs. Interesting variables are rotational speed, axial flow rate, temperature pattern, product viscosity and the dimensions and design of the SSHE.

(2) To describe qualitatively relations between flow patterns and axial and radial mixing effects.

(3) To describe quantitatively relations between mixing and temperature patterns, residence time distribution, heat transfer and power requirements in SSHEs.

Scope

The principle design of SSHEs is briefly described. We assume that the blades connected to the rotating cylinder in SSHEs complicate, but they do not change the fundamental flow patterns compared with those in a concentric annulus with a rotating inner cylinder without blades. We have therefore surveyed the vast literature on flow patterns in annulus with rotating cylinders without blades, with special emphasis on possible operating conditions in SSHEs. We also assume that the flow pattern controls the radial and the axial mixing and that these mixing effects control residence time distribution, temperature pattern and heat transfer. Models and measuring techniques for mixing effects, residence time distribution, heat transfer and the power required for rotation are discussed with emphasis on assumptions and results.

In equations, tables and figures we recast all symbols with our notations and in several cases we have calculated and recalculated values on basis of data given in the references to facilitate comparison of various data.

In this way we have evaluated results from the literature on residence time distribution, heat transfer and power requirements in SSHEs on the basis of results in the literature on flow pattern and mixing effects.

The sections on flow pattern, mixing effects and residence time distribution, heat transfer and power begin with general overviews. Together, these overviews constitute a summary of the literature. After each overview there are details and references. A short gereral overview on the performance of SSHEs can be found in Härröd and Maingonnat (1984).

PRINCIPAL DESIGN

Names like scraped surface heat exchangers, swept heat exchangers or swept surface heat exchangers are used in the literature in a confusing way. We would like to divide them into two different categories: scraped surface heat exchangers (SSHE) and scraped surface film evaporators.

Scraped Surface Heat Exchangers

In a SSHE, the product is pumped through a heat transfer tube. Rotating blades keep the heat transfer surface clean. The design may differ according to mixing performance, mechanical strength, dimensions, mounting and accessibility for inspection and cleaning.

Some information about manufacturers, trade names and sizes of SSHEs is presented in Table 1. The heat transfer area is important for the capacity of the equipment. The larger the gap between the cylinders, the larger the particles that can be processed in the equipment.

The most common type of SSHE consists of a heat transfer tube and blades mounted on a rotating inner cylinder (see Fig. 1).

Another type of SSHE consists of two static annular heat transfer tubes; a frame rotates in the gap between the two cylinders; the blades on the frame keep the heat transfer surfaces clean. With heat transfer surfaces on both sides of the gap the heat transfer area per volume increases. The configuration of the blades may provide more efficient radial mixing, particularly for high-viscosity products. The flow pattern with a static inner cylinder is probably different from the flow pattern when a rotating inner cylinder is used. However, we have not found any literature describing how this SSHE operates and this type of SSHE is not further discussed in this paper.

Scraped Surface Film Evaporators

In a scraped surface film evaporator the product falls down along the inner side of a vertical heat transfer tube by gravity. The heat transfer is promoted by rotation of blades that scrape the product off the surface

TABLE 1. Market survey of scraped surface heat exchangers

Manufacturer	Trade name	Heat transfer area m^2	Gap mm	Diameter mm	Remarks
Alfa Laval	Contherm	0.3-0.9	11-50	152	
Cherry Burell	Termutator Votator Vogt	0.3-0.9	6-50	152	
APV-Crepaco	Rota Pro	0.2-0.9	6-50	76-152	
Schröder	Kombinator	0.1-1.5	5-15	60-336	
Gerstenberg Agger	Prefector	0.3-0.8	6-14	105-180	
Fran Rica	Fran Rica	1.1-4.7	10-75	305-610	
Luwa	Thermalizer	0.3-18.0	?	100-1000	
Lehmann	KBF	1.3	15	250	
Terlet	Terlotherm	0.6-4.6	70		heat transfer and blades on both sides of the gap
Groen		0.7-12	15		
Fryma	Cool mix	1.5-6	6		

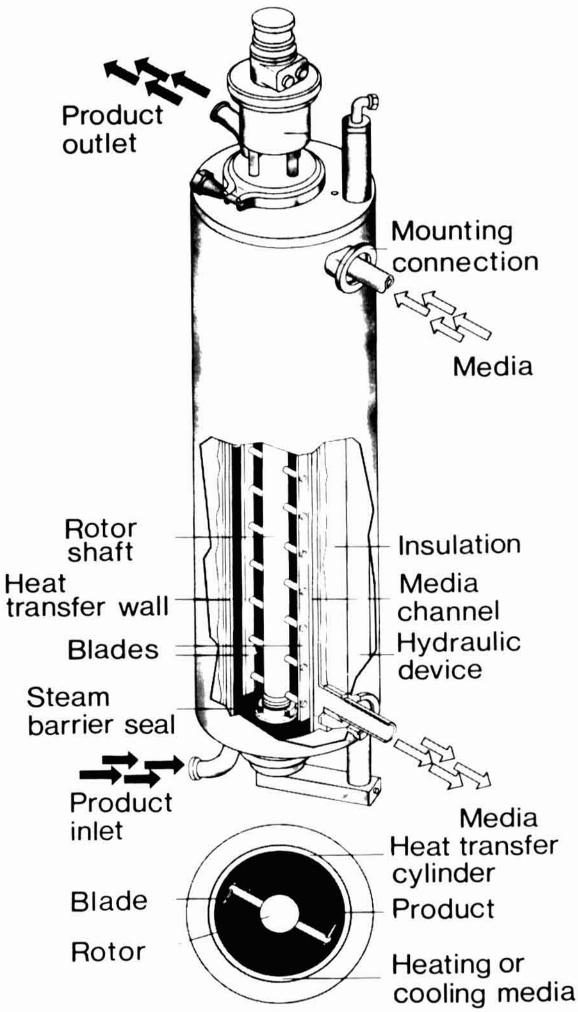

FIG. 1. PRINCIPAL DESIGN OF A SSHE (COURTESEY ALFA-LAVAL)

of the heat transfer tube. Centrifugal forces throw the product back onto the tube. Evaporated steam rises in the free space close to the rotor.

The flow pattern in scraped surface film evaporators cannot be expected to be similar to the flow pattern in an annulus with a rotating inner cylinder where the annulus is completely filled with liquid.

Scraped surface film evaporators are not further discussed in this survey, but more information can be found elsewhere (Kern and Karakas 1959; Lustenander *et al.* 1959; Bott and co-workers, 1963, 1966a,b, 1968, 1968a,b, 1969; Azoory and Bott 1970; Miyashita and Hoffman 1978; Rosabal *et al.* 1982a,b; Kohli and Sarma 1983).

FLOW PATTERNS

After the general overview, we survey the flow patterns in concentric annuli, and come closer to the real flow patterns in SSHEs by adding information on how different factors interact to determine the flow pattern. These factors are: axial flow, length of the equipment, time, radial temperature differences, eccentric cylinders, non-Newtonian fluids and blades.

General Overview of Flow Patterns in SSHEs

The flow in an annulus with axial flow and a rotating inner cylinder can be divided into different flow regimes (see Fig. 2). The rotational flow is characterized by a Taylor number, Ta, and the axial flow by an axial Reynolds number, Re_{ax}.

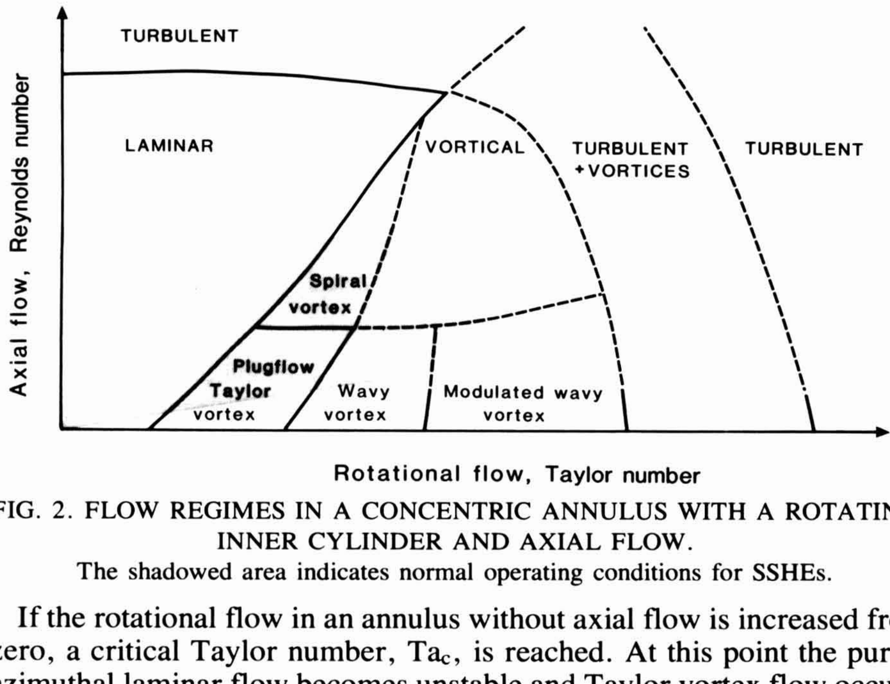

FIG. 2. FLOW REGIMES IN A CONCENTRIC ANNULUS WITH A ROTATING INNER CYLINDER AND AXIAL FLOW.
The shadowed area indicates normal operating conditions for SSHEs.

If the rotational flow in an annulus without axial flow is increased from zero, a critical Taylor number, Ta_c, is reached. At this point the purely azimuthal laminar flow becomes unstable and Taylor vortex flow occurs. In this flow, toroidal vortices encircle the inner cylinder and are stacked in the axial direction (see Fig. 3). The velocity now has radial and azimuthal components, but is still time-independent.

At a higher Ta, the Taylor vortex flow becomes unstable and wavy vortex flow, in which travelling azimuthal waves are superimposed on the vortices, appears. As Ta increases further, this periodic flow becomes unstable and a new flow; the modulated wavy vortex flow, appears. In the flow

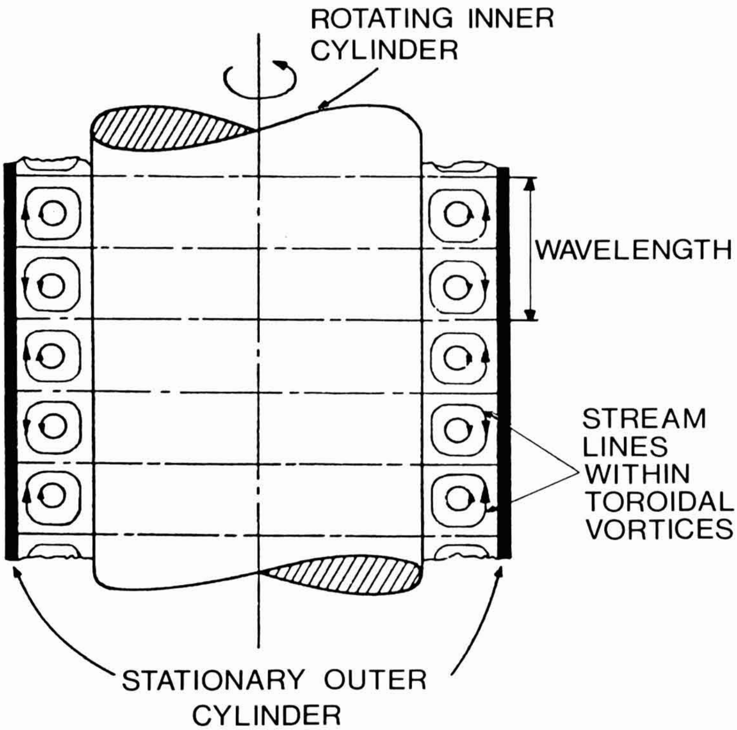

FIG. 3. PAIRS OF TAYLOR VORTICES WITH COUNTER-ROTATION; THIS FLOW OCCURS WHEN THE ROTATIONAL FLOW JUST HAS BECOME VORTICAL AND THE AXIAL FLOW IS ZERO OR VERY LOW

the amplitude of the waves as they travel around in the annulus is modulated. At very high Ta the flow becomes turbulent but a regular vortex pattern can still be recognized, and finally, at extremely high Ta the vortex pattern disappears and the flow is completely turbulent.

The transition from Taylor vortex flow to turbulent flow for very low radius ratio also depends on other factors; radial waves occur almost directly after the onset of Taylor vortex flow at radius ratios below 0.2; these radial waves occur later at higher radius ratios. The Taylor vortex flow is most stable at radius ratios from 0.5 to 0.7.

When we add axial flow to the system, this flow stabilizes the rotational flow. The transition to different vortex patterns appear at higher Taylor numbers as the axial flow increases. At very low axial Reynolds numbers and rotational flow with Taylor vortex flow, the vortices march through the annulus without being disturbed (see Fig. 3). However, at low axial flow the vortices start moving in a spiral (see Fig. 4).

The flow in a real SSHE is also complicated by several other factors like: length of the equipment, time-development of rotational and axial flows, radial temperature differences, eccentric cylinders, non-Newtonian

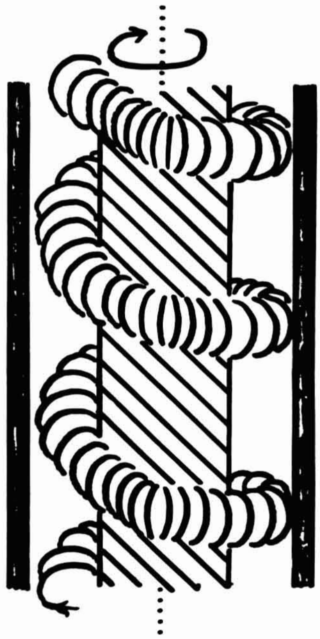

FIG. 4. TAYLOR VORTEX IN A SPIRAL; THIS FLOW OCCURS WHEN THE ROTATIONAL FLOW JUST HAS BECOME VORTICAL AND THE AXIAL FLOW IS LOW OR HIGH

fluids and blades. Because of the relative short annulus, fully developed flow may occur only in minor parts of the SSHE. Radial temperature differences in combination with high-viscosity fluids increase Ta_c on cooling and decrease Ta_c on heating in SSHEs. Eccentricity of the rotating cylinders increases Ta_c, particularly in short equipments. Complex flow behavior in the fluid may delay the transition to vortex flow. Blades on the rotating cylinder have only a limited effect on the transition to vortex flow.

Flow Patterns in Annuli Without Axial Flow

DiPrima and Swinney (1981) have made an excellent review of hydrodynamic instability theories and flow patterns from laminar to turbulent flow, between concentric rotating cylinders without axial flow. Illustrative photographs on different flow patterns have been published by several investigators, e.g. in (Coles 1965; Fenstermacher *et al.* 1979; Koschmieder 1979; Gorman and Swinney 1982).

Taylor Vortex Flow. Taylor (1923) showed the existence of a critical Taylor number value, Ta_c, which is a function of the radius ratio, with the following properties; for $Ta < Ta_c$ all initially infinitesimal axisymmetric disturbances that are periodic in the axial direction are damped and decay to zero with increasing time; for Ta > Ta_c there are some disturbances that will grow with time. Moreover, his experiments showed that this instability of Couette flow leads to a new steady secondary axisymetric flow, commonly referred to as Taylor vortices (see Fig. 3). The form of the regularly spaced vortices in the axial direction is usually described by a wavelength (see Fig. 3).

Critical Taylor number and wavelength values are defined as the combinations of Taylor number and wavelength that give rise to the lowest unstable Taylor number. Critical Taylor number and wavelength values have been calculated for a wide range of radius ratios, by introducing axisymmetric disturbances into a viscous incompressible laminar flow between infinitely long rotating cylinders, when the flow is described with the Navier-Stokes and the continuity equations and the instability is analyzed with the linear stability theory; details can be found in DiPrima and Swinney (1981) and references in that paper.

Results from calculations of critical Taylor numbers for different radius ratios are summarized in Table 2. We have transformed previous results into Ta_c to enable comparison with results in Table 3 and Table 4. It is worth noting that the original formula proposed by Taylor (1923) provide good approximation to Ta_c for of radius ratios from 1 to about 0.7.

TABLE 2. Critical values of Ta, for different values of D_s/d_t, calculated with the linear stability theory by Sparrow *et al.* (1964), Walowit *et al.* (1964), and Roberts (1965) and summarized in DiPrima and Swinney (1981). Note that the Taylor number and rotating Reynolds number are related as
$Ta = Re_r^2\ \pi^2(d_t - d_s)^3\ d_s^2/2(d_t + d_s)d_t^4$

d_s/d_t	Ta_c	d_s/d_t	Ta_c	d_s/d_t	Ta_c
1	1695.8	0.8	1994.6	0.35	4717.1
0.975	1724.3	0.75	2101.9	0.3	6523.8
0.9625	1737.7		2102.8	0.28	6345.2
0.95	1755.0	0.7	2230.3	0.25	7442.0
	1755.0	0.65	2384.2	0.2	10356.0
	1755.8	0.6	2572.0		10364.0
0.925	1787.7	0.5	3099.0	0.15	16317.0
0.9	1823.3		3099.9	0.10	32606.0
	1824.1		3099.9		32500.0
0.875	1861.6	0.4	3997.5		
0.85	1902.4	0.36	4551.4		

From the critical disturbance wavelength, the vortices can be expected to have an almost square cross section (see Fig. 3) which is consistent with the experimental observations dating back to Taylor (1923).

Wavy Vortex Flow. As the speed of the inner cylinder increases, a second critical Taylor number, Ta_w, is reached at which the axisymmetric Taylor vortex flow becomes unstable. This instability leads to wavy vortex flow, which can be denoted with the number of Taylor vortices (or $1/\lambda$) and the number of azimuthal waves. At increasing Ta values there is a tendency towards a decrease in the number of Taylor vortices (λ increases). The number of stable azimuthal waves is normally in the range 3-7 (Coles 1965; Ahlers *et al.* 1983; King and Swinney 1983). The number of vortices is not unique at a given Ta but depends on the initial conditions (Koschmeider 1979; Snyder 1969a,b). The wavespeed was about half that of the inner cylinder speed at the first appearance of wavy vortices, but the ratio decreased to about one third at higher inner cylinder speed (Coles 1965). The wavespeed decreases as the radius ratio decreases (King *et al.* 1984; Jones 1985).

Critical conditions for the onset of wavy vortex flow, Ta_w, λ_c and the number of azimuthal waves, have been calcuated for a narrow gap, by introducing an azimuthal disturbance into Taylor vortex flow. This was described by the Navier-Stokes and the continuity equations and with an axisymmetric disturbance (Davey *et al.* 1968; Eagles 1971; Nakaya 1975).

Weinstein (1975) extended the solution to a small gap and Cole (1976) recast these analytical results with

$$Ta_w = 1.11\ Ta_c(1 + 0.291(d_t - d_s)/d_s)^2 \qquad (1)$$

where Ta_c is Ta_c at $d_s/d_t = 1$.

Recent analytical calculations (Jones 1985) show that Ta_w/Ta_c rapidly increases when d_s/d_t becomes smaller than 0.75. ($Ta_w < 1.2\ Ta_c$ for d_s/d_t from 1 to 0.75; $Ta_w = 25\ Ta_c$ for d_s/d_t from 0.75 to 0.65).

Also experiments show that Ta_w depends strongly on the radius ratio; with $d_s/d_t = 0.95$, Ta_w is from 1.1 to 1.2 Ta_c (Snyder 1970); with $d_s/d_t = 0.87$, $Ta_w = 2\ Ta_c$ (King and Swinney 1983); with $d_s/d_t = 0.5$, Ta_w is very much larger, 100 Ta_c or greater (Snyder 1970; Kataoka *et al.* 1975).

For small radius ratios another wavy vortex flow appears. Harmonic generation makes the outward flow from the inner to the outer cylinder more concentrated and intense than the backflow; the resulting outgoing jet develops an instability in the form of axisymmetric waves if the gap is sufficiently wide. The wider the gap, the closer to the onset does this instability occur; for $d_s/d_t = 0.2$, the waves appear almost at the onset of vortex flow (Snyder 1970).

Taylor vortex cells with a size close to the gap size are most stable towards both classical rotational and jet induced waves d_s/d_t from 0.5 to 0.56 and $\lambda/(d_t-d_s)$ from 0.95 to 1.05 give Ta_w higher than 100 Ta_c (Jones, 1985; Cole 1981, 1983; Lorenzen *et al.* 1982).

Higher Instabilities and Turbulence. As the speed of the inner cylinder increases further, a third critical Taylor number, Ta_{mw}, is reached at which irregular disturbances appear in the wavy vortex flow. When the radius ratio is 0.88, Ta_{mw} = 100 Ta_c, and at 400 Ta_c the azimuthal waves disappear (see DiPrima and Swinney 1981 and references therein). Toroidal eddies remain up to 3×10^5 Ta_c, but cannot be clearly distinguished beyond 5×10^5 Ta_c, (Smith and Townsend 1982).

Finite Annulus Length Effects. Experiments show that the Ta_c value is rather insensitive to annulus length, while the Ta_w value depends on the ratio between the annulus length and the gap. Equation (1) applied on rather narrow annulus with finite length results in Ta_w values that are likely to be 10% too low at $1/(d_t-d_s) = 17.5$, 40% too low at $1/(d_t-d_s) = 7.5$ and over 300% too low at $1/(d_t-d_s) = 2.5$ (Cole 1976). Ta_c and Ta_w values have been calculated by an amplitude equation, which consider the length of the annulus, and these results were in agreement with the experimental results mentioned (Walgraef *et al.* 1984).

For cylinders of great or moderate length, compared with the gap, the azimuthal velocity can be expected to be nearly the same as that obtained by Couette flow, except for boundary layers at the ends, but there will also be slow circulation which has some axial structure in planes containing the axis of the cylinders. As the Taylor number increases, this circulary motion slowly develops with the possibility of smooth transitions in cellular structures until Ta approaches the Ta_c for infinitely long cylinders; then there is rapid, but smooth development of the classical Taylor vortex flow over most of the length of the cylinders. In short cylinders this axial and radial flow will be even more pronounced. This picture is consistent with the observation of "ghost" or "shadow" Taylor vortices at Ta values below Ta_c (DiPrima and Swinney 1981; Snyder and Lambert 1966; Burkhalter and Koschmieder 1973; Cole 1974a,b; Jackson *et al.* 1977; Mullin *et al.* 1982).

A numerical analysis with a finite difference procedure of the finite length problem with fixed end plates has been provided by Alziary de Roquefort and Grillaud (1978). Their results for $d_s/d_t = 0.933$ and $1/(d_t-d_s) = 5$, see Fig. 5, show a smooth transition with increasing Ta, from two cells at $Ta/Ta_c = 1.5 \times 10^{-5}$, through four cells and eight cells to, at $Ta/Ta_c = 1.37$, ten cells of equal size with the appearance of classical Taylor

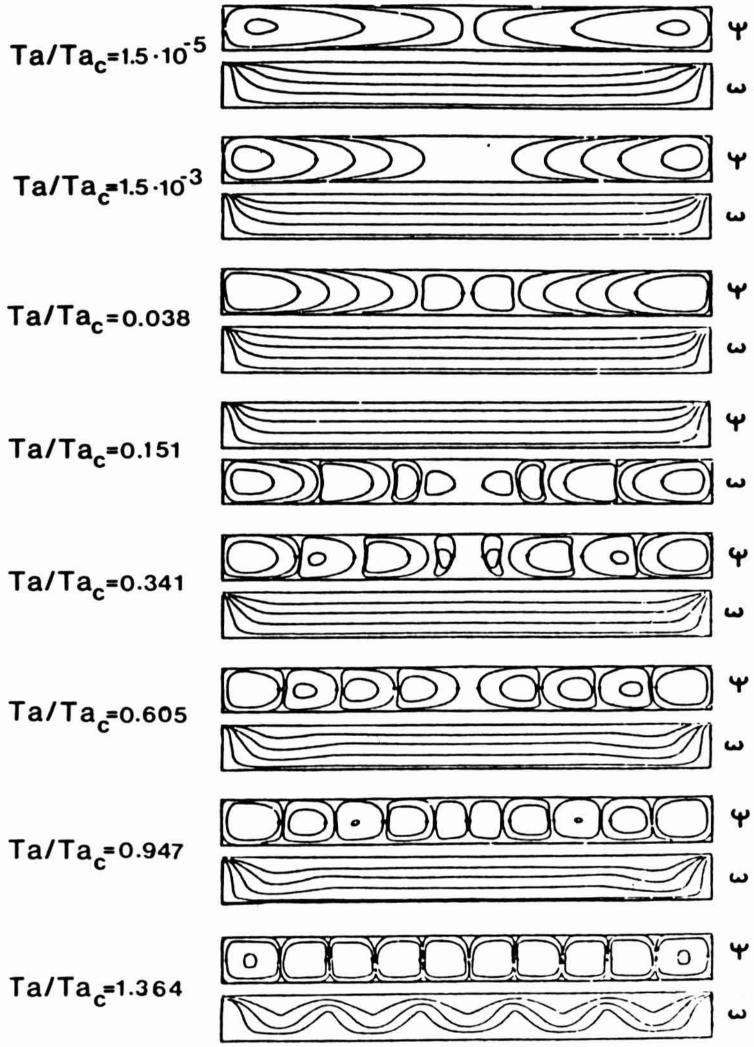

FIG. 5. CONTOUR PLOTS OF THE STREAM FUNCTION Ψ AND THE ANGULAR VELOCITY ω FOR AN ANNULUS WITH $d_s/d_t = 0.933$ AND $1/(d_t\text{-}d_s) = 5$ (Alziary de Roquefort and Grillaud 1978) We have calculated the ratio Ta/Ta_c from data given in the reference combined with Table 2.

vortex flow except for small end effects. For Ta/Ta_c between 0.95 and 1.36 the vortex intensity increased rapidly.

Numerical and experimental investigations (Lücke *et al.* 1984b) show that in a very short annulus with a large gap ($1/(d_t\text{-}d_s) = 0.525$; $d_s/d_t = 0.5066$) the rigid top and bottom plates strongly influence the flow pattern. At Ta well below Ta_c there are two vertically compressed vortices with an inward flow near the plates; at Ta = 3.5 Ta_c the flow becomes gradually assymetric, either the top or the bottom vortex grows, while the other one shrinks and is pushed into a corner near the inner cylinder. At large Ta the flow contains asymmetrically a single vortex, although a small remnant of the second vortex survives.

Time — Development of Rotational Flow. It takes some time after the critical conditions have been exceeded for the flow to develop an equilibrium flow pattern. Several analytical and experimental investigations have been performed (see Cooper *et al.* 1985, and references cited therein).

As an example, it takes about 3 s for the vortex to grow from the inner cylinder and completely fill the radial space when Ta = 1.12 Ta_c, at operating condition typical for an SSHE without axial flow. We have calculated this time using equations in an analytical investigation (Lücke *et al.* 1984a) together with assumed experimental data (N = 4 rps; d_t = 152 mm; d_s = 76 mm; η = 0.5 Pa s; ρ= 1000 kg/m^3) and Ta_c (Table 2).

Flow Patterns in Annuli With Axial Flow

DiPrima and Pridor's (1979) paper gives a good summary of the mathematical problem and of previous analytical and experimental papers on flow patterns between rotating cylinders with axial flow. Illustrative photographs of this combined Couette-Poiseuille flow can be found in Snyder (1962) and Gu and Fahidy (1985a,b).

Taylor Vortex Flow and Spiral Flow. Experimental investigations have shown that at very low Re_{ax}, pairs of toroidal vortices march through the annulus, see Fig. 3 (Kataoka *et al.* 1975, 1977; Takeuchi and Jankowski 1981). This situation agrees with the conclusions that the flow is characterized by only one frequency depending on the axial velocity of the vortices (Legrand *et al.* 1983) and the axial velocity profile is uniform (Simmers and Coney 1980). Experimental investigations have also shown that at low and higher Re_{ax} spiral flow occur, see Fig. 4 (Snyder 1962, 1965; Schwarz *et al.* 1964; Sorour and Coney 1979; Takeuchi and Jankowski 1981; Gu and Fahidy 1985a,b).

The critical conditions for onset of the moving toroidal vortex flow and the onset of spiral flow have been predicted from analytical calculations. Toroidal vortices are caused by axisymmetric disturbances and the spiral flow by nonaxisymmetric disturbances. The onset of the flow with moving toroidal vortices is characterized by critical Taylor number, axial wavelength and wave velocity values at given axial Reynolds number and radius ratio. The wave velocity describes how fast the vortices move in axial direction relative to the axial flow rate. The onset of spiral flow is also characterized by a critical angle, describing the inclination of the spiral (Takeuchi and Jankowski 1981; Ng and Turner 1982).

Results from calculations of critical Taylor numbers are summarized in Table 3 as functions of axial Reynolds numbers for radius ratios 0.95, 0.77 and 0.5. The theoretical onset of spiral flow is also indicated in the

TABLE 3. Critical Taylor numbers for assigned values of Re_{ax} and various radius ratios. Pairs of toroidal vortices are expected when axisymmetric disturbances are critical (denoted by t). Spiral flow is expected when non-axisymmetric disturbances are critical. Axisymmetric disturbances are also critical for the onset of turbulence at very high Re_{ax} (denoted by a). The results for radius 0.5 are from Takeuchi and Jankowski (1981) and for 0.95 and 0.77 from Ng and Turner (1982).

Re_{ax}	Critical Taylor numbers at various radius ratio		
	0.95	0.77	0.5
0.02	1754.86 t)	2056.88 t)	
2			3101.7 t)
10	1788.78 t)	2096.36 t)	
20	1891.32 t)	2215.69 t)	3329.5 t)
40	2297.97	2687.72	4039.4 t)
60			5025.1
80	4021.69	4577.40	6274.0
100			7017.8
120	6805.73	6825.28	7224.5
140			7031.5
160	9263.20	8069.78	6936.0
180			6608.1
200	11546.0	8809.15	6423.6
300	16740.7	9598.71	
400	21087.6	9839.89	
600	27498.4	9963.32	
1000	34383.7	9997.97	
2000	39545.4	10011.4	
4000	41288.4	10009.8	
6000	41638.5	10009.6	
8000	41768.1	10009.5	
10000	41823.3	10009.5	
12000	41854.8	10009.5	
15479	0.0 a)		

table. We have transformed previous results to allow direct comparison between Table 2 and Table 4.

For $Re_{ax} < 70$, there is very good correlation between experimental and analytical results. However, at higher Re_{ax} the analytical results predict a lower Ta_c than that found experimentally (Chung and Astill 1977; Hasoon and Martin 1977; Gravas and Martin 1978; Coney and Simmers 1979). The finite length of the experimental equipment and systematic errors in the experimental technique for determination of the onset of instability have been suggested as explanations of the deviations (Takeuchi and Jankowski 1981; Ng and Turner 1982).

Wavy Vortex Flow with Axial Flow. For $Re_{ax} < 80$, the onset of wavy vortex flow occurred at about 70 Ta_c in systems with radius ratios of 0.75 and 0.62 and annulus length to gap ratios of 20 and 34 respectively, (Kataoka *et al.* 1975, 1977).

Wavy vortex flow can be detected at $Re_{ax} = 500$ for radius ratios of 0.955 and 0.80. However, at $Re_{ax} > 1500$, a weak turbulence occurred directly after the onset of Taylor vortex flow (Wan and Coney 1980).

Time — Development of Rotational and Axial Flow. Sparrow and Lin (1964) developed a criterion for the length of development of axial velocity profiles in an annulus.

In a developing axial flow in an annulus with rotating inner cylinder, Taylor vortices originate near the inner wall, and grow radially outward, and the vortices move in the direction of flow. This leads to two length effects: one to the point where the instability occurs and a second to a point where the vortices are fully developed. The distance from the entrance to the point where vortices occur increases with increasing axial Reynolds number and decreases with increasing Taylor number (Astill 1964; Takeuchi and Jankowski 1981).

Astill (1964) evolved an emperical criterion for the "first discernible ripple" in developing tangential flow as a special form of Taylor number for $200 < Re_{ax} < 1{,}700$ and $13{,}800 < Ta < 312{,}000$ in an annulus where $d_s/d_t = 0.727$. On the basis of these results Martin and Payne (1972) developed a relationship between Ta, Re_{ax}, d_s, d_t and a point z, where "the first discernible ripple" occurs. Ripples will occur at $Ta > Ta_z$ for $0.5 < d_s/d_t < 0.98$ and $0.01 < L < 0.15$, where Ta_z and L are defined by Eq. (2) and (2a), respectively. However, the validity of the formula for radius ratios other than 0.727 remains to be established.

$$Ta_z = 1150\ L^{-1.175} \qquad (2)$$

$$L = 4\ z/(d_t\text{-}d_s)Re_{ax} \qquad (2a)$$

The development length is longer for the tangential velocity profile than for the axial velocity profile, in concentric annuli at $Re_{ax} = 1{,}200$ and Ta at 0 and at 100-600 Ta_c (Simmers and Coney 1979a).

Radial Temperature Difference

The effect of radial temperature differences on the stability of Couette flow between concentric cylinders has been calculated by Becker and Kaye (1962b) for a small gap and by Walowit *et al.* (1964), who also included variations of the radius ratio.

They assumed there to be no axial flow and that the fluid had constant thermal conductivity, specific heat and viscosity. For assigned radius ratio and modified Rayleigh number, they calculated critical Taylor number and wavelength values, with the same method as that described under "Flow patterns without axial flow". We have transformed the results of Walowit *et al.* (1964) in Table 4 to enable comparison with Tables 2 and 3.

TABLE 4
Critical Ta values for different values of ds/dt and of the modified Rayleigh number, calculated with the linear stability theory by Walowit *et al.* (1964). Note that in a SSHE, Ray* is > 0 at heating and < 0 at cooling.

Ray*	$Ta_c(d_s/d_t = 1)$	$Ta_c(d_s/d_t = 0.5)$
1.0	1088.7	2304.5
0.5	1326.7	2647.7
0	1697.3	3109.1
−0.5	2353.0	3761.1
−0.75	2913.2	4198.7
−1	3816.0	4747.4

The results in Table 4 indicate that radial temperature differences have no effect on the Ta_c for low viscosity products, which is in agreement with experiments, with water (Snyder 1965) and with air (Simmers and Coney 1980). However, we have applied the results in Table 4 on high viscosity fluids in a SSHE and found that the Ta_c is predicted to decrease with a factor 2 on heating and to increase with a factor 2 on cooling. We assumed the following conditions: radial temperature difference = 10 °C, $\eta = 0.5$ Pa s and other properties like water. Thus, radial temperature difference seems to be very important for the onset of Taylor vortices in a SSHE, but this remains to be experimentally verified.

Walowit (1963) has also calculated the effect of variable viscosity on the critical conditions for the small gap approximation.

Eccentric Cylinders

When the inner cylinder is eccentrically mounted in the apparatus, the gap size changes when the cylinder rotates. With low laminar rotational flow and no axial flow, the streamlines are compressed when the gap is narrow and expanded when the gap is wide. This leads to pulsating flow. The tangential velocity is high when the gap is narrow and low when the gap is wide; in between the two extremes, the radial flow expands or compresses the streamlines. The radial flow is very small compared with the tangential flow.

Laminar flow between eccentric cylinders has been described analytically and experimentally for a wide range of fluids and operating conditions (Beris *et al.* 1983, 1984; Suematsu *et al.* 1981; Kamel 1985).

Transition to Taylor vortex flow and wavy vortex flow occurs at higher critical Taylor numbers when the eccentricity increases, particularly in short equipments with large gaps (Cole 1976; Jackson *et al.* 1977).

Non-Newtonian Fluids

All analytical and experimental papers dealt with so far presume Newtonian fluids. However, complex flow behavior can change the results; analytical considerations show that transition to Taylor vortex flow is hindered for micropolar fluids (Sastry and Das 1985) and for thermoviscoelastic fluids (Narasimhan and Ghandour 1982).

Blades

In a SSHE with blades mounted on the rotating inner cylinder with no heat transfer and no axial flow, it was hard to detect precisely with visual methods the transition from laminar to Taylor vortex flow, but the transition occurred at about Ta_c in annuli without blades for radius ratios from 0.5 to 0.9 (Trommelen 1970; Trommelen and Beek 1971a; Weisser 1972). Thus, the blades do not seem to change the basic flow patterns.

MIXING EFFECTS AND RESIDENCE TIME DISTRIBUTION

Following the general overview, the theory of plug flow and axial dispersion is surveyed with special emphasis on assumptions and results. Experimental techniques for determination of axial dispersion coefficients are described and published results on annuli and SSHEs are summarized with operating conditions. Radial mixing effects, prerequisites for plug flow behavior and residence time distribution are also discussed.

General Overview of Mixing Effects in SSHEs

General. In the ideal continuous reactor, all molecules spend the same amount of time in the system, residence time distribution is minimal and the driving force is maximal. The process can be modelled with the plug flow model with perfect radial mixing.

In the nonideal continuous reactor, molecules have different axial velocities at different radii; this leads to residence time distribution. The axial flow causes an axial velocity profile and on this profile vortices can be superinduced. Vortices may e.g. originate from turbulence or from Taylor vortices. Vortices contribute to axial mixing (also called axial dispersion or back-mixing). In some cases the back-mixing can be modelled with plug flow and axial dispersion coefficients. Axial mixing increases the residence time distribution and reduces the heat transfer since axial mixing reduces the driving force for heat transfer. Radial mixing improves the heat transfer and reduces the residence time distribution.

Annuli and SSHEs. With laminar flow the radial mixing is very poor and the residence time distribution is controlled by the axial velocity profile caused by the axial flow. The plug flow with superimposed axial dispersion seems to be an unsuitable model for laminar flow.

Superimposed vortices on laminar axial flow lead to very efficient radial mixing. Almost perfect plug flow behavior has been found in an annulus without blades at Taylor vortex flow and very low axial flow, but it remains to be verified whether plug flow also exists in a SSHE. Wavy vortex flow and spiral flow lead to considerable back-mixing; the back-mixing effect is controlled by the axial mixing and axial flow rate ratio and increases with increasing Taylor number and decreasing axial flow rate. The plug flow with superimposed axial dispersion seems to be a good model for vortical flow.

The Plug Flow and Axial Dispersion Model

The first solution of the plug flow and axial dispersion model of any interest was provided by Danckwerts (1953). He solved, for mass transport, the problem of the back-mixing effects on the first order chemical reaction in a tubular reactor with no axial dispersion in the inlet and outlet lines.

Wehner and Wilhelm (1956) generalized Dankwerts' solution to include dispersion in the inlet and outlet lines. Their theoretical results predict that dispersion in the inlet and outlet lines does not change the theoretical solution for the reactor.

The temperature distribution in a continous heat exchanger with back-mixing have been presented (White and Churchill 1959; Miyauchi and Vermeulen 1963; Bott *et al.* 1968b; Penney and Bell 1969b). They assumed the following conditions:

(1) Plug flow with axial dispersion,
(2) Constant wall temperature throughout the heat exchanger,
(3) Uniform local heat transfer coefficient, both around the circumference and along the length of the exchanger,
(4) Constant physical properties of the liquid throughout the exchanger,
(5) The axial dispersion process operates uniformly throughout the liquid at any section,
(6) Negligible molecular thermal conduction in the liquid in the direction of the flow,
(7) Negligible thermal conduction of the equipment in the direction of the flow, and
(8) Feed liquid well mixed to uniform temperature at inlet

The solution can be recast using our heat transfer terminology in the following way:

$$\frac{T_x - T_w}{T_i - T_w} = fa\ e^{fm\ x} + fb\ e^{fn\ x} \tag{3}$$

$$fa = \frac{fm + fn}{fn\left((1 - \left(\frac{fm}{fn} \right)^2 e^{fm - fn} \right)} \tag{3a}$$

$$fb = \frac{fn + fm}{fm\left(1 - \left(\frac{fn}{fm} \right)^2 e^{fn - fm} \right)} \tag{3b}$$

$$fm = \frac{Bo}{2}(1 + \sqrt{1 + 4\ St/Bo}\ ) \tag{3c}$$

$$fn = \frac{Bo}{2}(1 - \sqrt{1 + 4\ St/Bo}\ ) \tag{3d}$$

Note that the temperature profile along the heat exhanger is dependent only on two dimensionless numbers, Bo and St.

Miyauchi and Vermeulen (1963) gave analytical solutions of general and specific cases of axial dispersion accompanying mass transfer or heat transfer. These cases also include solutions in which the wall temperature is not constant.

In the case with constant wall temperature the effect of back-mixing can be expressed by Eq. (4) and illustrated by Fig. 6.

$$\frac{\alpha_{\text{effective}}}{\alpha_{\text{surface}}} = \frac{-\ln(\text{fa}\ e^{\text{fm}} + \text{fb}\ e^{\text{fn}})}{\text{St}} \tag{4}$$

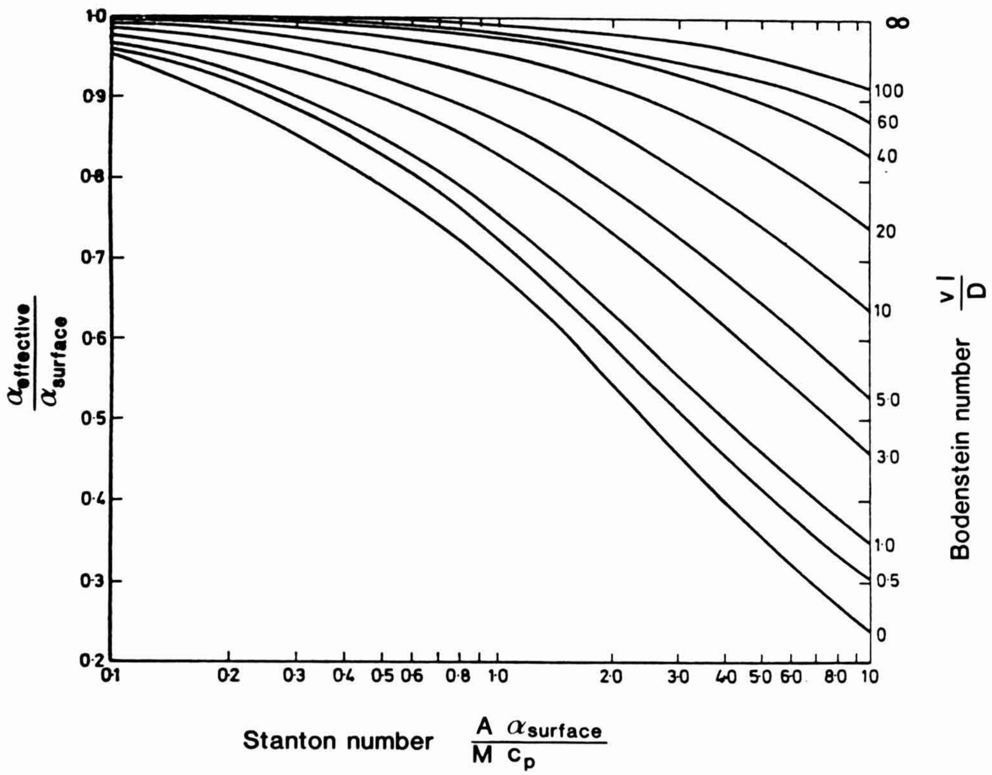

FIG. 6. REDUCTION OF THE DRIVING FORCE, $\alpha_{\text{EFFECTIVE}}/\alpha_{\text{SURFACE}}$, AS A FUNCTION OF STANTON NUMBER AND BODENSTEIN NUMBER (Bott *et al.* 1968b).

Restrictions. Plug flow with axial dispersion is an unsuitable model for laminar rotational flow, indicated by substantial radial temperature gradients have been observed in the outlet line of the heat exchanger at laminar rotational flow (Penney and Bell 1969b); and the control parameters in residence time distribution measurements deviate from the model at laminar rotational flow (Trommelen and Beek 1971a).

Axial Dispersion Coefficients

The axial dispersion coefficient can be expressed as dispersion of heat or as dispersion of mass. The experimental techniques for determination of the axial dispersion coefficients are first described and followed by a summary of published results for annuli and SSHEs.

Axial Dispersion of Heat. Miyauchi and Vermeulen (1963) showed that the temperature just inside the inlet of the heat exchanger is the only experimental measurement that has to be made in addition to those normally taken in heat transfer experiments, in order to be able to calculate the axial dispersion coefficient of heat and the real heat transfer coefficient.

In the case of constant wall temperature the equations for the temperature ratio in the inlet and at the exit of the heat exchanger can be expressed as:

$$\frac{T_{x=0} - T_w}{T_i - T_w} = fa + fb \tag{5}$$

$$\frac{T_{x=1} - T_w}{T_i - T_w} = fa\ e^{fm} + fb\ e^{fn} \tag{6}$$

The two unknown quantities Bo and St can be solved from these two equations. Bo contains the axial disperison coefficient and St contains the real heat transfer coefficient. Miyauchi and Vermeulen (1963) stated that if either St or Bo is known, the unknown quantity can preferably be solved on the basis of temperature jump ratio data. In the case of constant wall temperature, the jump ratio can be written:

$$\frac{T_{x=0} - T_i}{T_{x=1} - T_i} = \frac{fa + fb - 1}{fa\ e^{fm} + fb\ e^{fn} - 1} \tag{7}$$

Blaisdell and Zahradnik (1959) investigated the axial temperature profile obtained when heating water in a Votator. The temperature at the inlet was higher than predicted by the logarithmic temperature profile, which was the first indication of backmixing in a SSHE. Penny and Bell (1969b) obtained a dimensionless correlation between the axial dispersion and the operating parameters of the heat exchanger (see Fig. 7) from the experimental temperature jump ratio and the heat transfer coefficient at one internal point in the heat exchanger. Maingonnat and Corrieu (1983) calculated the axial dispersion from the experimental temperature jump ratio and the heat transfer coefficient from the axial temperature profile inside a SSHE. The values they obtained for the axial dispersion coefficient were greatly scattered (see Fig. 7).

Axial Dispersion of Mass. A much more widely used technique to determine the axial dispersion coefficient is the use of tracer tests. In this transient method some property of the inlet stream is varied by imposing a step, a delta function or a sinusoidal change, and the outlet stream response to this variation is measured. The axial dispersion coefficient is determined by comparison between the experimental data and the theoretical solution (Bischoff and McCracken 1966; Levenspiel 1972, 1979; Wen and Fan 1975).

Some investigations have expressed the axial dispersion of mass as functions of operating conditions or as a constant (see Table 5). Other investigations have expressed the axial dispersion in diagrams (see Fig. 7).

Comments on the Axial Dispersion Coefficients. With laminar rotational flow, large discrepancies occur between the different measurements presented in Fig. 7, probably because the plug flow and axial dispersion model is unsuitable to model laminar flow. With vortex flow and constant viscosity the axial dispersion increases with increasing Taylor number, (see Table 5).

Radial Mixing

With laminar flow the radial mixing is very poor in a SSHE, as observed in photographs (Tommelen and Beek 1971a); and indicated by substantial radial temperature gradients in the heat exchanger outlet line (Penny and Bell 1969a,b).

When Taylor vortices are present the radial mixing is very efficient. Kataoka *et al.* (1975) measured radial mixing in a Taylor vortex-cell and found it to be very high. Increased heat transfer has been observed at onset of vortex flow and the phenomenon has been related to increased radial mixing owing to the onset of Taylor vortices (Becker and Kaye 1962a; Ho *et al.* 1964; Trommelen and Beek 1971a; Payne and Martin 1974; Kataoka *et al.* 1977; Coeuret and Legrand 1981).

Improved design of the tube, shaft and blades may improve radial mixing, particularly in the laminar flow regime; for products with a viscosity higher than 5 Pa s, Bolanowski (1972) showed that eccentric mounted shafts improved the heat transfer by 52%; and Lineberry (1970) and Bolanowski (1972) claim that increased heat transfer is obtained if the blades are mounted in staggered positions or if oval tubes are used.

TABLE 5. Axial dispersion at different operating conditions.

Authors (Year)	Equations	Operating conditions: Products	ν $\frac{m^2}{s} \cdot 10^6$	Ta/Ta_c	Re_{ax}	n	N rps	d_t mm	d_s mm	l mm	d_s/d_t	Remarks
Van Lookeren Campagne (1966)	$D/\nu = 0.00956\ (Ta\ (d_t+d_s)/(d_t-d_s))^{0.55}\ 10^{-0.19(d_t-d_s)/d_s}$	water water-glycerol air	1 3-9 16	10-2500	12-430	0	0-30	26-43	29-82	740-1150	0.50-0.89	RTD measurements
	$D/\nu = 0.707\ (Ta\ (d_t+d_s)/(d_t-d_s))^{0.3}\ 10^{-0.19(d_t-d_s)/d_s}$	water water-glycerol air	1 3-9 16	2500-100000	14-4600	0	0.035-55	22-320	29-640	590-4665	0.30-0.89	
	$D/\nu = 0.243\ (Ta\ (d_t+d_s)/(d_t-d_s))^{0.35}\ 10^{-0.19(d_t-d_s)/d_s}$	water	1	10^5-10^8	56-4800	0	0.24-38	28-320	56-640	590-4665	0.40-0.60	
Trommelen,Beek (1971a)	$D/\nu = 1.15$	glycerol-water	200	0.6	1.2	2	8	56	76	452	0.74	D/ν much greater at 50 Ta_c
Weisser (1972)	$D/\nu = 0.0159\ (Ta\ (d_t+d_s)/(d_t-d_s))^{0.42}\ n^{1.5}$ cooling $D/\nu = 0.276\ (Ta\ (d_t+d_s)/(d_t-d_s))^{0.345}$ freezing											Comparison with exp. data in Figure 7.

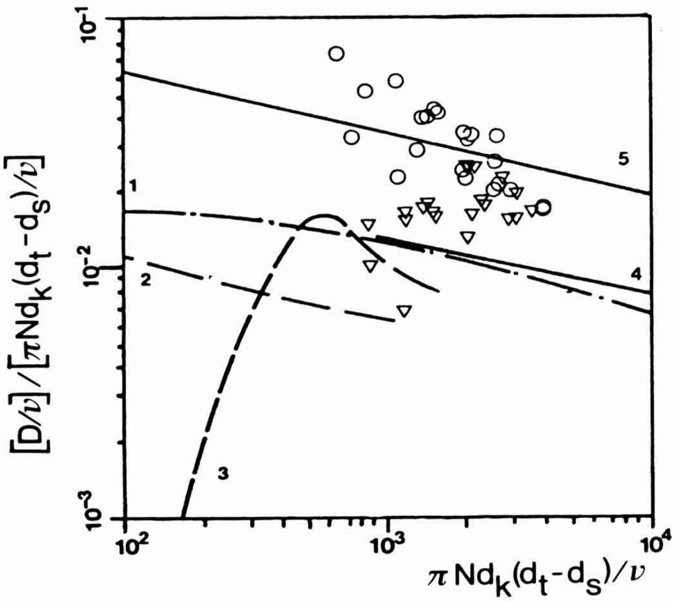

FIG. 7. CORRELATIONS BETWEEN THE AXIAL DISPERSION COEFFICIENT, VISCOSITY AND A MODIFIED ROTATIONAL REYNOLDS NUMBER

1 Croockewit *et al.* (1956), annulus, RTD;
2,3 Penney and Bell (1969b), 2 moderate clearance, 3 close clearance, rotating paddle, temp. jump;
4,5 Weisser (1972), 4 two blades, 5 four blades, comparison with 1, 2, 3;
∇,○ Maingonnat and Corrieu (1983), ∇ two blades, ○ four blades, SSHE, temp. jump.

(Maingonnat and Corrieu 1983; we have included informations about type of equipment and measuring techniques, and introduced ν on the y-axis to facilitate comparison with equations in Table 5).

Plug Flow

Almost perfect plug flow behavior has been found in an annulus without blades with Taylor vortex and with a small axial flow. Each vortex cell marched through the annular space, almost without any axial mixing between neighboring vortex cell. With wavy vortex flow or $Re_{ax} > 90$, the mixing between two vortices was considerable (Kataoka *et al.* 1975, 1977). The condition $Re_{ax} > 90$, coincides with the conditions for onset of spiral flow, as discussed before.

The circumferential mixing within a Taylor vortex-cell has been measured and described as function of Taylor number (Legrand and Coeuret 1986).

Calculations on the flow patterns in an infinitly long annulus without axial flow for $Ta < 200\ Ta_c$ show also no mixing between the vortex cells at Taylor vortex flow but considerably mixing between the cells at wavy vortex flow (Marcus 1984).

Radius ratio from 0.5 to 0.7 is the most favorable range to establish Taylor vortices without waves (Snyder 1970). We therefore expect that this range also is the most favorable range for establishing plug flow in a SSHE, but this remains to be verified.

Evaluation of Residence Time Distribution in SSHEs

Based on experimental investigations by Trommelen and Beek (1971a) and the relations between Ta_c, Re_{ax} and d_s/d_t from Table 3 in this paper we compare the shortest residence time in a SSHE at different flow patterns. With purely laminar flow, at $Ta = 0.006\ Ta_c$, the first trace reached the exit after 0.67 average residence time; this value is the same as that for laminar flow between two parallell plates. For laminar flow close to Ta_c, Ta at 0.6 and 0.9 Ta_c, the first trace reached the exit after about 0.5 average residence time. With vortical flow, at $Ta = 50\ Ta_c$ the back-mixing increases considerably; the first trace the reached exit after 0.2 average residence time.

The residence time distribution in SSHE have also been measured in several other papers. (Blaisdell and Zahradnik 1959; Chen and Zahradnik 1967; Milton and Zahradnik 1973; Bateson 1971). Their data are not detailed enough to allow the above kind of calculations but their results are in agreement with the results of Trommelen and Beek (1971a).

HEAT TRANSFER

After a general overview on heat transfer in SSHEs, the frequently used heat transfer model for SSHEs, the penetration theory with surface renewal, is reviewed, with the emphasis on assumptions, results and limits. Reynolds' analogy theory is mentioned. Back-mixing effects on heat transfer in SSHEs are discussed and followed by several dimensionless equations with operating conditions. Finally, we evaluate published equations and experimental results.

General Overview of Heat Transfer in SSHEs

The heat transfer is controlled by conduction into a thin layer at the heat transfer surface and by the speed of mixing of this layer into the rest of the fluid. Radial mixing improves heat transfer. Axial mixing reduces the driving force for heat transfer, i.e. the temperature difference between the product and the heat transfer medium, and thus axial mixing reduces the apparent heat transfer coefficient. The back-mixing effect is controlled by the axial mixing and the axial flow rate ratio.

With laminar flow the heat transfer is poor due to poor radial mixing. Experimentally determined heat transfer coefficients scatter considerably and no reliable equations are available.

With vortical flow the heat transfer is high due to efficient radial mixing. However, wavy vortex flow causes axial mixing. The back-mixing effect increases with increasing Taylor number and decreasing axial flow rate. A practical consequence of this phenomenon is that large SSHEs operate more efficiently than small SSHEs because the back-mixing effect is normally smaller in large equipment.

Changes in heat transfer due to changes in operating conditions are fairly well predicted with the equations for heat transfer, when the back-mixing effects are calculated with the plug flow and axial dispersion model. However, the different equations predict greatly varying levels of heat transfer; the highest heat transfer prediction is twice the lowest.

Penetration Theory with Surface Renewal

Penetration theory with surface renewal for mass transport was presented by Higbie (1935). Kool (1958) applied this model for heat transfer to equipment like SSHEs and described detailed assumptions, mathematics and results. He assumed that: (1) only molecular conduction transfers the heat into a film at the surface during the time that passes between two scrapings; and (2) at the scraping, the film at the surface is perfectly mixed with the bulk flow.

After some mathematics, Kool (1958) expressed the average rate of heat flux with Eq. (8). In a SSHE, the contact time becomes the time between two scrapings, (see Eq. 8c). Kool simplified Eq. (8) and expressed the heat transfer coefficient with Eq. (8d), for values of s from 0.2 to 30, with an error margin smaller than 1%.

$$k = k'(2s\pi^{-0.5} + \exp(s^2)^{\mathrm{erfc}(s)} - 1)s^{-2} \quad (8)$$

$$1/k = 1/\alpha + 1/k' \quad (8a)$$

$$s = k't^{0.5}(\lambda \rho c_p)^{-0.5} \quad (8b)$$

$$t = (nN)^{-1} \quad (8c)$$

$$\alpha = 1.24k's^{-1.03} \quad (8d)$$

Harriot (1959) and Latinen (1959) made the same assumptions as Kool (1958), but they also assumed that: the heat resistance on the side of the medium and in the heat transfer tube wall can be ignored.

With these assumptions, they expressed the heat transfer coefficient for the product side with Eq. (9) and rewrote it in dimensionless numbers with Eq. (9a)

$$\alpha = 2\pi^{-0.5}(\lambda \rho c_p nN)^{0.5} \quad (9)$$

$$\mathrm{Nu}_{pr} = 2\pi^{-0.5}(\mathrm{Re}_r \mathrm{Pr}\ n)^{0.5} \tag{9a}$$

The Nusselt number for the penetration theory with surface renewal, the Nu_{pr}, has been compared by several authors with experimentally found heat transfer coefficients. We discuss these results later in our evaluation of heat transfer in SSHEs.

Limits and Modifications of the Nu_{pr}. Latinen (1959) compared experimental investigations from Houlton (1944) and Skelland (1958) with the Nu_{pr} and concluded that the heat transfer mechanism in the transition regime must be different from the penetration theory assumptions and mentioned that following factors have been neglected in the penetration theory: (1) peripheral fluid velocities within the thin heat transfer layer, (2) entrance effects, and (3) axial flow effects.

Trommelen *et al.* (1971) suggest a slightly modified mechanism for heat transfer in SSHEs with: (1) penetration of heat by conduction in a thin layer close to the heat transfer surface during the time that passes between two scrapings; (2) partial temperature equalization in the boundary layer that builds up on the scraper blade; (3) convective radial transport from the heat transfer layer to the bulk of the liquid; Taylor vortices contribute to this radial transport.

Trommelen *et al.* (1971) multiplied the Nu_{pr} by a factor less than one to compensate for: (1) incomplete temperature equalization in the boundary layer, (2) effects of radial mixing, and (3) decrease in the heat transfer driving force due to axial mixing.

Reynolds Analogy Theory Between Momentum and Heat Transfer

Bjorklund and Kays (1959) and Simmers and Coney (1979b) have presented equations for heat transfer between the outer surface and the fluid in an annulus. Velocity profiles at different radii are assumed for Taylor vortices with an imposed axial flow. Together with Reynolds' analogy between momentum and heat transfer it is possible to derive equations of the type:

$$\mathrm{Nu} = f(\mathrm{Re}_{ax}, \mathrm{Ta}, \mathrm{Pr}, d_s/d_t) \tag{10}$$

These equations have not been compared with experiments in SSHEs.

Back-Mixing Effects on Heat Transfer

There are three possible mechanisms for axial heat transfer in a flowing mechanically agitated liquid stream in a conduit: (1) conduction along the conduit walls and along the agitator, (2) axial conduction in the liquid, and (3) axial convection in the liquid (commonly called back-mixing or axial dispersion).

A heat exchanger with no back-mixing can be modelled with plug flow and perfect radial mixing and no axial dispersion. In this ideal case, the mean temperature difference is equal to the logarithmic mean temperature difference. This gives the maximum driving force value for heat transfer. With back-mixing the temperature makes a jump at the inlet and the axial temperature profile is changed in the whole heat exchanger. Complete back-mixing gives the absolute minimum of the mean temperature difference. Every heat exchanger operates between the two extremes: no back-mixing and complete back-mixing.

If the back-mixing is considerable but ignored it results in erroneous use of the logarithmic mean temperature difference; the apparent heat transfer coefficient becomes smaller than the real heat transfer coefficient. When experimental data are reduced to dimensionless equations, the values for the physical properties of the product may also be erroneous, due to the unexpected axial temperature profile in the equipment. Together, these factors lead to a false correlation between the axial flow rate and the heat transfer coefficient, when back-mixing is falsely ignored (Penney and Bell 1967b).

Methods Used to Consider the Effect of Back-Mixing in SSHEs. Back-mixing can be ignored when the axial mixing and the axial flow rate ratio is low. The operating conditions for ignoring backmixing can be estimated in different ways.

Trommelen *et al.* (1971) and Weisser (1972), used the plug flow and axial dispersion model combined with axial dispersion coefficients. The plug flow and axial dispersion model can also be used to model SSHE as a chemical reactor, because it is possible to consider time and temperature relations simultaneously.

Another way to consider back-mixing is the temperature jump method. Maingonnat and Corrieu (1984) introduced this method and predicted the temperature jump at the inlet in a SSHE by the following equation, recast with our notations:

$$\frac{T_{x=0} - T_i}{T_{x=1} - T_i} = 0.8 - e^{-0.0366N(d_s(d_t - d_s))^{0.5}/v} \qquad (11)$$

With Eq. (11) they could predict the temperature at the inlet, $T_{x=0}$, and calculated the arithmetic mean temperature in the heat exchanger, $(T_{x=0} + T_{x=1})/2$, without any new measurements inside the SSHE. They used the arithmetic mean temperature to calculate the real heat transfer driving force and the physical properties of the product.

It is easier to reduce heat transfer experiments to a dimensionless equation with the temperature jump method than with the plug flow and axial dispersion model. However, the temperature jump method can probably not be used to model as SSHE as a chemical reactor, since the time aspect is not considered.

TABLE 6. Equations for estimation of inner surface heat transfer coefficient in SSHEs during heating or cooling.

Authors (Year)	Equations	Operating conditions: Products	Pr	Re_r	Re_{ax}	n	N rps	d_t mm	d_s mm	l mm	Remarks
Skelland Oliver Tooke (1962)	$Nu = 0.014\, Pr^{0.96}\, Re_{ax}^{1.0}\, (d_t\, N/\nu)^{0.62}\, (d_s/d_t)^{0.55}\, n^{0.53}$ $Nu = 0.039\, Pr^{0.70}\, Re_{ax}^{1.0}\, (d_t\, N/\nu)^{0.62}\, (d_s/d_t)^{0.55}\, n^{0.53}$	glycerol +water water+ glycerol	1000-4000 5-70	80-200 12600-26200	0.1-5.0 140-1060	2-5	1.7-12.5	76.2	25.4 35.6 45.7 57.2	489.4	high viscosity low viscosity
Dinglinger (1964)	$Nu = 0.489\, Re_r^{0.652}\, Pr^{0.33}$	sugar+water salt+water	7-55	2000-16000		2	0.5-1.2	162	24	350	
Uhl, Gray (1966)	$Nu = 0.308\, Re_r^{0.68}\, Pr^{0.33}\, (\eta/\eta_w)^{0.18}$										Data from Huggins (1931) Houlton (1944) and Skelland et al. (1962)
Trommelen (1967)	$Nu = Nu_{pr}\, (1\text{-}2.78(Re_{ax}\, Pr + 200)^{-0.18})$ $Nu = Nu_{pr}\, (1\text{-}3.28(Re_{ax}\, Pr)^{-0.22})$	glycerol +water	119-2650	300-3600	1-70	2 3 6	5-30	76	46 56 62 68	452	exp. data from Skelland et al. (1962) high viscosity $Re_{ax}\, Pr < 1500$
Nikolajew (1967)	$Nu = 0.00475\, (\frac{d_t\, v\, \rho}{\eta})^{0.89}\, (\frac{N\, d_k}{\nu})^{0.86}\, Pr^{0.58}\, (\frac{Pr_b}{Pr_w})^{0.25}$										
Ghosal Srimani Gnosh (1967)	$Nu = 0.123\, (d_t\, N/\nu)^{0.65}\, Re_{ax}^{0.79}\, Pr^{0.6}$	molasses glycerol	8-128			2	9.1-25.7	72.4	38.1	304.8	

TABLE 6. Cont. Equations for estimation of inner surface heat transfer coefficient in SSHEs during heating or cooling

Authors (Year)	Equations *	Operating conditions: Products	Pr	Re_r	Re_{ax}	n	N rps	d_t mm	d_s mm	l mm	Remarks
Sýkora Navrátil Karásek (1968)	$Nu = 0.80\ Re_r^{0.36}\ Pr^{0.37}\ n^{0.25}$	oils corn syrup	5000- 200000	1- 44	0.001- 0.9	1-4	0.7-1.7	152	108	380	$Re_r < 44$
	$Nu = 2.0\ Re_r^{0.48}\ Pr^{0.24}\ n^{0.15}$	oils	50- 6000	44- 8000	1-200						$Re_r > 44$
Penney Bell (1969a)	$Nu = 0.123\ Re_r^{0.78}\ Pr^{0.33}\ (\eta / \eta_w)^{0.18}$	mineral oil ethylene - glycol	500- 10000 15- 40	2- 10000	0.2- 260	2*	0-20	103.1	89* 97* 101.6* 102.6*	560	* Rotating flat blade covering the whole d_s $Re_r > 400$
Trommelen Beek van de Westelaken (1971)	$Nu = 2.26\ Re_r^{0.5}\ Pr^{0.25}\ n^{0.5}$	glycerol+ water	400- 4000	280- 8000	10- 200	2	4-33.3	76	46 56 62	452	$Re_r > Re_{rc}$ $m > 50\ kg/m^2s$
Weisser (1972)	$Nu = 1.2\ Re_r^{0.5}\ Pr^{0.33}\ n^{0.26}$	water+sugar water+ glycerol	7- 200	100- 19000	10- 1200	2,4	0.075- 0.75	162	80 100 120	350	$m > 5\ kg/m^2s$
Ramdas, Uhl Osborne, Ortt (1977)	$Nu = 57\ Re_r^{0.113}\ Pr^{0.063}\ (\eta / \eta_w)^{-0.018}\ Re_{ax}^{0.059}$	corn syrup oils	550000- 1600000 1300- 14000	0.02- 0.06 3-70	0.002- 0.01 0.5-10	2	0.01- 0.5	152.4	50.8	1828	0.063, - 0.018 and 0.059 fixed

TABLE 6. Cont. Equations for estimation of inner surface heat transfer coefficient in SSHEs during heating or cooling

Authors (Year)	Equations	Operating conditions: Products	Pr	Re_r	Re_{ax}	n	N rps	d_t mm	d_s mm	l mm	Remarks
Cuevas Cheryan Porter (1982)	$Nu = 1.09\ Re_r^{0.322}\ Pr^{0.33}\ (\eta / \eta_w)^{0.18}\ Re_{ax}^{0.504}$	water			1200-1800						
	$Nu = 0.00165\ Re_r^{0.637}\ Pr^{0.33}\ (\eta / \eta_w)^{0.18}\ Re_{ax}^{0.942}$	water	1.76-2.90	8600-730000	1800-3700	2	0.16-9.6	154	111	462	0.33 and 0.18 fixed
	$Nu = 0.352\ Re_r^{0.4}\ Pr^{0.33}\ (\eta / \eta_w)^{0.18}\ Re_{ax}^{0.468}$	soy extracts	3-50	3500-370000	60-1800		1.6-9.6				
Maingonnat Corrieu (1984)	$Nu = 2.6\ Re_r^{0.54}\ Pr^{0.33}$	water+ sugar	90-600	250-14000	4-20	2	1.6-6.7	130	79	370	back-mixing considered 0.33 fixed
	$Nu = 2.9\ Re_r^{0.49}\ Pr^{0.33}$					4			106		
Maingonnat Benezech Corrieu (1985)	$Nu = 1.69\ Re_r^{0.32}\ Pr^{0.33}$	alginate	13000-40000	5-55		2	1.6-6.7	130	106	370	back-mixing considered 0.33 fixed non-Newtonian fluids
	$Nu = 0.28\ Re_r^{0.90}\ Pr^{0.33}$		2500-10000	17-270							
	$Nu = 0.165\ Re_r^{0.96}\ Pr^{0.33}$		1000-3000	64-580							
	$Nu = 1.25\ Re_r^{0.60}\ Pr^{0.33}$		300-600	46-2200							

TABLE 7. Equations for estimation of inner surface heat transfer coefficient in SSHEs during freezing or crystallization

Authors (Year)	Equations	Conditions	Products	Pr	Re_r	Ra_{ax}	n	N rps	d_t mm	d_s mm	l mm	Remarks
Dinglinger (1964)	$Nu = 141000\, Re_r^{0.83}\, Pr^{3.32-0.332 \ln (Pr)}\, (T_i^*/T_e^*)^{1.76-0.22 \ln (T_i^*/T_e^*)}$		sugar+ water salt+ water	7-55	2000-16000		2	0.5-1.2	162	24	350	
Weisser (1972)	$Nu = 1.41\, Re_r^{0.5}\, Pr^{0.45}\, n^{0.5}$		water-sugar water-glycerol	7-200	100-19000	10-1200	2 4	0.075-0.75	162	80 100 120	350	$\dot{m} > 6$ kg/m^{2}s standard dev. 12% max error 25%
Ay Wenzlau Gramlich (1979)	$Nu = 8.161\, Re_{rs}^{0.666}\, Pr^{-0.51}$		P-Nitroacetophenon- P-Nitroetylbenzol				2	0-6.66	84		1500	average deviation $\pm$ 25%
Wenzlau Ay Gramlich (1982)	$Nu = 0.053\, Re_{rs}^{0.53}\, Pr^{1.3}\, (1 - c_v / c_{max})^{1.35}$ $Nu = 0.00475\, Re_{rs}^{1.0}\, Pr^{1.1}\, (1 - c_v / c_{max})^{1.6}$	$Re_{rs} < 900$ $Re_{rs} > 900$	P-Nitroacetophenon- P-Nitroetylbenzol P-Nitrochlorbenzen- O-Nitrochlorbenzen		300-5000		2	0-6.66	84		1500	max error < $\pm$ 20%

TABLE 8. Comparison between experimentally found Nu and Nu_{pr}. We have divided the experiments according to viscosity and calculated Re_r and Re_{ax} from data given in the references

Exp. data (year)	Products	Viscosity Pa s	Re_r	Re_{ax}	Nu/Nu_{pr}
Houlton (1944)	water	0.0004	30000-200000	3000-7000	1.15
Harriott (1959)	water	0.0004	80000-340000	1000-3000	1.10
Cuevas, Cheryan (1982)	water	0.0004	370000 370000 36000 36000	2200 650 2200 650	4.0 0.8 1.4 1.1
van Boxtel de Fielliettaz Goethart (1984)	water	0.0004	220000 41000	1950 1760	1.1 0.9
Harriott (1959)	oil carrot pure	0.04 0.1	 400-4000	high 15-60	0.8-1.2 0.6
van Boxtel de Fielliettaz Goethart (1984)	high viscosity foods	>2	<40	<0.4	0.2-0.5

Experimental Results Summarized with Dimensional Analysis

Many authors have summarized their heat transfer experiments in SSHEs with dimensional analysis. We have gathered several equations including operating conditions during heating and cooling in Table 6 and during freezing in Table 7.

Evaluation of Heat Transfer in SSHE

Experimentally determined heat transfer have been reported to range from 0.2 Nu_{pr} to 4 Nu_{pr} (see Table 8). This considerable difference between theory and experiment has been explained by entrance effects, axial flow and axial mixing effects and radial mixing effects (Latinen 1959; Trommelen *et al.* 1971).

In the following analysis of the literature on heat transfer in SSHE we assume that the flow pattern controls the mixing effects and the mixing effects control the heat transfer. Let us also bear in mind that backmixing is considerable in the vortex flow regime, and the backmixing effect increases with increasing Re_r and decreasing Re_{ax}.

The rotational flow is expected to be laminar for $Re_r < 250$, vortical for Re_r values from 250 to 100,000, and turbulent for $Re_r > 100{,}000$. The axial flow is expected to be laminar for $Re_{ax} < 15{,}000$. We have calculated these rough criteria using Tables 2 and 3, in combination with the operating conditions in Table 6. The onset of turbulence has been regarded to be the same phenomenon as the disappearance of vortices at very high Ta.

Penetration Theory with Surface Renewal, Nu_{pr}. The penetration theory with surface renewal predicts that the Nu_{pr} is independent of viscosity (see Eq. 9). The powers of Re_r and Pr are identical in Eq. (9a). However, several equations in Table 6 indicate a Nu viscosity-dependency by different powers of Re_r and Pr.

When the contact time, $(N\ n)^{-1}$, is the rate-controlling factor the power of N and n become 0.5, which is expressed as 0.5 in the powers of Re_r and of n in the Nu_{pr}, (see Eq. 9, and 9a). Values below 0.5 of these powers indicate the presence of some other rate-controlling factor. Values above 0.5 indicate that there is some factor dependent on the Re_r and n, that improves the Nu above reduced contact time.

The Nu_{pr} is based on optimistic assumptions. Nu values greater than Nu_{pr} therefore require special attention to be explained.

A possible way to explain why the Nu can be greater than Nu_{pr} is to consider the heat resistance in the tube wall; in this way the real driving force is reduced and the real Nu increases and the Nu ranges from 1.10 to 1.14 Nu_{pr}, for normal operating conditions in a SSHE. We calculated these values, using Eq. (8d) together with the following data: $k = 2000$

W/m² °C, λ = 0.6 W/m °C, ρ = 1000 kg/m³, c_p = 4200 J/kg °C, n = 2 and N from 1 to 10 rps.

Nu values greater than Nu_{pr} can also be expressed by viscosity-dependency. Trommelen *et al.* (1971) predicted the Nu from 0.3 Nu_{pr} to 0.45-Nu_{pr} for his experimental conditions (Pr from 2000 to 400). However, if his equation is extrapolated to experimental conditions for water (Pr = 2), the equation predicts the Nu to be 1.7 Nu_{pr}. In principle, dimensionless equations should not be extrapolated beyond the experimental conditions, but this example indicates that Nu viscosity-dependency might express Nu values greater than Nu_{pr}. However, it does not explain why the Nu becomes greater than Nu_{pr}.

Laminar flow. The heat transfer at laminar flow is considerably less than predicted by the Nu_{pr}. The Nu varies from 0.2 Nu_{pr} to 0.5 Nu_{pr} (see Table 8).

In Table 6, three equations are valid for laminar flow and the power of Re_r varies in these equations from 0.11 to 0.36. This indicates some factor other than contact time to be the rate-controlling factor. Poor radial mixing is the rate-controlling factor at laminar rotating flow.

The experimental data scatter considerably; the relative standard deviation between equations and experimental data available was 25% (see Appendix A). This indicates that the heat transfer is very hard to predict and that there are no methods available to describe heat transfer when the rotational flow is laminar in a SSHE.

Transition from Laminar to Vortical Flow. Some equations in Table 6 are valid for a rather narrow range around Re_{rc} and in these equations the power of Re_r varies from 0.6 to 0.96. The factor that improves Nu more than reduced contact time and which is dependent on Re_r, is the onset of vortex flow followed by improved radial mixing. This is in agreement with several observations (Becker and Kaye 1962a; Trommelen and Beek 1971a; Payne and Martin 1974; and Kataoka *et al.* 1977).

Vortical flow. With vortical flow, back-mixing is considerable in SSHEs (Trommelen 1970; Weisser 1972; and Maingonnat and Corrieu 1984). If back-mixing is falsely ignored, a false dependence on axial flow rate occurs (Penney and Bell 1967b). None of the equations in Table 6 considering back-mixing, shows any dependence on axial flow rate. Therefore, equations in Table 6 with some dependence on axial flow rate are excluded in the following discussion.

Vortical flow provides intense radial mixing and therefore, we expect the same viscosity in the bulk as at the wall. In this way the factor (η/η_w) becomes equal to 1 and can thus be omitted.

The power of Re_r varies from 0.48 to 0.54 when vortical flow is expected in Table 6 and these powers are very close to 0.5, the power of

Re_r in Nu_{pr}. This indicates that the heat transfer is controlled by the contact time at vortical flow.

The heat transfer at vortical flow has been reported to vary from 0.3 to 1.4 Nu_{pr}. This variation seems to depend on the viscosity; the greatest heat transfer takes place for low viscosity products like water (see Table 8); and the smallest heat transfer for high viscosity products, as predicted by equations in Table 6. The power of Pr varies from 0.24 to 0.33 while the power of Re_r is close to 0.5 (see Table 6). This indicates that the radial mixing decreases when the viscosity increases at constant Re_r.

The equations presented by Weisser (1972) and Trommelen *et al.* (1971) predicted the changes in heat transfer due to different operating conditions fairly well; the relative standard deviation was about 8% (see Appendix A). This indicates that when Taylor vortices are present in SSHEs the changes in heat transfer can be predicted fairly well, provided that back-mixing is considered.

If we look at the equations which consider back-mixing and divide these equations with the equation of Trommelen *et al.* (1971), we find that the equation of Weisser (1972) predicts the Nu at a level of about 0.80 of that of Trommelen's equation; the corresponding ratio for the equation of Maingonnat and Corrieu (1984) is 1.25. This indicates that equations derived in one type of SSHE can hardly be applied to another SSHE, because of too large differences with regard to predicted heat transfer coefficient levels.

Turbulent Rotational Flow. The heat transfer at turbulent rotational flow is great or very great, from Nu_{pr} to 4 Nu_{pr}. The Nu decreases when Re_{ax} decreases and in some cases the Nu is almost constant at 1.1 Nu_{pr} (see Table 8).

We suggest the following explanation for these results: Turbulent eddies remove the film more frequently than at each scraping and perfect radial mixing takes place. This leads to an Nu value far greater than the Nu_{pr}. However, at low axial flow rates the back-mixing reduces the apparent Nu to a value slightly above the Nu_{pr}.

In industrial applications, however, turbulent rotational flow appears almost only during cleaning processes, resulting in only minor interest heat transfer equations with this flow pattern.

POWER REQUIRED TO ROTATE SHAFT AND BLADES

A general overview of the mechanical power requirement in SSHEs is followed by a presentation of analytical and semi-analytical approaches to power requirements with special emphasis on assumptions and results.

Results from dimensional analyses are presented with operating conditions. Finally, we evaluate the published relationships.

General Overview of Mechanical Power Requirements in SSHEs

The total power required for rotation consists of the power required to maintain the rotational flow in the annulus and the power required to rotate the blades. The total power is mainly controlled by the design of the blades. However, most papers have not presented details on the blade design and the differences between predicted powers are tremendous.

The maximum power requirements occurs at laminar flow and experiments can be extended by an equation to higher rotational speeds and higher viscosities provided that the blade design and flow regime are the same.

With laminar flow, the mechanical power required to rotate the shaft and blades is considerably and can exceed 10% of the heat-transferred power in SSHEs. With vortex flow, the mechanical power can usually be ignored in comparison with the heat-transferred power.

Analytical and Semi-Analytical Approaches

The total power required for rotation consists of the power required to maintain the rotational flow in the annulus and the power required to rotate the blades (Trommelen and Beek 1971b).

Power Required by Viscous Rotating Flow in an Annulus. The mean torque on the inner cylinder for laminar Couette flow and Taylor vortex flow has been calculated analytically (DiPrima and Eagles 1977; Kirchgässner and Sorger 1969). By multiplying their mean torque with the angular velocity, the required power can be recast in the following way:

$$\mathrm{Ne} = \frac{4\pi^3(d_s/d_t)^2}{(1 - (d_s/d_t)^2)\mathrm{Re}_r} \left|-1 + G_t/G_l\right| \quad G_t = 0 \text{ for Ta} < \mathrm{Ta}_c \qquad (12)$$

where G_l is the dimensionless torque due to laminar Couette flow and G_t is the dimensionless Taylor vortex torque. G_t/G_l can be expressed as

$$G_t/G_l = C_1(\mathrm{Ta} - \mathrm{Ta}_c) + C_2(\mathrm{Ta} - \mathrm{Ta}_c)^2 \qquad (12a)$$

where C_1 and C_2 values are given in Table 9, and the Ta_c is given in Table 2 or Table 3. Equation (12) is in agreement with experimental results of Snyder and Lambert (1966), but is only valid for laminar flow and Ta values slightly higher than Ta_c (see Table 9).

TABLE 9

Coefficients C_1 and C_2 as functions of the radius ratio, d_s/d_t, to be used in Eq. (12a) for calculation of the mean torque on the inner cylinder with Taylor vortex flow in the annulus. (DiPrima and Swinney 1981; DiPrima and Eagles 1977; Sorger 1969).

d_s/d_t	C_1	C_2	Restrictions
1	9.0×10^{-4}	-8.4×10^{-7}	$Ta < 1.1\ Ta_c$
0.95	7.9×10^{-4}	-6.8×10^{-7}	$Ta < 1.1\ Ta_c$
0.5	1.4×10^{-4}	-3.8×10^{-8}	$Ta < 1.35\ Ta_c$

Donnelly and Simon (1960) and van Lookeren Campagne (1966) found experimentally that the Ne was proportional to Re_r^{-1} below Re_{rc} and proportional to $Re_r^{-0.5}$ above Re_{rc}.

Entrance effects can be ignored as the power required to impart kinetic rotational energy to the fluid is small compared with the power measured (Trommelen and Boerema 1966).

Axial flow has no influence on the power requirements for agitation of Newtonian fluids in a SSHE, as shown analytically (Yamada 1962) and experimentally (Trommelen and Boerema 1966; and Coney and Simmers 1979).

Power Required by the Blades. Trommelen and Beek (1971b) developed a formula for estimation of power requirements for the blades in a SSHE, with parameters related to centrifugal forces, viscous forces and the contact area between the blades and the tube wall. These three parameters have to be determined from experimental data. The formula is too voluminous to be recast in this paper.

Power requirements for very low Re_r values have been calculated analytically for hinged blades by Toh and Murakami (1982a) and for floating blades by Toh and Murakami (1982b). They considered: the shape of the blades, the number of blades in a set, the scraping angle of the blades and the slit in the blades. The equations are too voluminous to be recast in this paper, but to provide an example the results of some calculations have been illustrated in Fig. 8. Only the friction between the blades and the tube wall have to be determined from experimental data. There is very good agreement between the analytical and experimental values (see Fig. 8).

On freezing the power requirements increase considerably and are hard to predict, due to increased friction when scraping the crystals away from the tube wall (Weisser 1972; Dinglinger 1964).

Dimensional Analysis

Equations based on dimensional analysis and operating conditions from several investigations are presented in Table 10. For many types of stir-

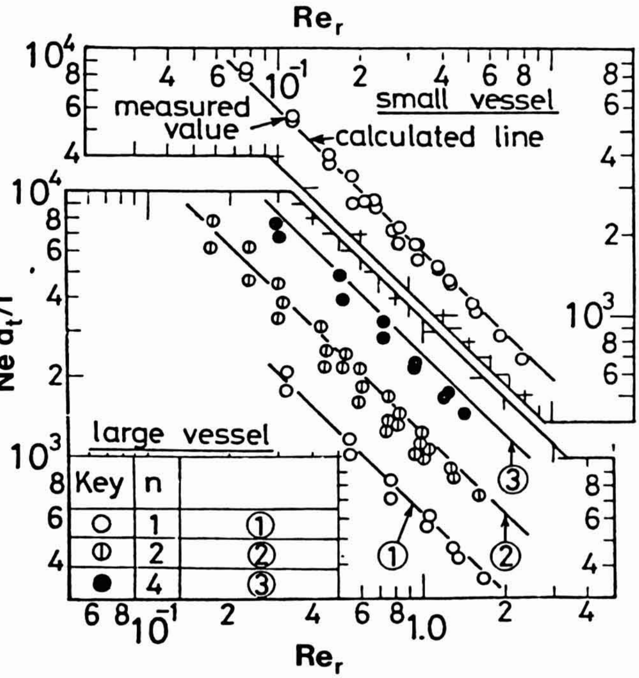

FIG. 8. POWER REQUIREMENTS FOR FLOATING SCRAPER BLADES IN VESSELS; A COMPARISON BETWEEN CALCULATED AND MEASURED VALUES

		Large Vessel	Small Vessel
Inner diameter,	m	0.208	0.1325
Length of blade,	m	0.200	0.11
Thickness lf blade,	m	0.002	0.002
Width of blade,	m	0.028	0.028
β_1 (see Fig. 8b)	rad	$\pi/6$	$\pi/6$
β_2 (see Fig. 8b),	rad	0.471	0.524
Assumed friction coefficient (Toh and Murakami 1982b)		0.1	0.15

rers the power number, Ne, is a unique function of the rotational Reynolds number, Re_r, and the result can be successfully summarized by dimensional analysis. However, in a SSHE the Ne increases with decreasing viscosity at a given Re_r (Trommelen and Beek 1971b; Weisser 1972). Trommelen and Beek (1971b) suggested that scraping in a SSHE causes this deviation.

Evaluation of Mechanical Power Requirements in SSHEs

We have evaluated published relationships for prediction of the power required to rotate shafts and blades in SSHEs in Appendix B. Our results and conclusions of the evaluation are presented below.

Principles for Sizing Motors for SSHEs. The power requirement for rotation reaches its maximum at maximum rotational speed and maximum viscosity. The equations in Table 10 cannot be used to size motors for SSHEs since the design of the blades seems to be of primary importance and there is insufficient detailed information to assess the equations in the literature.

For laminar flow the Ne seems to be proportional to Re_r^{-1} for SSHEs as well. Therefore, with a given rotor and blade design the proportional constant can be determined from one experiment in which the Ne and Re_r are known. By extrapolation the power can be estimated for a desired maximum viscosity at any rotational speed, provided that all design factors except the length of the equipment is kept constant from the experiment to the estimation. Thus, it seems possible to size motors for SSHEs fairly well by extending the results from one experiment. However, this remains to be verified.

Influence of Power Dissipation on Temperature Conditions. The estimated mechanical power requirements for rotation can be found in Appendix B. The heat-transferred power can be estimated by a combination of heat transfer coefficients in Table 8, heat transfer area based on the size of the equipment in Appendix B, and by a temperature difference. In the following comparison we assume the temperature difference to be 50 °C and our conclusion is then: (1) At laminar flow, the power required for rotation of shaft and blades in viscous products can exceed 10% of the heat-transferred power in SSHEs; and (2) At vortex flow the heat transfer is efficient and in most cases the power dissipated into the fluid can be ignored in comparison with the heat-transferred power. However,

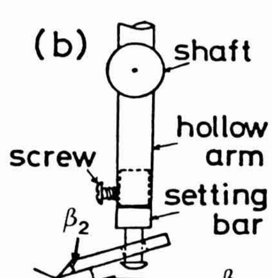

FIG. 8b. DETAILS OF ATTACHING FLOATING BLADE TO SHAFT
(Toh and Murakami 1982b)

TABLE 10. Power required to rotate shaft and blades in SSHEs described with dimensional analysis.

Authors (Year)	Equations		Operating conditions								Remarks
			Products	Re_r	η Pa s	N rps	n	d_s mm	d_t mm	l mm	
Skelland Leung (1962)	$Ne = 35656\ Re_r^{-1.27}\ \eta^{0.59}$		glycerol	90-250		5.25 12.50	2-5	25.4 35.6 45.7 57.2	76	460	
Dinglinger (1964)	$Ne = 36522\ Re_r^{-1.20}$			20-20000			2				
Leung (1967)	$Ne = 27322\ Re_r^{-1}\ \eta^{0.59}$										experimental data of Skelland, Leung (1962) and Trommelen, Boerema (1966)
Trommelen Beek (1971b)	$P = 251\ (N\ d_t)^{1.79}\ \eta^{0.68}\ l\ n^{0.66}\ (d_t - d_s)^{-0.31}$	SI units	glycerol water	20-2300	0.1-1.5	4.0-33	2 4 6	46 56 62 68	76	460	
	$P = 276\ (N\ d_t)^{1.52}\ \eta^{0.68}\ l\ n^{0.68}\ (d_t - d_s)^{-0.31}$	SI units	glycerol water	10-1000	0.1-1.2	3.3-33	1	34 38 43	50	260	0.68 and -0.31 kept constant. experimental data of Trommelen, Boerema (1966)
Weisser (1972)	$P = 344\ (N\ d_t)^{1.79}\ \eta^{0.47}\ l\ n_w^{0.53}$	SI units		150-6100	0.001-0.2	0.075-0.75	2 4	80 100 120	162	350	
	$Ne = 1066\ Re_{rw}^{-1.20}\ \eta^{0.47}\ n_w^{0.66}$										

these conclusions remain to be experimentally verified. The main uncertainty is the power required for rotation, but the uncertainty regarding heat transfer during laminar flow is also considerable.

SUMMARY AND RECOMMENDATIONS

This is a summary of today's knowledge and some recommendations for future work on the performance of scraped surface heat exchangers, SSHEs.

The flow pattern controls the desired radial mixing and the undesired axial mixing. The axial flow is always laminar and the rotational flow is laminar or vortical in SSHEs. The power required to rotate the shaft and blades in SSHEs is mainly controlled by the design of the blades.

Laminar Flow

With laminar flow the radial mixing is poor, resulting in poor heat transfer. The heat transfer results are greatly scattered and no equations are available. The power required for rotation may be considerable but no equations are available. The residence time distribution is controlled only by the axial flow profile. Some important problems remain to be solved: (1) reduction of the scattering of heat transfer results, probably by improvements of the measuring technique, (2) description of heat transfer with equations as functions of the operating conditions, (3) description of power required for rotation with equations for various operating conditions with careful consideration of blade design, and (4) improvement of the radial mixing efficiency, probably by improving the shaft and blade design.

Transition Laminar — Vortex Flow

The transition to vortex flow in a SSHE is hard to predict precisely, because factors like axial length, axial flow rate and radial temperature differences make it hard to fulfil the presumptions for available analytical solutions. Another complicating factor is the axial temperature profile, which changes the physical properties of the fluid, particularly its viscosity. An important task that remains to be solved is the development of a simple method for distinguishing between laminar and vortex flow in SSHEs.

Vortex Flow

With vortex flow the radial mixing is very efficient, which leads to high heat transfer and perhaps to plug flow behavior. However, vortex flow also causes axial mixing which reduces the apparent heat transfer coefficient and increases the residence time distribution.

Back-mixing can be modelled with plug flow and axial dispersion. The axial dispersion coefficient can be determined from temperature or residence time distribution measurements. However, results presented on axial dispersion coefficient are considerably scattered. Available equations for heat transfer differ considerably but each equation predicts the effect of changes in operating conditions fairly well. Some tasks that remain to be solved are: (1) reduction of the scattering axial dispersion coefficient of heat or mass; (2) correlation of the axial dispersion coefficient to operating conditions; (3) development of better equations for heat transfer; (4) experimentally verification of plug flow in SSHE, and (5) improvement of design and choice of operating condition to faciliate use of SSHEs at optimal operating conditions.

APPENDIX A
EVALUATION OF SOME EQUATIONS FOR HEAT TRANSFER IN SSHEs

Background

Back-mixing is considerable in SSHEs and some authors have considered this phenomenon before they reduced their experimental heat transfer data to equations predicting heat transfer coefficients (see Table 6). The plug flow with axial dispersion model seems to be a good model for prediction of the effects of back-mixing in SSHEs. Some equations for the axial dispersion coefficient in annuli with rotating inner cylinder but without blades have been published (see Table 5).

We have combined these equations and evaluated them by comparing with experimental data. We have also divided the experimental data into the laminar and the vortex flow regimes respectively.

Methods

Experimental Data. Detailed experimental results on cooling in a SSHE are available (Trommelen 1970, Tables A5-A9). We have calculated the heat transfer power from the sum of "sensible heat" and "frictional heat" in his tables. Some information on physical properties are missing in his paper but we have assumed the following properties for his water glycerol mixtures: density 1000 kg/m^3, specific heat 3000 J/kg °C and thermal conductivity 0.3 W/m °C.

Equations. From Table 6 we have chosen two heat transfer equations which consider back-mixing (Trommelen and Beek 1971b; Weisser 1972). We modelled the back-mixing with Eq. (4) in this survey and calculated the axial dispersion coefficient from the equation of Weisser (1972) in Table 5.

Evaluation Technique. We calculated a heat transfer coefficient ratio, defined as the ratio between the experimentally found heat transfer coefficient and the calculated effective heat transfer coefficient. We then divided the experiments, by comparing the Re_r from the experiments and the Re_{rc} from Table 2 into three groups: only laminar flow, only vortex flow and all experimental data together. For each group of data, we calculated an average heat transfer coefficient ratio and the relative standard deviation for this ratio.

Results and Conclusions

The results from our calculations are presented in Table A1. From this table we can see that the equation of Weisser (1972) predicts the heat transfer coefficients to be about 80% of those of Trommelen and Beek (1971b).

For laminar flow, the experimental data scatter considerably; the ratio between relative standard deviation and average heat transfer ratio is from 20 to 24%.

The corresponding ratio for vortex flow is from 7 to 9%, which indicates more predictable operating conditions.

TABLE A1

Comparison of calculated effective heat transfer coefficient, calc, and experimentally found heat transfer coefficient, exp. The standard deviation for the ratio calc/exp. is abbreviated std.

EQUATIONS (Year)	FLOW PATTERN	RESULTS $\frac{\text{Calc}}{\text{Exp}}$	$\frac{\text{Std exp}}{\text{Calc}}$
Weisser (1972)	Only laminar	0.84	0.20
	Only vortex	0.72	0.07
	Both laminar and vortex	0.77	0.16
Trommelen and Beek (1971b)	Only laminar	0.98	0.24
	Only vortex	0.89	0.09
	Both laminar and vortex	0.92	0.17

APPENDIX B
EVALUATION OF POWER REQUIRED TO ROTATE THE SHAFT AND BLADES IN SSHEs

Background

Several relationships have been presented for the predicton of the power required for the rotation of shaft and blades in SSHEs. In this appendix we compare these relationships with one another and with expected experimental values which are divided into different flow regimes.

Methods

Expected Experimental Data. We assume that the equations of Weisser (1972) and of Trommelen and Beek (1971b) in Table 10 cover the respective experiments fairly well. We therefore assume that these equations represent "experimental values" for the two ranges of operating conditions, respectively.

The range of the experimental conditions is extended to a very low Taylor number, in order to cover the operating conditions in Toh and Murakami (1982a,b). In this range we assume the equations of Toh and Murakami (1982a,b) to be the most reliable.

Equations. The following relationships have been evaluated: All equations in Table 10, the analytical solution for the power required by viscous flow in an annulus (Eq. 12) and the semi analytical solution for the power required by the blades (Fig. 8). Equation (12) is not valid for $Ta > 1.4\ Ta_c$ and for this flow regime we extended the value of Ne from Eq. (12) at $1.4\ Ta_c$ with the empirical relation $Ne = C\ Re_r^{-0.5}$ (Donnelly and Simon 1960; van Lookeren Campagne 1966).

Evaluation Technique. The axial flow was assumed to be zero and the Ta_c was chosen from Table 2. Ta_c was used in Eq. (12) and when we divided the experimental conditions into the laminar and the vortex flow regimes.

To facilitate interpretation of the results we present them as power ratios; the predicted power required for agitation divided by the value from Weisser (1972). The Weisser value (1972) is presented in Watts.

Results and Discussion

None of the authors listed in Table 10 consider any influence from different flow patterns on the power requirements.

Laminar Flow. The results from our calculations on laminar flow conditions are presented in Table B1.

TABLE B1. Evaluation of the power required for rotation at *laminar* flow in SSHEs. The following conditions were kept constant in the calculations: blades = 2 and density = 1000 kg/m^3. Ta_c was chosen from Table 2 for each radius ratio, $Re_{ax} = 0$. The equations used are empirical (Table 10), analytical for annulus (Eq. 12), and semi-analytical for blades (Fig. 8)

	OPERATING CONDITIONS						PREDICTED POWER REQUIREMENTS						
Source	visc. Pa s	N rps	d_s mm	d_t mm	l mm	Ta/Ta_c	Weisser Watts	Trommelen/Weisser	Skelland/Weisser	Dinglinger/Weisser	Leung/Weisser	annulus/Weisser	blade/Weisser
Weisser	0.2	0.075	80	162	350	$3\ 10^{-3}$	0.03	1.5	11	9	6	0.015	0.3
		0.75				$3\ 10^{-1}$	1.6	1.5	10	9	9	0.025	
Trommelen	0.4	4	46	76	460	$9\ 10^{-2}$	16	2.2	19	17	20	0.076	
		10				$7\ 10^{-1}$	82	2.2	18	17	24	0.092	
	1.5	4				$6\ 10^{-3}$	32	2.6	51	42	38	0.14	0.8
		33				$4\ 10^{-1}$	1409	2.6	45	43	58	0.22	
Extended	10	0.1	76	152	400	$2\ 10^{-6}$	0.4	2.5	210	130	42	0.10	2.0
		1				$2\ 10^{-4}$	22.2	2.5	180	130	69	0.17	4.0
		10				$2\ 10^{-2}$	1336	2.5	160	130	110	0.27	4.8
	100	1				$2\ 10^{-6}$	75	3.4	980	600	200	0.50	11.0
	1000	1				$2\ 10^{-8}$	255	4.6	5400	2800	600	1.5	34

The differences in predicted power requirements for the equations are tremendous. The ratio between the lowest and the highest prediction ranges from 30 to 5000.

Our assumption, that the level of Weisser's equation is correct for his operating conditions and the level of Trommelen's equation is correct for his operating conditions, leads us to the following conclusions about the viscosity exponent.

(1) 0.66 is too low. The equations of Weisser (1972) and Trommelen and Beek (1971b) have an exponent of about 0.66 and these equations predict too small changes in power requirements due to changes in viscosity.

(2) 1.0 is about right. The equation of Leung (1966) has an exponent of 1.0 and this equation predicts fairly consistently values ten times too high.

(3) 1.2 is too high. The equations of Dinglinger (1964) and Skelland and Leung (1962) have exponents higher than 1.2 and their equations predict far too high values at high viscosity values.

Trommelen and Boerema (1966) found the blade resistance to be far greater than the resistance from the rotating flow in the annulus. Our calculations predict this ratio to be about 20:1. Thus, the design of the blades are of primary importance in the laminar flow regime. Toh and Murakami (1982a,b) have investigated this problem. However, in other investigations the information on blade design is not detailed enough. Differences in blade design may be one reason for the tremendous differences reported.

Thus, for a given blade design, Ne seems to be proportional to Re_r^{-1} at laminar flow in a SSHE.

The only experimental conditions in Table 10, which covers radius ratios from 0.75 to 0.9 is Trommelen and Beek (1971b). Their equation is the only equation in Table 10 which considers the size of the gap. They predict that the power increases as the gap decreases.

Vortex Flow. The results from our calculations on vortex flow conditions are presented in Table B2.

The differences between the equations are sometimes small and sometimes very big. However, the power required to maintain the vortices is always less and sometimes far less than predicted by the other equations. Thus, the blade design is the main factor controlling the power requirements also in the vortex flow regime.

The power requirements for most stirrers can be described by

$$P = C\ N^2\ d_t^2\ 1\ \eta^2 \tag{B1}$$

TABLE B2. Evaluation of the power requirements for rotation at *vortex* flow in SSHEs. The following conditions were kept constant in the calculations: blades=2 and density=1000 kg/m^3. Ta_c was chosen from Table 2 for each radius and Re_{ax} presumed to be zero. The equations used are empirical (Table 10), analytical for viscous flow in an annulus without blades (Eq. 12) extended with the empirical equation for an annulus $Ne = C\ Re_r^{-0.5}$ when Ta greater than 1.4 Ta_c.

OPERATING CONDITIONS							PREDICTED POWER REQUIREMENTS						
Source	visc.	N	d_s	d_t	l	Ta/Ta_c	Weisser	Trommelen/Weisser	Skelland/Weisser	Dinglinger/Weisser	Leung/Weisser	annulus/Weisser Eq.12	annulus/Weisser $Re^{-0.5}$
	Pa s	rps	mm	mm	mm		Watts						
Weisser	0.001	0.075	80	162	350	130	0.0016	0.74	0.22	0.25	0.46		0.003
		0.2				930	0.0092	0.74	0.21	0.26	0.57		0.006
		0.75				13000	0.099	0.74	0.19	0.26	0.75		0.016
	0.01	0.075				1.3	0.0054	1.0	1.2	1.2	1.4	0.003	
		0.2				9.3	0.031	1.0	1.2	1.2	1.7		0.006
		0.75				130	0.33	1.0	1.1	1.2	2.2		0.016
Trommelen	0.1	4	46	76	460	1.4	7.7	1.9	6.8	6.8	10	0.004	
		10				8.9	40	1.9	6.5	6.9	12		0.076
		20				36	137	1.9	6.2	6.9	15		0.13
		33				97	335	1.9	6.0	7.0	16		0.18
	0.4	20				2.2	285	2.2	17	18	28	0.22	
		33				6.0	700	2.2	17	18	31		0.31

or in dimensionless numbers:

$$Ne = C\ Re_r^{-1} \tag{B1b}$$

Trommelen and Boerma (1966) and Trommelen and Beek (1971b) noticed that Ne increased when the viscosity decreased if Re_r was kept constant. Trommelen and Beek (1971b) explained this phenomenon with scraping effects in SSHEs.

We would like to suggest another explanation based on flow pattern effects. Assume that

$$P_{total} = P_{blades} + P_{vortex} \tag{B2}$$

The P_{vortex} is constant when Re_r is constant, see the analytical (Eq. 12) and empirical results (Donnelly and Simon 1968; van Lookeren Campagne 1966).

Assume that P_{blades} can be described with Eq. (B1). Combine this assumption with the definition of Re_r and keep Re_r, d_t and l constant while the viscosity changes and the result is:

$$P_{blades} = C_1 \eta^3 \tag{B3}$$

Combine Eq. (B2), constant $P_{vortex} = C_2$ and Eq. (B3) and the result is:

$$P_{total} = C_2 + C_1 \eta^3 \tag{B4}$$

Our calculations, Table (B2) indicate that P_{vortex} ranges from 5 to 15% of the experimental values for the operating conditions of Trommelen and Beek (1971b). If this is true, P_{vortex} cannot be ignored in comparison with P_{blades} and the P_{total} does not decline as rapidly as Eq. (B1) predicts when the viscosity decreases. The same conclusion expressed with dimensionless numbers becomes: Ne increases at constant Re_r when the viscosity decreases in a SSHE if P_{vortex} can not be ignored in comparison with P_{blades}.

LIST OF SYMBOLS

A	heat transfer area	m^2
a	$\lambda/\rho\ c_p$ thermal diffusivity	m^2s^{-1}
C, C_1, C_2, ...	constants	—
c_p	specific heat	$J\ kg^{-1}K^{-1}$
c_v/c_{max}	concentration ratio of solids in a suspension	—

D	axial dispersion coefficient	m^2s^{-1}
D_m	axial mass dispersion coefficient	m^2s^{-1}
D_t	axial thermal dispersion coefficient	m^2s^{-1}
d_s	shaft diameter	m
d_t	tube diameter	m
d_k	diameter of the cylinder described by the rotating blades	m
fa, fb, fn, fm	values of functions defined in Eq. (3a-d)	—
k	overall heat transfer coefficient	$W\ m^{-2}K^{-1}$
k'	heat transfer coefficient media + wall, see Eq. (8a)	$W\ m^{-2}K^{-1}$
l	length of annulus	m
M	mass flow rate	$kg\ s^{-1}$
m	mass flow density	$kg\ s^{-1}m^{-2}$
N	rotational velocity	rotation s^{-1}
n	number of blades	
P	power required to rotate shaft and blades	W
s	constant defined in Eq. (8b)	—
t	contact time	s
T	temperature	°C
T_1	fluid temperature at inner cylinder	°C
T_2	fluid temperature at heat transfer surface	°C
T_f	temperature freezing point	°C
T_{cm}	temperature cooling medium	°C
T_x	temperature at x, x = 0 at inlet, x = 1 at outlet	°C
T_i	temperature before inlet	°C
T_w	temperature at heat transfer wall	°C
v	average axial flow rate	$m\ s^{-1}$
z	point where "the first discernable ripple" occurs	m
α	surface heat transfer coefficient	$W\ m^{-2}K^{-1}$
$\alpha_{effective}$	surface heat transfer coefficient, effective	$W\ m^{-2}K^{-1}$
$\alpha_{surface}$	surface heat transfer coefficient, at the surface	$W\ m^{-2}K^{-1}$
γ	thermal expansion coefficient	K^{-1}
η	dynamic viscosity	Pa s
η_w	dynamic viscosity at wall	Pa s
λ	thermal conductivity	$W\ m^{-1}K^{-1}$
λ	wave length vortical flow	m

λ_c	critical vortical wavelength	m
ν	kinematic viscosity	m^2s^{-1}
ρ	density	$kg\ m^{-3}$

LIST OF DIMENSIONLESS NUMBERS

Bo	$v\ 1/D$	Bodenstein number
L		dimensionless length, defined in Eq. (2a)
Ne	$P/\rho\ N^3\ \eta\ d_k^4\ 1$	Newton number
Nu	$\alpha d_t/\lambda$	Nusselt number
Nu_{pr}		Nu from penetration theory with surface renewal (see Eq. 9a)
Pe	$v(d_t - d_s)/a$	Peclet number
Pr	$\eta c_p/\lambda$	Prandtl number
Pr_b		Pr in the bulk
Pr_w		Pr at the wall
Ray*	$\dfrac{Pr\gamma(T_2-T_1)(d_t-d_s)}{4\ d_s\ \ln(d_t/d_s)}$	modified Rayleigh number
Re_{ax}	$v(d_t - d_s)\rho/\eta$	axial Reynolds number
Re_r	$Nd_t^2\rho/\eta$	rotational Reynolds number
Re_{rc}		critical Re_r, laminar-Taylor vortex
Re_{rs}	$N\ d_k^2\rho/\eta_s$	Re_r with viscosity of suspension
Re_{rw}		Re_r with the viscosity at the wall
St	$\alpha\ A/M\ c_p$	Stanton number
T*	$\dfrac{T_f - T}{T_f - T_{cm}}$	dimensionless temperature
T_i^*		T* at inlet
T_e^*		T* at exit
Ta	$\dfrac{(2\pi N)^2(d_t - d_s)^3 d_s^2}{\nu^2\ 8(d_t + d_s)}$	Taylor number
Ta_c		critical Ta, laminar-Taylor vortex
Ta_w		critical Ta, Taylor vortex-Wavy vortex
Ta_{mw}		critical Ta, Wavy vortex-Modulated wavy vortex
Ta_z		critical Ta, for developing flow (see Eq. 2)

REFERENCES

AHLERS, G., CANNELL, D. S. and LERMA, M. A. D. 1983. Possible mechanism for transitions in wavy Taylor-vortex flow. Phys. Rev. A. *27*(2), 1225-1227.

ALZIARY DE ROQUEFORT, T. and GRILLAUD, G. 1978. Computation of Taylor vortex flow by a transient implicit method. Computers and Fluids *6*, 259-269.

ASTILL, K. N. 1964. Studies of the develping flow between concentric cylinders with the inner cylinder rotating. J. Heat Transfer *86*, 383-392.

AY, P., WENZLAU, H. and GRAMLICH, K. 1979. Zur Modellierung des Wärme- und Stofftransportes in Kratzkühlerkristallisatoren; Teil I: Wärmetransport. Chem. Tech. Leipzig *31*(7), 341-344.

AZOORY, S. and BOTT, T. R. 1970. Local heat transfer coefficients in a model "falling film" scraped surface exchanger. Can. J. Chem. Eng. *48*(4), 373-377.

BATESON, R. N. 1971. The effect of age distribution on aseptic processing. Chem. Eng. Progr. Symp. Ser. *67*(108), 44-52.

BECKER, K. M. and KAYE, J. 1962a. Measurements of diabatic flow in an annulus with an inner rotating cylinder. J. Heat Transfer *84*(5), 97-105.

BECKER, K. M. and KAYE, J. 1962b. The influence of a radial temperature gradient on the instability of fluid flow in an annulus with an inner rotating cylinder. J. Heat Transfer *84*(5), 106-110.

BERIS, A., ARMSTRONG, R. C. and BROWN, R. A. 1983. Perturbation theory for viscoelastic fluids between eccentric rotating cylinders. J. Non-Newton. Fluid Mech. *13*, 109-148.

BERIS, A., ARMSTRONG, R. C. and BROWN R. A. 1984. Finite element calculations of viscoelastic fluid flow between eccentric rotating cylinders. J. Rheol. *28*(4), 490-491.

BISCHOFF, K. B. and McCRACKEN, E. A. 1966. Tracer tests in flow systems. Ind. Eng. Chem. *58*(7), 18-31.

BJORKLUND, I. S. and KAYS, W. M. 1959. Heat transfer between rotating concentric cylinders J. Heat Transfer *81*, 175-186.

BLAISDELL, J. L. and ZAHRADNIK, J. W. 1959. Longitudinal temperature distribution in a scraped-surface heat exchanger. Food Technol. *13*(11), 659-662.

BOLANOWSKI, J. P. 1972. Technical advances in heat transfer aid cooling of peanut butter. Candy and Snack Industry *137*(2). 16, 18, 20, 21.

BOTT, T. R. and AZOORY, S. 1968. Scraped surface heat transfer with Unit Mesh scrapers. Brit. Chem. Eng. *13*, 130-132.

BOTT, T. R., AZOORY, S. and PORTER, K. E. 1968a. Scraped-surface heat exchanger. Part 1. Hold up and residence time studies. Trans. Inst Chem. Engrs. *46*, T33-36.

BOTT, T. R., AZOORY, S. and PORTER, K. E. 1968b. Scraped-surface heat exchanger. Part 2. The effects of axial dispersion on heat transfer. Trans. Inst. Chem. Engrs. *46*, T37-42.

BOTT, T. R. and NAIR, B. 1969. The behaviour of some pseudoplastic solutions in "scraped film" heat transfer equipment. The Chemical Engineer *76*(232), CE361-62.

BOTT, T. R. and ROMERO, J. J. B. 1963. Heat transfer across a scraped surface. Can. J. Chem. Eng. (Oct.), 213-219.

BOTT, T. R. and ROMERO, J. J. B. 1966. The characteristic dimension in scraped surface heat transfer. Can. J. Chem. Eng. (Aug.), 226-230.

BOTT, T. R. and SHEIKH, M. R. 1966. Evaporation at a scraped surface. Chem. Eng. Progr. Sym. Ser. *62*(64), 97-103.

BURKHALTER, J. E. and KOSCHMIEDER, E. L. 1973. Steady supercritical Taylor flows. J. Fluid Mech. *58*(3), 547-560.

CHEN, A. C. Y. and ZAHRADNIK, J. W. 1967. Residence time distribution in a swept surface heat exchanger. Trans. ASAE *10*(4), 508-511.

CHUNG, K. C. and ASTILL, K. N. 1977. Hydrodynamic instability of viscous flow between rotating coaxial cylinders with fully developed axial flow. J. Fluid Mech. *81*(4), 641-655.

COLE, J. A. 1974a. Taylor vortices with short rotating cylinders. J. Fluids Eng. *96*, 69-70.

COLE, J. A. 1974b. Taylor vortex behaviour in annular clearances of limited length. Proc. Australasian Conf. Hydraulics and Fluid Mech., 5th, 514-521.

COLE, J. A. 1976. Taylor-vortex instability and annulus-length effects. J. Fluid Mech. *75*(1), 1-15.

COLE, J. A. 1981. Wavy vortex onset and cylinder radius ratio. In Proc. 2nd Taylor vortex flow working party, pp. 11-12, (Tufts University, Medford, Mass.).

COLE, J. A. 1983. The effect of cylinder radius ratio on wavy vortex onset. In Proc. 3rd Taylor vortex flow working party (Nancy), pp.1-4.

COLES, D. 1965. Transition in circular Couette flow. J. Fluid Mech.*21*(3), 385-425.

CONEY, J. E. R. and SIMMERS, D. A. 1979. A study of fully-developed, laminar, axial flow and Taylor vortex flow by means of shear stress measurements. J. Mech. Eng. Sci. *21*(1), 19-24.

CROOCKEWIT, P., HONIG, C. C. and KRAMERS, H. 1955. Longitudinal diffusion in liquid flow through an annulus between a stationary outer cylinder and a rotating inner cylinder. Chem. Eng. Sci. *4*(3), 111-118.

COOPER, E. R., JANKOWSKI, D. F., NEITZEL, G. P. and SQUIRE, T. H. 1985. Experiments on the onset of instability in unsteady circular Couette flow. J. Fluid Mech. *161*, 97-113.

CUEVAS, R., CHERYAN, M. and PORTER V. L. 1982. Performance of a Scraped-Surface Heat Exchanger under ultra high temperature conditions: A Dimensional Analysis. J. Food Sci. *47*, 619-625, 641.

CUEVAS, R. and CHERYAN, M. 1982. Heat transfer in a vertical, liquid-full scraped-surface heat exchanger — application of the penetration theory and Wilson plots models. J. Food Process Eng. *5*(1), 1-21.

DANCKWERTS, P. V. 1953. Continuous flow systems. Chem. Eng. Sci. *2*(1), 1-13.

DAVEY, A., DI PRIMA, R. D. and STUART, J. T. 1968. On the instability of Taylor vortices. J Fluid Mech. *31*(1), 17-52.

DINGLINGER, G. 1964. Die Wärmeübertragung im Kratzkühler. Kältetechn. *16*(6), 170-175.

DI PRIMA, R. C. and EAGLES, P. M. 1977. Amplification rates and torques for Taylor-vortex flows between rotating cylinders. Phys. Fluids *20*, (2)171-175.

DI PRIMA, R. C. and PRIDOR, A. 1979. The stability of viscous flow between rotating concentric cylinders with an axial flow. Proc. Roy. Soc. London, Ser. A *366*, 555-573.

DI PRIMA, R. C. and SWINNEY, H. L. 1981. Instabilities and transition in flow between concentric rotating cylinders. In *Hydrodynamic Instabilities and the Transition to Turbulence*, (Swinney and Gollub, ed.). pp. 139-180, Springer, Berlin, Heidelberg, New York.

DONNELLY, R. J. 1958. Experiments on the stability of viscous flow between rotating cylinders. I. Torque measurements. Proc. Roy. Soc. London, Ser. A 246, 312-325.

DONNELLY, R. J. and SIMON, N. J. 1960. An empirical torque relation for supercritical flow between rotating cylinders. J. Fluid Mech. *7*, 401-418.

EAGLES, P. M. 1971. On stability of Taylor vortices by fifth-order amplitude expansions. J. Fluid Mech. *49*(3), 529-550.

FENSTERMACHER, P. R., SWINNEY, H. L. and GOLLUB, J. P. 1979. Dynamical instabilities and the transition to chaotic Taylor vortex flow. J. Fluid Mech. *94*(1), 103-129.

GHOSAL, J. K., SRIMANI, B. N. and GNOSH, D. N. 1967. Study of the heat transfer rate in a steam-heated Votator. Indian Chem. Eng. *9*(2), T53-58.

GORMAN, M. and SWINNEY, H. L. 1982. Space-time symmetry in doubly periodic circular Couette flow. NATO Adv. Study Inst. Ser., Ser. B 77, 295-301.

GRAVAS, N. and MARTIN, B. W. 1978. Instability of viscous axial flow in annuli having a rotating inner cylinder. J. Fluid Mech. *86*(2), 385-394.

GU, Z. H. and FAHIDY, T. A. 1985a. Visualization of flow patterns in axial flow between horizontal coaxial rotating cylinders. Canadian J. Chem. Eng. *63*, 14-21.

GU, Z. H. and FAHIDY, T. Z. 1985b. Characteristics of Taylor vortex structure in combined axial and rotating flow. Canadian J. Chem. Eng. *63*, 710-715.

HAASON, M. A. and MARTIN, B. W. 1977. The stability of viscous axial flow in an annulus with rotating inner cylinder. Proc. Roy. Soc. London, Ser. A 352, 351-380.

HARRIOTT, P. 1959. Heat transfer in scraped-surface exchangers. Chem. Eng. Progr. Symp. Ser. *54*(29), 137-139.

HIGBIE, R. 1935. The rate of absorption of a pure gas into a still liquid during short periods of exposure. Trans. AIChE *31*, 365-389.

HO, C. Y., NARDACCI, J. L. and NISSAN, A. H. 1964. Heat transfer characteristics of fluids moving in a Taylor system of vortices. A.I.Ch.E. J. *10*(2), 194-202.

HOULTON, H. G. 1944. Heat transfer in the Votator heat exchanger. Ind. Eng. Chem. *36*(6), 522-528.

HÄRRÖD, M. 1982. Scraped surface heat exchanger. Literature and market survey. Unpublished observations.

HÄRRÖD, M. and MAINGONNAT, J. F. 1984. Performance of scraped surface heat exchangers. In Thermal Processing and Quality of Foods, (P. Zeuthen *et al.*, eds.), pp. 318-323, Elsevier, London.

JACKSON, P. A., ROBATI, B. and MOBBS, F. R. 1977. Secondary flows between eccentric rotating cylinders at subcritical Taylor numbers. In *Superlaminar Flow in Bearings*, pp.9-14. Proc. 2nd Leeds-Lyon Symp. on Tribology 1975. (Inst. Mech. Engrs., London).

JONES, C. A. 1985. The transition of wavy Taylor vortices. J. Fluid Mech. *157*, 135-162.

KAMEL, M. T. 1985. Flow of a polar fluid between two eccentric rotating cylinders. J. Rheol. *29*(1), 37-48.

KATAOKA, K., DOI, H., HONGO, T. and FUTAGAWA, M. 1975. Ideal plug flow properties of Taylor vortex flow. J. Chem. Eng. Japan *8*(6), 472-476.

KATAOKA, K., DOI, H. and KOMAI, T. 1977. Heat/mass transfer in Taylor-vortex flow with constant axial flow rates. Intern. J. Heat Mass Transfer *20*, 57-63.

KERN, D. Q. and KARAKAS, H. J. 1959. Mechanically aided heat transfer. Chem. Eng. Progr. Symp. Ser. *29*, 141-148.

KING, G. P. and SWINNEY, H. L. 1983. Limits of stability and irregular flow patterns in wavy vortex flow. Phys. Rev. A. *27*(2), 1240-1243.

KING, G. P., LI, Y., LEE, W., SWINNEY, H. L. and MARCUS, P. S. 1984. Wave speeds in wavy Taylor-vortex flow. J. Fluid Mech. *141*, 365-390.

KIRCHGÄSSNER, K. and SORGER, P. 1969. Branching analysis for the Taylor problem. Quart. J. Mech. Appl. Math. *22*(2), 183-209.

KOHLI, R. K. and SARMA, S. C. 1983. Application of scraped surface heat exchanger for making Ghee. Trans. ASAE *26*(4), 1271-1274.

KOOL, J. 1958. Heat transfer in scraped vessels and pipes handling viscous materials. Trans. Inst. Chem. Engrs. *36*, 253-258.

KOSCHMIEDER, E. L. 1979. Turbulent Taylor vortex flow. J. Fluid Mech. *93*(3), 515-527.

LATINEN, G. A. 1959. Discussion of the paper "Correlation of scraped film heat transfer in the Votator" (A. H. Skelland). Chem. Eng. Sci. *9*(4), 263-266.

LEGRAND, J., COEURET, F. and BILLON, M. 1983. Struture dynamique et transfert de matière liquide-paroi dans le cas do l'écoulement laminaire tourbillonnaire de Couette-Poiseuille. Intern. J. Heat Mass Transfer *26*, 1075-1085.

LEGRAND, J. and COEURET, F. 1986. Circumferential mixing in one-phase and two-phase Taylor vortex flows. Chem. Eng. Sci. *41*(1), 47-53.

LEUNG, L. S. 1967. Power consumption in a scraped surface heat exchanger. Trans. Inst. Chem. Engrs. *45*(5), T179-81.

LEVENSPIEL, O. 1972. *Chemical Reaction Engineering*. 2nd ed. John Wiley & Son, New York.

LEVENSPIEL, O. 1979. Chemical Reactor Omnibook. OSU Book Stores, Corvallis, Oregon.

LINEBERRY, D. D. 1970. The application of scraped surface heat exchangers with eccentrically mounted shafts. Dairy and Food Eng. Conf. Proc. Mich. St. Univ. 18th Ann., 159-173.

LORENZEN, A., PFISTER, G. and MULLIN, T. 1982. End effects on the transition to time-dependent motion in the Taylor experiment. Phys. Fluids *26*, 10-13.

LUSTENADER, E. L., RICHTER, R. and NEUGEBAUER, F. J. 1959. The use of thin films for increasing evaporation and condensation rates in process equipment. J. Heat Transfer *81C*, 297-307.

LÜCKE, M., MIHELCIC, M. and WINGERATH, K. 1984a. Propagation of Taylor vortex fronts into unstable circular couette flow. Phys. Rev. L. *52*(8), 625-628.

LÜCKE, M., MIHELCIC, M., WINGERATH, K. and PFISTER, G. 1984b. Flow in a small annulus between concentric cylinders. J. Fluid Mech. *140*, 343-353.

MAINGONNAT, J. F.and CORRIEU, G. 1983. A Study of the thermal performance of a scraped-surface heat exchanger. Part II. The effect of the axial diffusion of heat. Entropie, *19*(111), 37-49. Translated to English in Intern. Chem. 1986.*26*(1),55-68.

MAINGONNAT, J. F. and CORRIEU, G. 1984. A new approach to modelling the thermal behaviour of a scraped surface heat exchanger. In *Engineering and Food*, Vol. 1, (McKenna, ed.) pp. 79-88, Elsevier.

MAINGONNAT , J. F., BENEZECH, T. and CORRIEU, G. 1985. Performances thermiques d'un échangeur de chaleur à surface raclée traitant des produits alimentarires newtoniens et non newtoniens. Rev. Gén. Therm. Fr. No 279 (mars), 299-304.

MARCUS, P. S. 1984. Simulation of Taylor-Couette flow. Part 2. Numerical results for wavy-vortex flow with one travelling wave. J. Fluid Mech. *146*, 65-113.

MARTIN, B. W. and PAYNE, A. 1972. Tangential flow development for laminar axial flow in an annulus with a rotating inner cylinder. Proc. Roy. Soc. London, Ser. A 328, 123-141.

MILTON, J. L. and ZAHRADNIK, J. W. 1973. Residence time distribution of a votator pilot plant using a non newtonian fluid. Trans. ASAE *16*(6), 1186-1189.

MIYASHITA H. and HOFFMAN, T. W. 1978. Local heat transfer coefficients in scraped-film heat exchanger. J. Chem. Eng. Japan *11*, 444-450.

MIYAUCHI, T. and VERMEULEN, T. 1963. Longitudinal dispersion in two phase continuous flow operations. I & EC Fund. *2*(2), 113-126.

MULLIN, T., PFISTER, G. and LORENZEN, A. 1982. New observations on hysteresis in Taylor-Couette flow. Phys. Fluids *25*(7), 1134-1136.

NAKAYA, D. 1975. The second stability boundary for circular Couette flow. J. Phys. Soc. Japan *38*(2), 576-585.

NARASIMHAN, M. N. L. and GHANDOUR, N. N. 1982. Taylor stability of a thermoviscoelastic fluid in Couette Flow. Intern. J. Eng. Sci. *20*(2), 303-309.

NG, B. S. and TURNER, E. R. 1982. On the linear stability of spiral flow between rotating cylinders. Proc. Roy. Soc. London, Ser. A 382, 83-102.

NIKOLAJEW, L. K. 1967. Heat transfer in horizontal scraped surface heat exchanger. Pistschew. Tech. *4*, 146-147.

PAYNE, A. and MARTIN, B. W. 1974. Heat transfer to laminar axial flow in concentric annulus from a rotating inner cylinder. Proc. 5th Intern. Heat Transfer Conf. Japan Soc. Mech. Engrs. and Soc. Chem. Engrs. Japan, Heat transfer 1974, II (FC2.7), 80-84.

PENNEY, W. R. and BELL, K. J. 1967a. Close-clearence agitators. Part 1. Power requirements. Ind. Eng. Chem. *59*(4), 40-46. Corrections in *59*(6), 17.

PENNEY, W. R. and BELL, K. J. 1967b. Close-clearence agitators. Part 2. Heat transfer coefficients. Ind. Eng. Chem. *59*(4), 47-54.

PENNEY, W. R. and BELL, K. J. 1969a. Heat transfer in a thermal processor agitated with a fixed clearence thin, flat blade. Chem. Eng. Progr. Symp. Ser. *65*(92), 1-11.

PENNEY, W. R. and BELL, K. J. 1969b. The effect of back mixing on the mean temperature difference in an agitated heat exchanger. Chem. Eng. Progr. Symp. Ser. *65*(92), 21-33.

RAMDAS, V., UHL, V. W., OSBORNE, M. W. and ORTT, J. R. 1977. Heat transfer to viscous materials in a continuous-flow, scraped-wall, commercial-size heat exchanger. A. I. Ch. E. Nat. Heat Transfer Conf., 24-31.

ROBERTS, P. H. 1965. Appendix in Experiments on the stability of viscous flow between rotating cylinders. VI. Finite-amplitude experiments. Proc. Roy. Soc. London, Ser. A 283, 531-556.

ROSABAL, Kh. M., DOMANSKII, I. V. and SHISHKIN, A. V. 1982a. Retentivity of rotary apparatus with sectioned blades. Communication II. Zh. Prikl. Khim. *55*(4), 845-850.

ROSABAL, Kh. M., DOMANSKII, I. V. and SHISHKIN, A. V. 1982b. Heat transfer in a vertical rotary apparatus with hinged sectioned blades. Communication III. Zh. Prikl. Khim. *55*(5), 1077-80.

SASTRY, V. U. K. and DAS, T. 1985. Stability of Couette flow and Dean flow in micropolar fluids. Intern. J. Eng. Sci. *23*(11), 1163-1177.

SCHWARZ, K. W., SPRINGETT, B. E. and DONNELLY, R. J. 1964. Modes of instability in spiral flow between rotating cylinders. J. Fluid Mech. *20*(2), 281-289.

SIMMERS, D. A. and CONEY, J. E. R. 1979a. The effect of Taylor vortex flow on the development length in concentric annuli. J. Mech. Eng. Sci. *21*(2), 59-64.

SIMMERS, D. A. and CONEY, J. E. R. 1979b. A Reynolds analogy solution for the heat transfer characteristics of combined Taylor vortex and axial flows. Intern. J. Heat Mass Transfer *22*, 679-689.

SIMMERS, D. A. and CONEY, J. E. R. 1980. Velocity distributions in Taylor Vortex flow with imposed laminar axial flow and isothermal surface heat transfer. Intern. J. Heat Fluid Flow *2*, 85-91.

SKELLAND, A. H. P. 1958. Correlation of scraped-film heat transfer in the Votator. Chem. Eng. Sci. *7*(3), 166-175.

SKELLAND, A. H. P. and LEUNG, L. S. 1962. Power consumption in a scraped-surface heat exchanger Brit. Chem. Eng. *7*(4), 264-267.

SKELLAND, A. H. P., OLIVER, D. R. and TOOKE, S. 1962. Heat transfer in a water cooled scraped-surface heat exchanger. Brit. Chem. Eng. *7*(5), 346-353.

SMITH, G. P. and TOWNSEND, A. A. 1982. Turbulent Couette flow between concentric cylinders at large Taylor numbers. J. Fluid Mech. *123*, 187-217.

SNYDER, H. A. 1962. Experiments on the stability of spiral flow at low axial Reynolds numbers Proc. Roy. Soc. London, Ser. A 265, 198-214.

SNYDER, H. A. 1965. Experiments on the stability of two types of spiral flow. Annals of Physics *31*, 292-313.

SNYDER, H. A. 1969a. Wavenumber selection at finite amplitude in rotating Couette flow. J. Fluid Mech. *35*(2), 273-298.

SNYDER, H. A. 1969b. Change inf waveform and mean flow associated with wavelength variations in rotating Couette flow. J. Fluid Mech. *35*(2), 337-352.

SNYDER, H. A. 1970. Waveforms in rotating Couette flow. Intern. J. Nonlinear Mech. *5*, 659-685.

SNYDER, H. A. and LAMBERT, R. B. 1966. Harmonic gereration in Taylor vortices between rotating cylinders. J. Fluid Mech. *26*(3), 545-562.

SOROUR, M. M. and CONEY, J. E. R. 1979. An experimental investigation of the stability of spiral vortex flow. J. Mech. Eng. Sci. *21*(6), 397-402.

SPARROW, E. M. and LIN, S. H. 1964. The developing laminar flow and pressure drop in the entrance region of annular ducts. J. Basic Eng. *86*, 827-834.

SPARROW, E. M., MUNRO, W. D. and JONSSON, V. K. 1964. Instability of the flow between rotating cylinders: the wide gap problem. J. Fluid Mech. *20*(1), 35-46.

SUEMATSU, Y., ITO, T. and MUKAI, R. 1981. Two dimensional flow between Eccentric rotating cylinders. Bull. JSME Japan Soc. Mech. Engrs. *24*(197), 1928-1937.

SÝKORA, S., NÁVRATIL, B. and KÁRASEK, O. 1968. Heat transfer on scraped walls in the laminar and transitional regions. Collection Czech. Chem. Commun. *33*(2), 518-528.

TAKEUCHI, D. I. and JANKOWSKI, D. F. 1981. A numerical and experimental investigation of the stability of spiral Poiseuille flow. J. Fluid Mech. *102*, 101-126.

TAYLOR, G. I. 1923. Stability of a viscous fluid contained between two rotating cylinders. Phil Trans. Roy. Soc. London, Ser. A 223, 289-343.

TOH, M. and MURAKAMI, Y. 1982a. Effect of scraping angle, or thichness or tip angle of blades on power consumption of a fluid-loaded hinged scraper blade. J. Chem. Eng. Japan. *15*(3), 242-244.

TOH, M. and MURAKAMI, Y. 1982b. Power consumption of a fluid-loaded floating scraper blade. J. Chem. Eng. Japan *15*(6), 493-495.

TROMMELEN, A. M. and BOEREMA, S. 1966. Power consumption in a scraped-surface heat exchanger Trans. Inst. Chem. Engrs. *44*(9), T329-334.

TROMMELEN, A. M. 1967. Heat transfer in a scraped surface heat exchanger. Trans. Inst Chem. Engrs. *45*(5), T176-178.

TROMMELEN, A. M. 1970. Physical aspects of scraped-surface heat exchangers. Ph D Thesis at UNI Delft.

TROMMELEN, A. M. and BEEK, W. J. 1971a. Flow phenomena in a scraped-surface heat exchanger. Chem. Eng. Sci. *26*(11), 1933-1942.

TROMMELEN, A. M. and BEEK, W. J. 1971b. The mechanism of power consumption in a Votator-type scraped-surface heat exchanger. Chem. Eng. Sci. *26*(12), 1977-1986.

TROMMELEN, A. M, BEEK, W. J. and VAN DE WESTELAKEN, H. C. 1971. A mechanism for heat transfer in a Votator-type scraped-surface heat exchanger. Chem. Eng. Sci. *26*(12), 1987-2001.

UHL, V. W. and GRAY, J. B. 1966. *Mixing — Theory and Practice*, Vol. 1. Academic Press, New York and London.

VAN BOXTEL, L. B. J. and DE FIELLIETTAZ GOETHART, R. L. 1984. Heat transfer to water and some highly viscous food systems in a water-cooled scraped surface heat exchanger. J. Food Process Eng. *7*(1), 17-35.

VAN LOOKEREN CAMPAGNE, N. 1966. Longitudinal dispersie in de stroming door een ringspleet met draaiende binnencilinder. Ph D Thesis Groningen.

VOGT, C. W. 1930. (to Vogt Instant Freezers Inc.) USA Pat. 1, 783, 685, appl. 17 III 1928, publ. 2 XII 1930.

WALGRAEF, D., BORCKMANS, P. and DEWEL, G. 1984. Onset of wavy Taylor vortex flow in finite geometries. Phys. Rev. A *29*(3), 1514-1519.

WALOWIT, J. 1963. The stability of Couette flow between rotating cylinders in the presence of a radial temperature gradient. Ph. D. Thesis, Rensselaer Polytechnic Institute, Troy, New York.

WALOWIT, J., TSAO, S. and DI PRIMA, R. C. 1964. Stability of flow between arbitrarily spaced concentric cylindrical surfaces including the effect of a radial temperature gradient. J. Appl. Mech. *31*, 585-593.

WAN, C. C. and CONEY, J. E. R. 1980. Transition Modes in Adiabatic spiral vortex flow in narrow and wide annular gaps. Intern. J. Heat Fluid Flow *2*(3), 131-138.

WEHNER, J. F. and WILHELM, R. H. 1956. Boundary conditions of flow reactor. Chem. Eng. Sci. *6*(1), 89-93.

WEINSTEIN, M. 1975. Linear and non-linear instability between two eccentric cylinders. Ph. D. thesis, University of London.

WEISSER, H. 1972. Untersuchungen zum Warmeubergang im Kratzkuhler. Ph D Thesis at Karlsruhe Universitat (T. H.)

WEN, C. Y. and FAN, L. T. 1975. Models for flow systems and chemical reactors. Marcel Dekker, New York.

WENZLAU, H., AY, P. and GRAMLICH, K. 1982. Zur Modellierung des Warme- und Stofftransportes in Kratzkuhlerkristallisatoren; Teil II: Stofftransport. Chem. Tech. Leipzig *34*(4), 179-182.

WHITE, R. R. and CHURCHILL, S. W. 1959. Experimental foundations of chemical engineering. A. I. Ch. E. J. *5*(3), 354-360.

YAMADA, Y. 1962. Resistance of flow through an annulus with an inner rotating cylinder. Bull. JSME Japan Soc. Mech. Engrs. *15*(18), 302-310.

MILK CONCENTRATION BY DIRECT CONTACT HEAT EXCHANGE

A. H. ZAIDA and S. C. SARMA

National Dairy Research Institute
Karnal, India

P. D. GROVER

Indian Institute of Technology
Delhi, India

and D. R. HELDMAN

National Food Processors Association
Washington, DC, USA

Accepted for Publication October 1, 1986

ABSTRACT

Milk was concentrated from 9% T.S. to 50% T.S. in batches by direct injection of hot air/nitrogen. The rates of evaporation were found satisfactory. Process was found energy efficient with thermal economy of 1.49 which approximates to that of a double effect evaporator. Inspite of high gas temperature (120 − 140°C) the bulk temperature of milk did not exceed 40°C which is advantageous from a nutritional view point. Lower processing temperature did not adversely affect the bacterial growth and it remained within permissible limit.

INTRODUCTION

Transfer of heat between two fluids can be achieved either through a metal barrier or by direct contact. The former is a conventional and

Journal of Food Process Engineering 9 (1986) 63-79. All Rights Reserved.

established method of heating. The other form of heat transfer is direct contact heat transfer (DCHT), where an immiscible fluid medium is injected directly in the form of tiny droplets or bubbles, through a continuous liquid phase. DCHT has been an active area of research in the past 3 decades owing to its following advantages. (1) Higher heat transfer coefficients which are due to the intense agitation of continuous phase and circulation within dispersed phase (drops or bubbles). (2) Efficient heat transfer under small temperature differentials. (3) Absence of scaling as high temperature heat transfer surface is eliminated. (4) Simple and inexpensive equipment which needs minimum maintenance. (5) Higher operational flexibility as interfacial heat transfer area can be altered substantially by changing the sparger design, which in turn changes the bubble/drop size.

Application of gas-liquid heat transfer is found to be of specific advantage in the processing of heat sensitive products. It is observed that by sparging of hot gases through liquids, the moisture content can be reduced appreciably at temperatures much below the liquid boiling point. In addition, the agitation associated with gas bubbling, maintains uniform liquid temperature, and thus prevents the localized overheating. Both these influences reduce the nutrient losses to a minimum during processing.

Initial developments in the field of DCHT were limited to liquid-liquid systems. Excellent reviews of the work on liquid-liquid direct contact heat transfer have been presented by Sideman and Shabtai (1964), Sideman (1966) and Kehat and Sideman (1970). Industrial application of DCHT has started with the development of water desalination plants (Wilke *et al.* 1963 and Sukhatme and Hurwitz 1964).

Available literature on gas-liquid heat transfer is limited. Initial reports were pertaining to the packed column (Peisakhov and Chartkov 1940; Turkhan and Zhideleve 1946; Mcadams *et al.* 1949 and Taecker and Hougen 1949) and foam apparatus (Mukhlenov and Tumarkina 1954, 1955). The experimental fluids for all the early studies were air and water. In early 1960's the heat transfer coefficients for bubbles originating at single orifice were estimated and simplified correlations, governing sensible heating were developed (Licht and Conway 1950; Heertjes *et al.* 1954 and Bhagde *et al.* 1973). A few researchers also studied the evaporation by direct sparging of hot gases. But their work was limited to water and steam/air systems (Schmidt 1977).

More detailed investigations on the machanism of heat transfer for sensible and latent heating was undertaken by Zaidi (1983). Large number of gas-liquid combinations were studied, and generalized correlations and models were developed.

The application of DCHT in food processing started with the work of Abichandani *et al.* (1978) and Zaidi *et al.* (1979), who studied the manufacture of ghee from butter by direct sparging of hot nitrogen. Milk being heat sensitive, is concentrated conventionally under vacuum. As the processing temperatures in DCHT are lower than the conventional evaporation temperature the product so obtained will have high nutritive value. However, the same may result in enhanced microbial growth. In addition the excessive agitation, resulting from DCHT may rupture to some extent the fat globule membrane and produce free fat. Both of the later effects if appreciable, could result in deterioration of the product quality.

A study of the concentration of milk by direct contact heat transfer was undertaken with the following objectives: (1) To determine the thermal economy for the process and its comparison with that of multiple effect evaporation. (2) To determine the bacterial growth rate during the process. (3) To estimate free fat formation in milk resulting from agitation during the heat exchange process.

THEORETICAL CONSIDERATIONS

Microbial growth is expected to be exponential in nature. Thus a plot of bacterial population on logarithmic scale vs time is usually a straight line. Such a growth can be mathematically expressed as:

$$\text{Log } N_F - \text{Log } N_0 = t/D \tag{1}$$

Where 't' is the time required for the population to increase from the initial population (N_0) to some population (N_F) at a later time.

The Eq. (1) is similar to the first order rate equation. Thus the microbial growth rate can be easily expressed by first order reaction rate constant (k). However, it is to be noted that the bacterial growth in an actual sense can not be described by first order reaction, since from kinetic theory, it is applicable only to monomolecular reactions. Nevertheless it provides a useful tool for representing the rate of bacterial multiplication and predicting the influence of various parameters on the same.

The energy efficiency of an evaporator is usually expressed by "thermal economy" (T.E.), which is defined as,

$$\text{T.E.} = \frac{\text{Quantity of water evaporated}}{\text{Quantity of steam consumed}} \tag{3}$$

The thermal economy of an evaporator increases with the increase in number of evaporator effects, because subsequent effects use vapor from the previous effect as the heating medium.

For evaporation by DCHT, the conventional definition of thermal economy is not applicable. For the purpose of comparison the economy for DCHT can be defined as:

$$\text{T.E.} = \frac{\text{Latent heat required for evaporation of water}}{\text{Heat supplied by the heating gas}} \tag{4}$$

Sparging of hot gases through liquid results in simultaneous evaporation and vaporization. The rate of vaporization (W_V) depends upon the mean difference in partial pressure of vapor between gas and liquid (Δpm) and the mass transfer coefficient (K). The rate of sensible heat transfer (qs) from gas depends upon the mean temperature difference between the gas and liquid (ΔTm) and heat transfer coefficient (U). Mathematically:

$$W_V = K\ A\ \Delta pm \tag{5}$$

$$\text{and } qs = U\ A\ \Delta Tm \tag{6}$$

Where 'A' is the interfacial area.

If W_E represents the rate of evaporation, and W_T the total rate of water transfer, then

$$W_T = W_V + W_E$$

For the transfer of vapor, from liquid phase to gas phase, the system needs latent heat, which usually is obtained at the expense of sensible heat of gas. When latent heat requirement is higher than the supply of sensible heat, the system consumes a part of sensible heat of liquid, too. In that case the liquid temperature drops till the steady state is achieved where the latent heat consumed equals the heat supplied by the gas.

For noninsulated systems, the drop in liquid temperature below ambient, may result in the flow of heat from surroundings to the system. A schematic diagram for such a system, showing mass and energy balance is presented in Fig. 1. The mass balance gives:

$$W_E + M_{G1} = M_{G2}$$

or

$$M_G(1 + h_1) = M_G(1 + h_2) - W_E$$

or

$$M_G(h_2 - h_1) = W_E \tag{7}$$

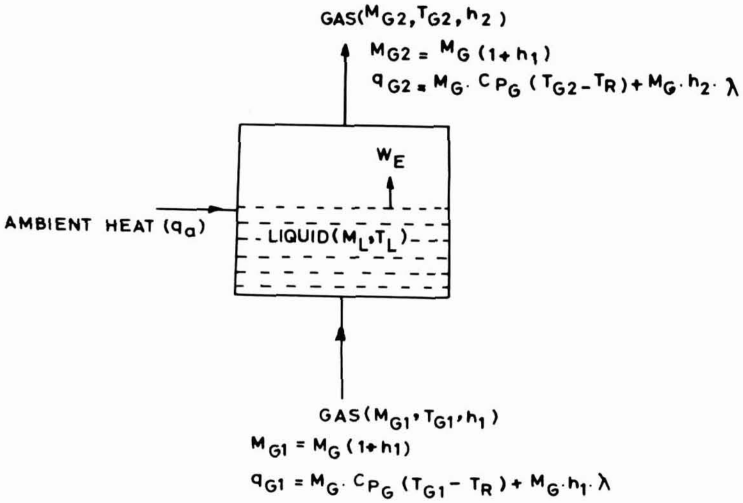

FIG. 1. MASS AND ENERGY BALANCE

From, heat balance

$$q_{G1} + q_a = q_{G2}$$

or
$$M_G \cdot Cp_G(T_{G1} - T_R) + M_G \cdot h_1 \cdot \lambda + q_a = M_G \cdot Cp_G \cdot (T_{G2} - T_R) + M_G \cdot h_2 \cdot \lambda$$

or
$$M_G \cdot Cp_G \cdot (T_{G1} - T_{G2}) + M_G \cdot \lambda(h_1 - h_2) + q_a = 0 \qquad (8)$$

or
$$M_G \cdot Cp_G \cdot (T_{G1} - T_{G2}) - W_E \cdot \lambda + q_a = 0$$

or
$$W_E \cdot \lambda = M_G \cdot Cp_G \cdot (T_{G1} - T_{G2}) + q_a$$

Thus, Thermal economy
$$= \frac{W_E \cdot \lambda}{M_G \cdot Cp_G \cdot (T_{G1} - T_{G2})}$$

$$= \frac{M_G \cdot Cp_G \cdot (T_{G1} - T_{G2}) + q_a}{M_G \cdot Cp_G(T_{G1} - T_{G2})}$$

$$= 1 + \frac{q_a}{q_G} \qquad (9)$$

Thus DCHT systems, where q_a is the sensible heat supplied by the gas, besides consuming the sensible heat of gas, may consume a part of ambient heat also. In that case the heat economy of DCHT systems will be greater than unity.

MATERIALS AND METHODS

The experimental set-up was designed for concentration of milk in batches. From economic considerations, it was decided to recycle the nitrogen. The basic requirements of the experimental apparatus were to have a regulated and measured quantity of hot gas and its recirculation after the condensation of entrained vapors, its recompression and reheating. A gas-liquid contactor with sparger and provision for temperature measurement was also needed. With the above requirements in mind, the apparatus shown, in Fig. 2, was developed.

The apparatus consisted of a glass column of 7.5 cm diameter and 33 cm length. The column was closed at both the ends using metallic cups having gaskets and secured in position by three vertical tie rods. Lateral openings were provided in the column for the insertion of thermocouples at proper locations. Sparger plates having 94 holes of 0.20 cm diameter drilled at 0.63 cm triangular pitch were provided in the lower cup.

The gas supply was maintained by a 2.0 HP, oil free, reciprocating compressor with 0.90 m^3 receiver and a pressure cut-off switch. A diaphragm-type pressure regulator was used at the receiver outlet to prevent variation in gas flow rate.

The gas heater consisted of a helical copper tube of sufficient length immersed in an oil bath having a wide temperature range (upto 300 °C) and proper temperature control.

The condenser used was a tube-in-tube type and was designed to operate with a small pressure drop. This was essential in order to protect the glass column from damage. A silicagel drying column was used to remove the traces of moisture from the hot gas before its recycling. Separate connections were provided for circulating hot gas through a drying column for the regeneration of drying gel at regular intervals.

Temperatures were measured by calibrated copper-constantan thermocouples. All thermocouples were connected to a digital millivoltmeter through a selector switch.

For the estimation of the rate constant for microbial growth (k) it was essential to maintain other parameters constant. The total solid concentration was maintained constant by recycling of condensate through the barometric leg. The experimental arrangement is shown in Fig. 3.

The preheated batches of milk with measured total solids (% TS) were placed in the glass column. Hot air/nitrogen (110 °-140 °C) was sparged through the product at the fixed flow rate (0.8×10^{-3} to 2.25×10^{-3} m^3/s). Milk samples were removed at regular intervals of 30 min and were analyzed by gravimetric method for % TS.

Bacterial populations were estimated by the determination of standard plate count (SPC). Both air and nitrogen were used as heating media. Trials

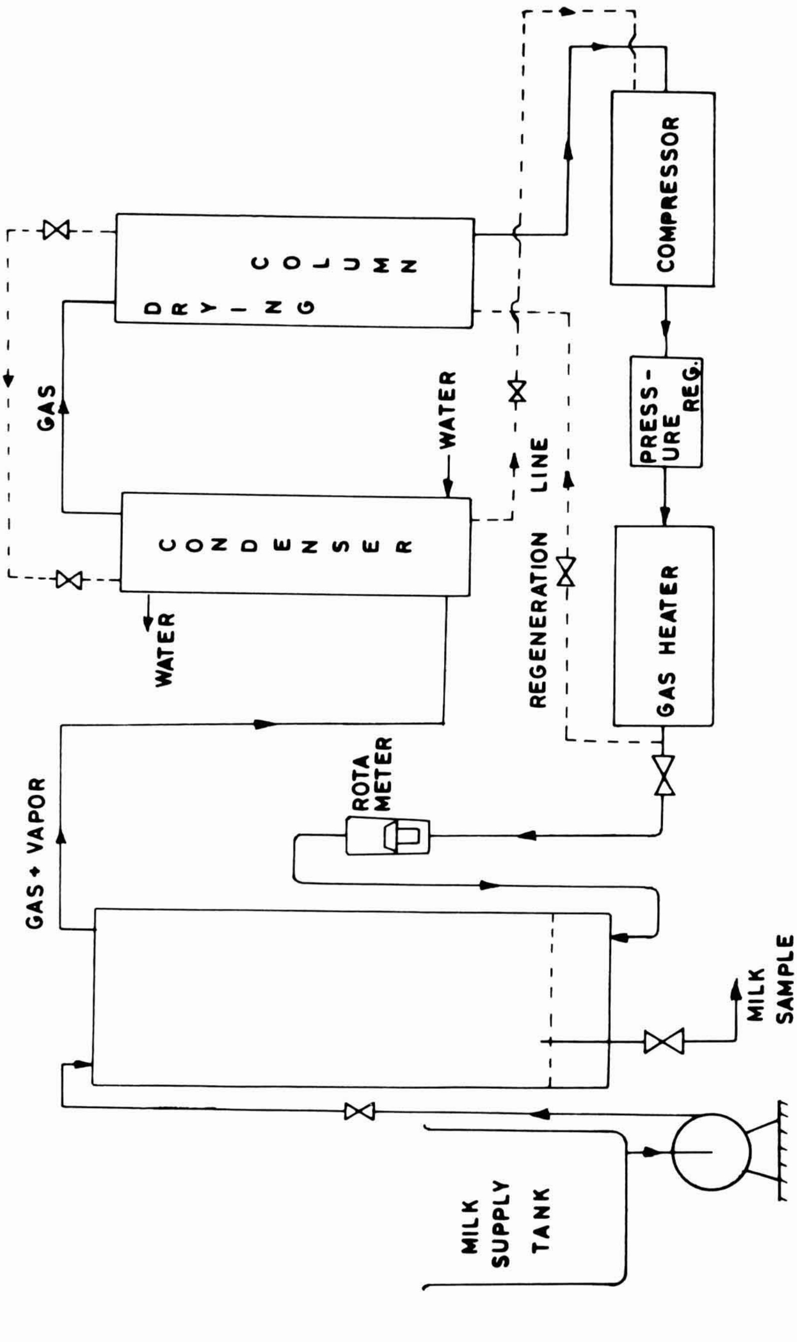

FIG. 2. SCHEMATIC FLOW DIAGRAM OF EXPERIMENTAL APPARATUS

with nitrogen provided an opportunity to study the bacterial growth in an oxygen free environment. Tryptone-dextrose-agar (TDA) was used as the plating media. Plates were incubated for 48 h both at 37 °C and 50 °C to determine the growth pattern of mesophilic and thermophilic bacteria. Before each trial the glass column was thoroughly cleaned by detergent, sanitizer and iodine bound disinfectant, and was dried by hot air. Swab tests were conducted to ensure cleanliness of the equipment. To investigate the effect of agitation on free fat formation, buffalo whole milk samples (6.1% fat) were subjected to gas sparging for various processing timings. Since the available procedure for the estimation of free fat is applicable only to milk powder, the samples were freeze dried and free fat in freeze dried powder was determined by the method of Hall and Hedrick (1971). The increase in free fat during processing was determined by comparison with unprocessed samples. Free fat in fluid milk was calculated from the values obtained for powder.

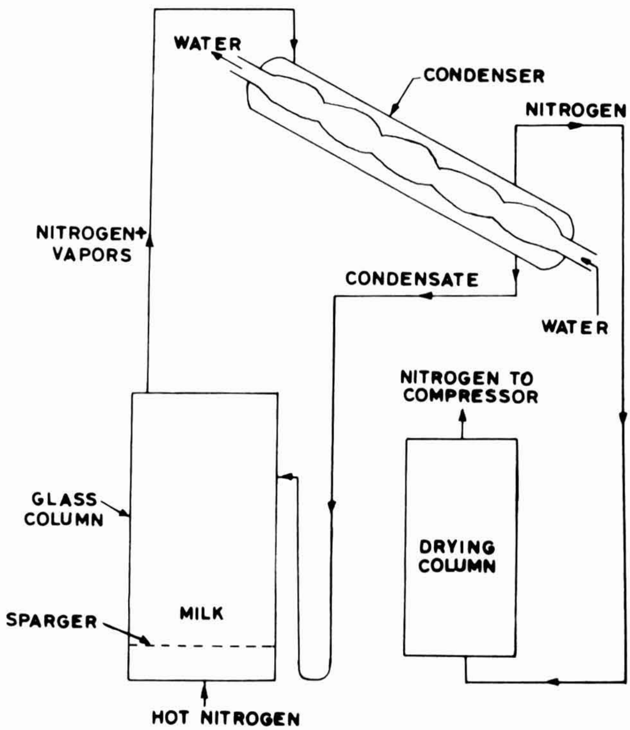

FIG. 3. CONDENSATE RECYCLING FOR BACTERIOLOGICAL STUDIES

RESULTS AND DISCUSSION

One of the objectives of our study was to determine the feasibility of milk concentration by DCHT and to estimate the thermal economy of the process. The results of five experiments conducted on milk concentration are presented in Table 1. Thermal economy was calculated by Eq. (4). The thermal economy was found to vary between 1.32 to 1.65 (mean 1.48), which is approximately equal to that of a double effect evaporator. The comparison shows that the process has a favorable energy efficiency.

Batch concentration of milk was studied. A concentration of 35% TS (generally required for spray drying) was obtained in 2 to 2.5 h with a gas flow rate of 7 kg/h per kg of raw milk. Although the sensible heat of gas is low, due to a low specific heat of gas, the evaporation rates obtained for the process are good. The reasons would include accompanied vaporization along with the evaporation, as explained earlier. Thus the process does not need high gas rates as usually required in gas heating systems.

During the process the bulk liquid temperature did not increase beyond 40 °C, which is much lower when compared to the temperatures in the vacuum pan and multiple effect evaporator (60 °-70 °C). Initially gas sparging resulted in slight increase in temperature if initial temperature of liquid was very low. On the contrary it resulted in quick initial drop in temperature, if the initial temperature of milk was sufficiently high. Subsequently the liquid pool stabilized at a temperature much lower than the boiling temperature of liquid. A typical time temperature plot for observations 1 & 2 of Table 1 is presented in Fig. 4. It is evident that after

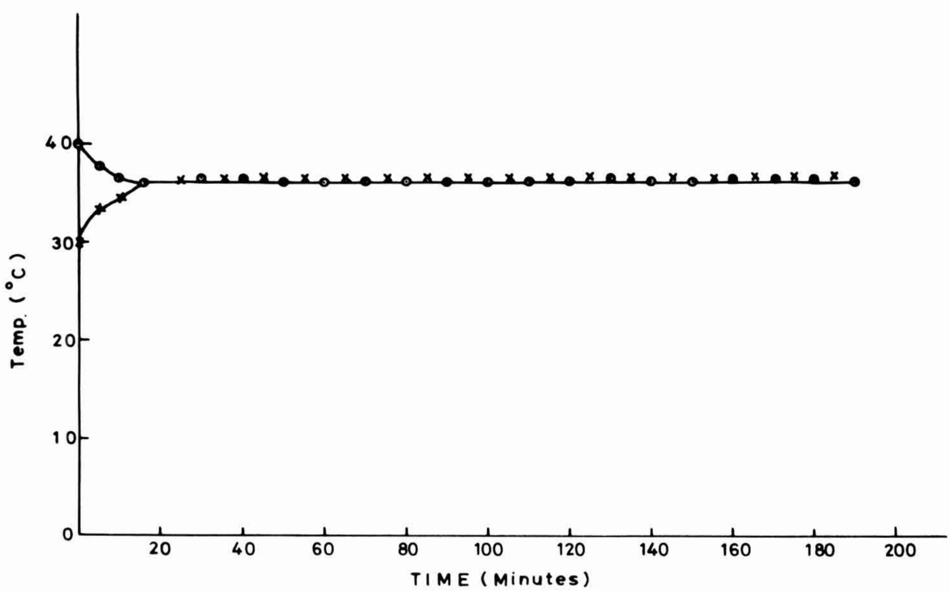

FIG. 4. TIME-TEMP. PLOT FOR MILK CONCENTRATION

X———X Observation 1, Table 1, Initial milk temp. 30 °C

⊙———⊙ Observation 2, Table 1, Initial milk temp. 40 °C

TABLE 1. Heat economy for evaporation by DCHT

S.No.	Milk			Air		% Total solids		Water evaporated	Heat economy
	Type	(Qty per batch) x 10^{-3} (m^3)	Temp. (°C)	(Flow rate) x 10^{-3}(m^3/sec.)	Temp. (°C)	Initial	After 2.0 hrs	in 2.0 hrs x 10^{-3} (m^3)	
1.	Skim	0.75	37.0	1.00	100.0	8.20	16.30	0.372	1.65
2	Skim	0.75	37.0	1.00	105.0	10.11	18.47	0.339	1.49
3	Skim	1.20	37.9	1.75	135.0	11.10	50.65	0.937	1.55
4	Skim	1.50	39.1	2.25	140.0	9.20	31.89	1.060	1.32
5	Whole Buffalo (5.8% fat)	0.50	38.0	0.80	109.0	12.10	28.59	0.288	1.40

initial adjustments, the major portion of heat supplied by the gas was picked up by the liquid in the form of latent heat. The following reasons are offered in support of this observation.

The introduction of hot gas into the liquid results in simultaneous heat and mass transfer through the gas film surrounding the gas bubble. Heat is transferred from gas to interface due to high gas temperature, causing evaporation. Since the vapor pressure is higher at the interface compared to partial pressure in the gas, the vapor diffuses into the bubble. Evaporation at bubble interface ceases when the gas gets saturated. If the bubble temperature still remains higher than the bulk liquid temperature after saturation then, some sensible heating of liquid may take place with the corresponding rise of liquid temperature. This temperature increase causes a vapor pressure increase which results in further evaporation. Thus the process of sensible heating if present would be quite slow. When liquid temperature is low enough to cause high temperature differentials and low pressure gradients some sensible heating occurs. However, the liquid attains a steady state in a short time, when the sensible heat supplied by the gas equals the heat required for evaporation.

Preliminary investigations indicated that the gas sparging through milk caused foaming. It was observed that the foaming could be suppressed by creating the back pressure. A back pressure of the order of 8 cm of mercury was found to be sufficient to arrest the foaming. In addition, the increase in system pressure was found to increase the bulk temperature. Thus in cases where processing at some higher temperature is desired due to bacteriological or other reasons, creation of additional back pressure might be useful.

During experiments, scaling was not observed on the sides of the glass column, but did occur on the sparger plate. Although milk deposits on the sparger plate do not reduce the heat transfer efficiency, it may cause difficulties in equipment cleaning. The sparger design could be improved by reducing the hole pitch, which in-turn would keep the blind area minimum.

Low temperature concentration of milk is advantageous from the view point of higher nutritional value but may result in higher bacterial populations. In this study investigation involved an estimation of bacterial growth rates to ascertain the quality deterioration due to bacterial growth. Bacterial growth rates for 12 milk samples, under various processing conditions are listed in Table 2. A plot betwween (N_F/N_0) versus time on semilog coordinates gave a straight line (Fig. 5). This confirms that the growth pattern is exponential as expected. The correlation coefficients (R^2) for various plots are also listed in Table 2 and are above 0.9 for most of the experiments.

TABLE 2. S. P. C. readings and rate constant for microbial growth

Sr. No.	Milk				Gas		Ratio of initial to final count (N_F/N_O) at					k (1/min)	R^2
	Type	T.S. %	Bulk temp (°C)	Initial count x 10^{-4}	Type	Temp (°C)	0.5 hr	1.0 hr	1.5 hr	2.0 hr	2.5 hr		
						CASE - A (WITH FIXED MILK CONCENTRATION)							
1.	Boiled	9.97	37.3	0.02	Air	100	9.30	100.0	112.5	147.5	207.50	2.005	0.797
2.	Pasteu-rized	8.89	37.0	1.90	Air	107	12.26	17.42	30.63	39.00	48.94	1.072	0.865
3.	-do-	22.0	37.6	2.50	Air	120	3.04	8.40	14.00	23.20	29.60	1.346	0.941
4.	-do-	35.53	37.0	2.60	Air	115	3.00	4.23	4.61	12.30	19.23	1.092	0.946
5.	-do-	50.90	40.0	1.80	Air	105	2.00	10.0	17.77	25.55	36.11	1.494	0.926
6.	-do-	9.13	37.4	0.18	Air	121	1.97	2.86	4.52	9.10	29.97	1.230	0.968
7.	Raw	14.18	38.3	1.20	Air	105	2.84	7.08	10.83	20.0	53.30	1.494	0.941
8.	-do-	8.82	38.0	16.00	N_2	109	1.12	1.375	1.47	1.72	1.81	0.247	0.969
9.	Pasteu-rized	8.93	37.0	0.50	N_2	115	1.06	1.160	1.40	1.84	2.32	0.346	0.984
10.	Raw	9.10	37.7	16.0	N_2	105	3.12	2.500	3.62	4.50	5.62	0.693	0.976
						CASE - B (WITH CHANGING CONCENTRATION)							
11.	Boiled	9.0 - 18.9	37.5	0.002	Air	120	4.50	15.45	29.54	35.91	61.82	1.571	0.910
12.	Pasteu-rized	10.0 - 42.0	37.0	0.130	N_2	125	1.05	1.14	1.25	1.40	1.78	0.220	0.932

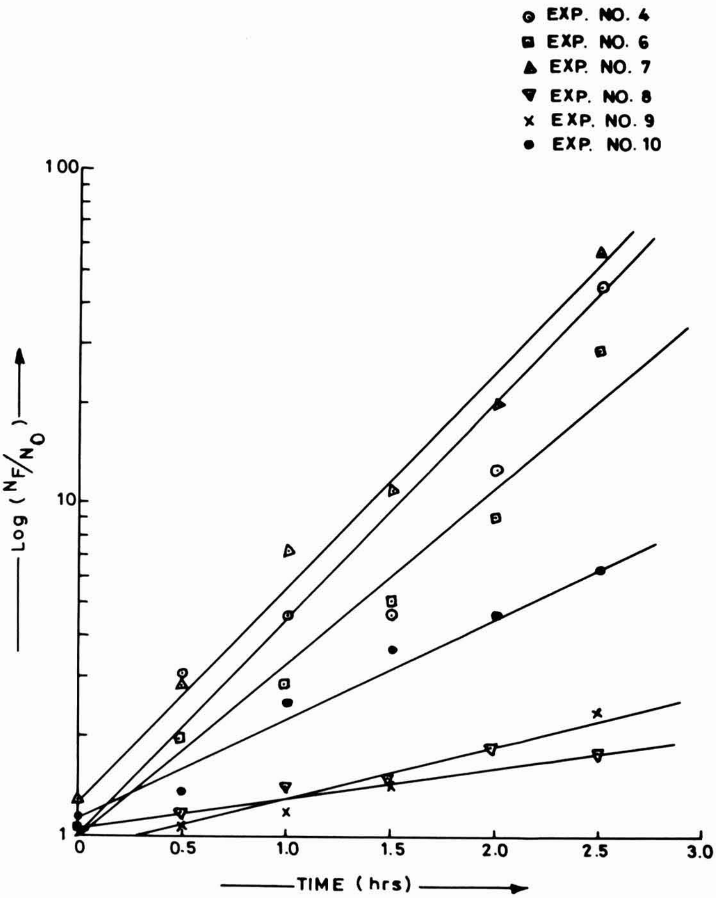

FIG. 5. EXPONENTIAL GROWTH OF MICROBES

As per the criterion suggested by IS-1479 (1960) pasteurized milk with SPC values below 30,000 is graded as good. Similarly raw milk with SPC values below one million is graded as good. It is observed from the table that the heating of both pasteurized and raw milk by nitrogen does not deteriorate its quality and it remains in the same grade, even after undergoing concentration for 2 h. Also the processing of pasteurized milk with air maintains the microbial growth within permissible range of good quality milk. Thus it is concluded that while heating raw milk, though nitrogen can be used, it is preferable to pasteurize the milk before its concentration.

First order rate constants (k), as obtained from an exponential curve, are listed in Table 2. From the values of rate constant the influence of various parameters affecting microbial growth may be summarized as follows: (1) It is observed that with the increase in gas temperature, the growth rate (or k value) decreases. This is revealed by comparison of k values for experiments 6 and 9, 8 and 9 and 9 and 10. The reason might be the higher lethal effect with gas at a higher temperature which results in the destruction of more bacteria at bubble interface before cooling. In the present study although the maximum gas temperature used was 140 °C, the use of higher temperatures up to 200 °C, as used in spray drying is recommended. This will also enhance the evaporation rate, reduce the gas-liquid ratio and simplify the gas handling operation. Comparison of k values for experiments 1 and 2 also indicate the same trend. However, in trial 1 the k value is much higher as compared to that in 2. This vast difference might be due to the additional influence of higher milk solids in experiment 1. (2) It is noted that with an increase in % TS in milk the k value or microbial growth rate increased, (compare trials 3 and 6 and 8 and 10). This must be associated with the higher nutrient content in the higher solids product, resulting in more rapid microbial growth. (3) Milk bacteria are usually aerobic in nature. Thus it was expected that the processing in oxygen free environment will retard the microbial growth. Appreciably lower k values (for experiments 8, 9, 10 and 12) for processing with nitrogen are observed in this study. A comparison between experiments No. 2 and 8 which are for identical conditions show that the k value for air is about 4 times higher compared to nitrogen. For experiment number 11 where the data were collected for increasing concentration, the k value is found to be much smaller (0.22). The reason for this might be the combined effect of processing by nitrogen and increase in milk solid concentration. (4) As the bulk temperature remained quite close for most of the trials, no specific effect of bulk temperature on microbial growth rate was observed.

The increase in free fat content of milk for various time intervals was estimated and is presented in Table 3. It was observed that free fat con-

TABLE 3. Increase in free fat content during processing

Sample Number	Processing time (min)	% Free fat in powder	% Free fat in milk
0	0	10.03	1.462
1	30	11.05	1.608
2	60	13.00	1.895
3	90	14.70	2.143
4	120	15.25	2.223
5	150	23.63	3.545

tent in milk increased from 1.46% to 3.54% in a duration of 2.5 h. This increase in free fat is appreciable and powder obtained from such high free fat milk would have reduced storage life. Thus it is recommended that milk after concentration by DCHT should be homogenized before, drying, if it is to be converted to powder.

CONCLUSIONS

Batch concentration of milk, by injection of hot noncondensible gases was studied in detail. Thermal economy of the process has been estimated and the average value was found as 1.48, which is close to that of a double effect evaporator. S.P.C. results do not show adverse microbial growth, inspite of low processing temperatures. Reaction rate constant for the bacterial growth were determined and the factors affecting the same are discussed.

However, since S.P.C. value is not the only parameter to establish the milk quality, it is recommended that some more trials like thermal stability test, alcohol test and sensory test may be conducted for the milk samples. Powder obtained from milk concentrated by DCHT may be studied for shelf-life also.

NOTATIONS

A = Interfacial area (m^2)
Cp = Specific heat (kcal/kg − °C)
D = Time for microbial growth by one log cycle (s)
h = humidity of gas (kg of vapor/kg dry air)
K = Mass transfer coefficient (kg moles/s-m^2-pascal)
k = rate constant for microbial growth
M = Mass flow rate (kg/s)
N = Microbial population
Δpm = Mean difference in partial pressure and the vapor pressure (Pascals)
q = rate of heat transfer (kcal/s)
T = Temperature (°C)
t = time for microbial growth (s)
ΔTm = Mean temperature difference between gas and liquid (°C)
U = Overall heat transfer coefficient (kcal/m^2-s-°C)
W = Rate of moisture removal (kg/s)
λ = latent heat of vaporization (kcal/kg)

SUFFIX

0 = Initial
1 = Inlet conditions
2 = Outlet conditions
G = Gas
E = Evaporation
F = Final conditions
R = Reference
S = Sensible heat
T = Total
V = Vaporization

REFERENCES

ABICHANDANI, H. and SARMA, S. C. 1978. Process feasibility of ghee making by direct contact heat exchange. J. Food Sci. Tech. (India), *15*, 5, 177.

BHAGDE, S. S., GIRADKAR, J. B. and MENE, R. S. 1973. Studies on heat transfer during bubble formation. Indian J. Technol. *11*, 281.

HEERTJES, P., HOLVE, W. A. and TALSMA, H. 1954. Transfer of heat to single originating bubbles. Chem. Eng. Sci. *3*, 122.

HALL, C. W. and HEDRICK, T. O. 1971. *Drying of Milk and Milk Products*. AVI Publishing Co., Westport, Conn.

KEHAT, E. and SIDEMAN, S. 1970. Heat transfer by direct liquid-liquid contact, recent advances in liquid-liquid extraction (C. Hanson, ed.) pp. 454-494. Pergamon Press, London.

LICHT, W. and CONWAY, C. J. B. 1950. Mechanism of solute transfer in spray towers. Ind. Eng. Chem. *42*, 1151.

MCADAMS, W. H., POHLENZ, J. B. and JOHN, R. C. 1949. Transfer of heat and mass between air and water in a packed tower. Chem. Eng. Prog. *45*, 4, 241.

MUKHLENOV, I. P. and TUMARKINA, E. S. 1954. Heat transfer in foam apparatus. J. Appl. Chem. USSR, *27*, 125.

MUKHLENOV, I. P. and TUMARKINA, E. S. 1955. heat transfer in foam aparatus-II. J. Appl. Chem. USSR, *28*, 323.

PIESAKHOV, I. L. and CHARTKOV, B. A. 1940. Analysis of packed columns. J. Chem. Ind. *9*, 211.

SCHIMDT, H. 1977. Bubble formation and heat transfer during dispersion of superheated steam in saturated water. Int. J. Heat Mass Trans. *20*, 6, 635.

SUKHATME, S. P. and HURWITZ, M. 1964. Heat transfer in the liquid-liquid spray tower, PB.166315, Office of Saline Water, U.S. Dept. of Interior, Washington, D.C.

SIDEMAN, S. and SHABTAI, H. 1964. Direct contact heat transfer between a single drop and an immiscible liquid medium. Canadian J. of Chem. Eng. *6*, 107.

SIDEMAN, S. 1966. Direct contact heat transfer between immiscible liquids. In, Advances in Chemical Engineering, Vol. 6, Academic Press, New York.

TAECKER, R. C. and HOUGEN, D. A. 1949. Heat and mass transfer from gas film in flow of gases through commerical tower packing. Chem. Eng. Prog. *45*, 3, 188.

TURKHAN, E. Y. and ZHIDELAVA, K. P. 1946. Analysis of packed towers, J. Chem. Ind. *11*, 6.

WILKE, C. R., CHENG, C. T., LEDESMA, V. L. and PORTE, J. W. 1963. Direct contact heat transfer for sea water evaporation. Chem. Eng. Prog. *59*, 12, 69.

ZAIDI, A. H., ABHICHANDANI, H. and SARMA, S. C. 1979. Lactose content and particle size distribution of ghee residue obtained from direct contact heat exchange. J. Food Sci. Tech. (India). *16*, 5, 217.

ZAIDI, A. H. 1983. Direct contact gas-liquid heat exchange. Ph.D. thesis, Indian Institute of Technology. N. Delhi (India).

TRANSPORTATION OF FROZEN FOOD IN INSULATED CONTAINERS — THEORETICAL AND EXPERIMENTAL RESULTS

G. S. MITTAL

School of Engineering
University of Guelph
Guelph, Ontario, N1G 2W1

and

K. L. PARKIN

Dept. of Food Science
University of Wisconsin
Madison, Wisconsin 53706

Accepted for Publication September 24, 1986

ABSTRACT

A study was conducted on the ability of two insulated containers to maintain the low temperature of ice cream in an ambient environment. A mathematical model was solved using Continuous System Modeling Program (CSMP) and finite difference technique to predict the temperature distribution in the product with time. The model predicted the temperature profiles within ±5% of the experimental data.

INTRODUCTION

During the regional distribution of frozen foods, difficulties arise that can lead to a substantial loss in quality of these products. During the partial unloading of goods at the initial destinations along a delivery route, subsequent and proper low temperature maintenance is made difficult due to the repeated opening of the refrigerated van doors, allowing exchange of warm air for chilled air inside the transport. Consequently, the refrigeration load is progressively increased as the delivery route is traversed and as a result, product temperature rises and its quality (or shelf-life) in turn deteriorates.

An alternative to this traditional means of retail distribution of frozen foods is to pack these products in insulated containers each of which will be destined for a specific retail destination in route. During the unloading process, the goods remaining in the transport are insulated or protected from the adverse conditions of warm-chilled air exchange. Therefore, the product being unloaded at the end of the delivery route should have an internal temperature similar to the initial loads that were dispensed. In this study the mathematical model was developed for insulated containers with frozen food. The model was solved using digital computer. The simulated results were compared with experimental data. Ice cream was chosen as a model product to study due to its extreme sensitivity to improper temperature control.

MATERIAL AND METHODS

Insulated containers were supplied by Acerado Ltd. of Ontario, Canada. Two units were examined; Model A which had a fiberglass shell and Model B, the shell of which was composed of plywood. The capacity of these two containers was 1.508 and 1.778 m^3, respectively. The walls of the containers were 5.0 cm thick with the fiberglass thickness of 3.18 mm (4.45 cm insulation), and a plywood thickness of 6.35 mm on the sides and 9.53 mm on the top (3.8 cm and 3.2 cm insulation, respectively). These units possessed an R rating of about 14 (2.47 $K.m^2/W$).

An economy brand of ice cream was supplied in 2 liter round plastic buckets, 4 to a sleeve. These were packed in rectangular shaped boxes made from thick paper. While the composition of the product was unknown, it can be assumed to be in the range of 8-11% milk fat, 12-15% sugar, 0-4% corn syrup solids, 10-12% milk solids-nonfat and 0.5% stabilizer-emulsifier with 36-38% total solids.

Containers were loaded with ice cream and allowed to equilibrate at cold room temperature (-20 to $-25\,°C$) overnight. During the loading of the sleeves of ice cream, thermocouples were placed as diagrammed in Fig. 1A and 1B. Thermocouples were placed at the center of 9 ice cream buckets, at the exterior of each of the same 9 buckets and at various ambient locations both inside and outside the insulated container. To facilitate the placement of the thermocouples within the container, a 1.27 cm hole was drilled through which the thermocouple leads entered. Following the placement of all of the thermocouples, this hole was filled with a silicone-based caulking material to prevent air exchange. After the equilibrium period, the cabinet doors were secured shut and the cabinet transferred

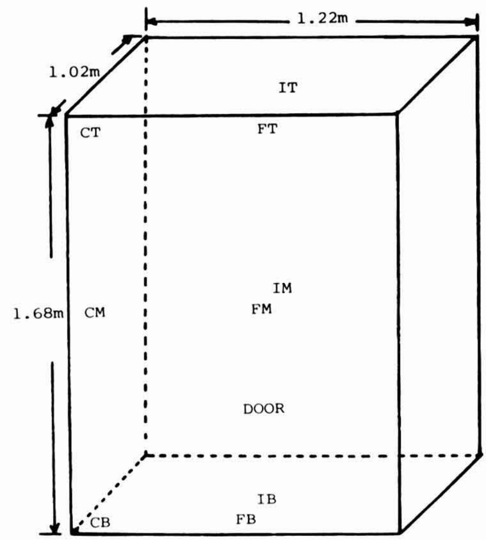

FIG. 1A

FIG. 1B

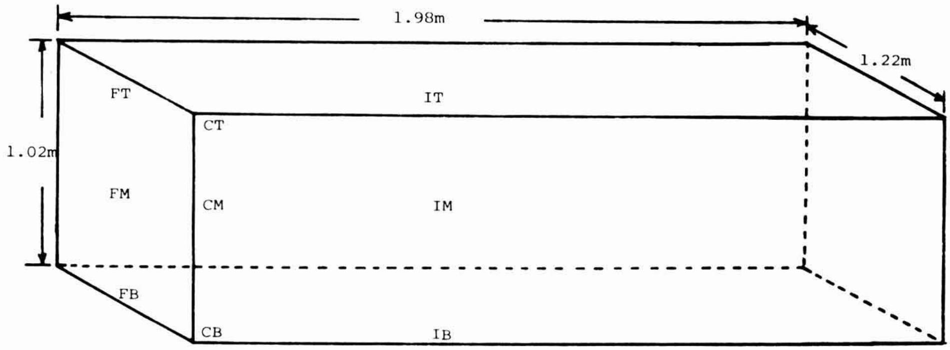

FIG. 1A-B. PLACEMENT OF ICE CREAM CARTONS AND THERMOCOUPLES IN INSULATED CONTAINERS
(A = fiberglass, B = plywood).

A: 9 cartons high (1.68 m), 6 cartons deep (1.02 m) and 6 cartons wide (1.22 m)
B: 5 cartons high (1.02 m), 6 cartons deep (1.22 m) and 10 cartons wide (1.98 m)

Coding for carton location:

C = Corner	T = Top
F = Face	M = Middle
I = Interior (center)	B = Bottom

For both containers, thermocouples were placed at the center of each coded carton and at the outside of the bottom of each of these cartons. Thermocouples were also placed at the inner and outer wall for the door, top side and door seam of the container as well as at ambient temperature.

to ambience (20-30 °C). Thermocouple leads were interfaced with a data logger and temperatures at each of the locations were monitored every 10 min for approximately 24 h. Due to space limitations and dimensions of the experimental site, it was necessary to leave cabinet B on its side throughout the course of the study. A pallet was used to prevent direct contact of the cabinet with the floor.

MODELING

The heat transfer through the container is three dimensional with conduction inside the container and through the walls, and convection outside the container. The formulation of the mathematical model in terms of dimensionless temperature is (Arpaci 1966):

$$\theta = (T - T_\infty)/(T_0 - T_\infty) \tag{1}$$

$$T = f(x,y,z,t) \tag{2}$$

$$\frac{\delta\theta}{\delta t} = \left(\frac{\delta^2\theta}{\delta x^2} + \frac{\delta^2\theta}{\delta y^2} + \frac{\delta^2\theta}{\delta z^2} \right) \tag{3}$$

Initial and boundary conditions are:

$$\theta(x,y,z,0) = 1 \tag{4}$$

$$\frac{\delta\theta}{\delta x}(0,y,z,t) = 0 \tag{5}$$

$$\frac{\delta\theta}{\delta y}(x,0,z,t) = 0 \tag{6}$$

$$\frac{\delta\theta}{\delta z}(x,y,0,t) = 0 \tag{7}$$

$$-K \frac{\delta\theta}{\delta x}(X,y,z,t) = h_v\, \theta(X,y,z,t) \tag{8}$$

$$-K \frac{\delta\theta}{\delta y}(x,Y,z,t) = h_h\, \theta(x,Y,z,t) \tag{9}$$

$$-K \frac{\delta\theta}{\delta z}(x,y,Z,t) = h_v\, \theta(x,y,Z,t) \tag{10}$$

The symbols are defined at the end. The thermal diffusivity (α) varies in x, y and z directions. This is a complex transient heat transfer problem with no conventional analytical solution.

The model was solved using finite difference technique. Equation (3) can be written as:

$$\frac{\delta\theta}{\delta t}(x_n,y_n,z_n) = \alpha[(\theta(x_{n-1},y_n,z_n) - 2\theta(x_n,y_n,z_n) + \theta(x_{n+1},y_n,z_n))/\Delta x^2$$
$$+ (\theta(x_n,y_{n-1},z_n) - 2\theta(x_n,y_n,z_n) + \theta(x_n,y_{n+1},z_n))/\Delta y^2 + (\theta(x_n,y_n,z_{n-1})$$
$$- 2\theta(x_n,y_n,z_n) + \theta(x_n,y_n,z_{n+1}))/\Delta z^2]$$

Only the space coordinates were eliminated as a variable by dividing the space into 125 small cube like shapes. Figure 2 shows the arrangements of three dimensional finite element grid. Grid #4 at the interface of wall and ice-cream boxes, in all three directions, contained the thermal mass of wall and ice-cream proportional to their masses. Similar procedure was used for grid #5. Due to similarity only 1/8 of the total space was simulated. Continuous System Modeling Program (CSMP) was used to simulate the system. The following assumptions were made: (1) Uniform initial temper-

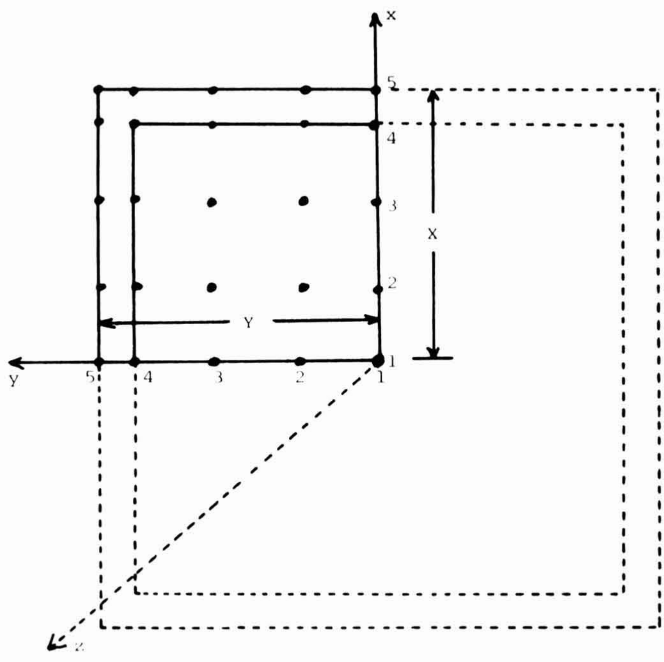

FIG. 2. ARRANGEMENTS OF FINITE DIFFERENCE GRIDS

ature of the container and food material. (2) Constant thermal properties of the food material. (3) Negligible convection heat transfer due to air inside the container. (4) Ambient temperature to be a step function of time.

The data used in the simulation is tabulated in Table 1. The thermal properties of ice cream were taken from Earle (1983) and of insulation from Kreith and Black (1980). The heat transfer coefficients were calculated for vertical and horizontal flat plates for natural convection (Kreith and Black 1980).

TABLE 1
DATA USED IN THE SIMULATION

	Ice Cream	*Insulation*
Specific heat, J/(kgK)	1880	1880
Density, kg/m^3	845	80
Thermal conductivity, W/(m · K)	0.8	0.0257
Thermal diffusivity, m^2/h	0.001858	0.000616
Heat transfer coefficient, W/(m^{2}K)		
vertical walls 1.6 to 3.0		
horizontal walls — lower 4.0		
— upper 1.0		

	Fiberglass	*Plywood*	
X, m	0.546	0.546	
Y, m	0.775	0.927	
Z, m	0.444	0.444	
Thermal resistance, Km^2/W	2.467	Top:	2.062
		Bottom and walls:	2.379

RESULTS AND DISCUSSION

Temperature Profile

Fiberglass Container. Figure 3 illustrates the temperature profiles at corner-top, corner-bottom, interior-middle and face-bottom positions in the container along with ambient temperature changes during 24 h test. The ambient temperature varied between 20.5 and 28.1 °C (25.2 °C average). It was not possible to keep the ambient temperature constant. As expected, the minimum temperature change was in the interior-middle and maximum at the corner-top positions. The maximum temperature drop in the container was 13.7 °C (i.e. 0.57 °C/h) for these test conditions. In the center of the container, there was no appreciable difference between ice cream and environment temperatures. This is due to the exchange of heat between ice cream and air. The test results indicated more heat transfer

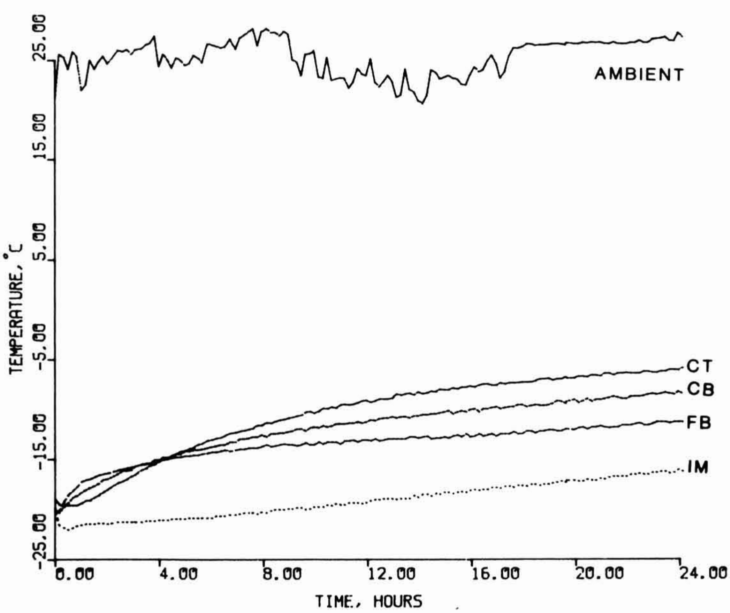

FIG. 3. AMBIENT TEMPERATURE CHANGES AND TEMPERATURE PROFILES IN FIBERGLASS CONTAINER

CT: center-top, CB: center-bottom, FB: face-bottom, and IM: interior-middle.

from the top of the container compared to the bottom. This may be due to more convective heat transfer at the top. In transports, the heat transfer at the top and bottom of the container should be similar since the van offers a closed system yielding a normalization of the environment compared to the open-air environment employed in this study.

Figure 4 shows the temperature profiles at interior and exterior sides of the container wall. There was no appreciable difference in these temperatures for the solid walls as well as for door wall. Inner side wall temperature was lower than the inner door temperature because there was a good contact of ice cream boxes with the side walls. There was no contact of ice cream boxes with the door wall due to the pattern of loading. The results indicate uniform heat transfer from all the container walls with negligible additional heat transfer taking place at the door seam.

Plywood Container. Figure 5 shows the ambient temperature and temperature profiles at the corner-top, corner-bottom, face-bottom and interior-bottom locations. The results are similar to those obtained for fiberglass container. There was less difference between corner-center and corner-bottom temperatures due to smaller height of the container. In this test, the door wall was positioned at the top of the container. The maximum heat was lost from the top-corner location. The temperature was

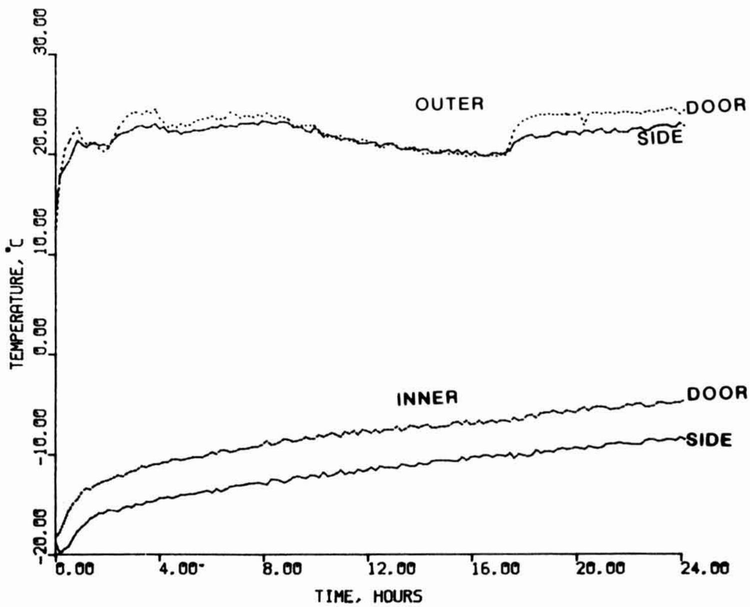

FIG. 4. INNER AND OUTER WALL TEMPERATURE VARIATIONS IN FIBERGLASS CONTAINER

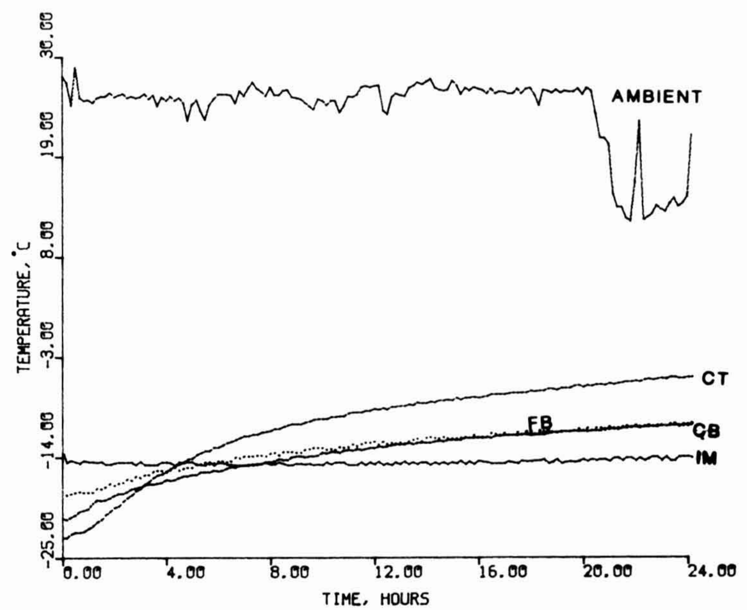

FIG. 5. AMBIENT TEMPERATURE CHANGES AND TEMPERATURE PROFILES IN PLYWOOD CONTAINER

CT: center-top, CB: center-bottom, FB: face-bottom, and IM: interior-middle (door facing up).

reduced to $-5.2\,°C$ from $-22.8\,°C$, a drop of $17.6\,°C$ (i.e., $0.73\,°C/h$) for the test conditions employed.

Figure 6 illustrates the variations in inner and outer wall temperatures for the plywood container. These results also indicate uniform heat transfer from all the sides and minimum additional heat transfer at the door seam.

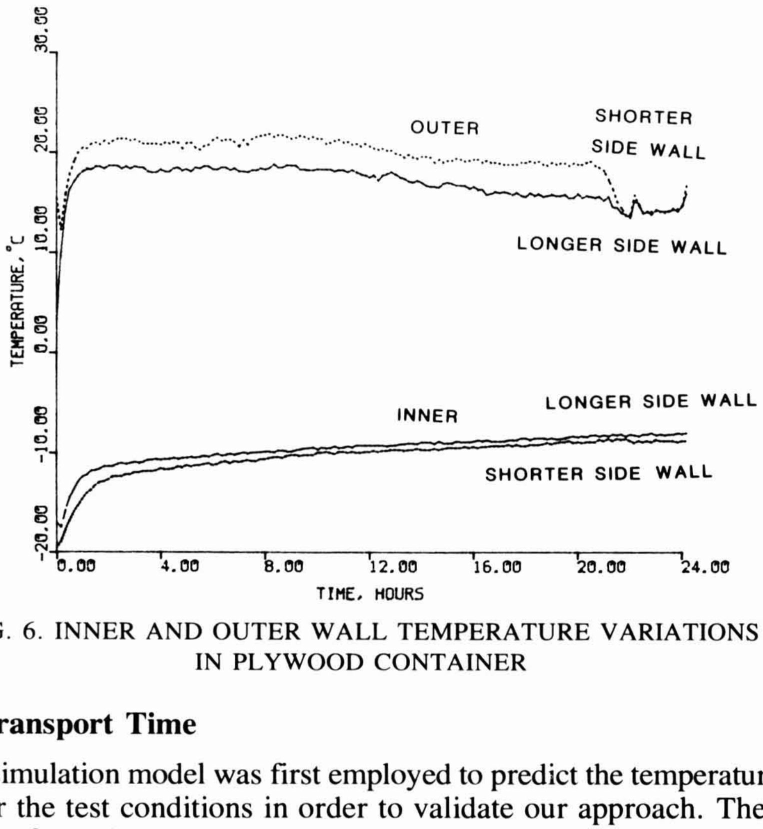

FIG. 6. INNER AND OUTER WALL TEMPERATURE VARIATIONS IN PLYWOOD CONTAINER

Safe Transport Time

The simulation model was first employed to predict the temperature profiles for the test conditions in order to validate our approach. The comparison of predicted and experimental values indicated that the above-mentioned method can predict the temperatures within $\pm 5\%$.

Using this approach, the recommended storage times at various ambient and initial ice cream temperatures were calculated and presented in Fig. 7 and 8. The figures will be useful in predicting the maximum holding time of the ice cream stored in these containers under various conditions.

The maximum holding times presented here are based on the increase in temperature to $-18\,°C$ at the top-corner location in the containers. This location represents the worst case in obtaining temperature at the other locations in the container.

If required, dry ice can be used at the sides and top of the containers to further decrease the initial ice cream temperature or in the event of anticipated extended storage periods. The maximum recommended storage

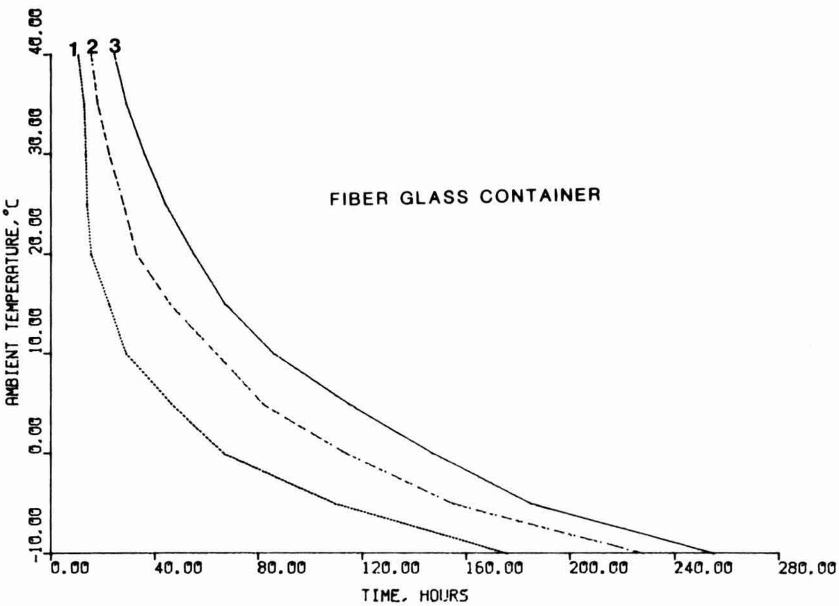

FIG. 7. SAFE STORAGE TIME OF ICE CREAM IN FIBERGLASS CONTAINER FOR DIFFERENT AMBIENT AND INITIAL ICE CREAM TEMPERATURES

1: −30 °C, 2: −35 °C and 3: −40 °C initial ice cream temperature. The maximum safe temperature of ice cream was considered to be −18 °C.

time will be proportionally increased. However, without further testing, we are unable to suggest any relationship between the amount of added dry ice and the extension of a safe holding period. The uniformity of dry ice distribution is very important to protect all the ice cream. Putting dry ice at one location will not provide uniform temperature in the container.

Figures 7 and 8 were also compiled under the assumptions of constant ambient temperature and the containers poised in the upright position. It is recommended that in the event of fluctuating ambient temperatures, the highest temperature be used to predict maximum holding time. The temperature of −18 °C (0 °F) was chosen as the maximum product temperature that should be encountered since it is generally recognized that ice cream quality deteriorates rapidly above this temperature.

NOMENCLATURE

- C specific heat, J/(kgK)
- h_h heat transfer coefficient on horizontal surface, W/(m^{2}K)
- h_v heat transfer coefficient on vertical surface, W/(m^{2}K)

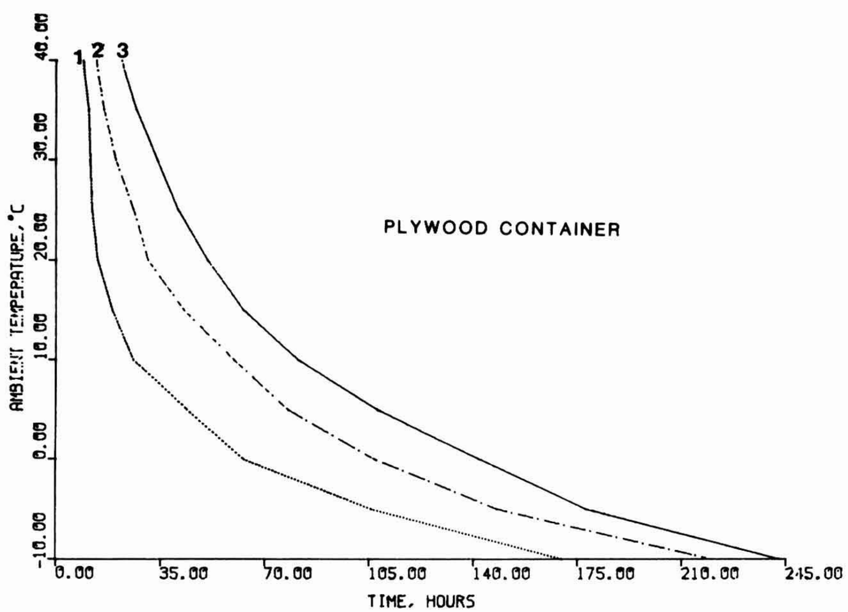

FIG. 8. SAFE STORAGE TIME OF ICE CREAM IN PLYWOOD CONTAINER FOR DIFFERENT AMBIENT AND INITIAL ICE CREAM TEMPERATURES

1: −30°C, 2: −35°C and 3: −40°C initial ice cream temperature. The maximum safe temperature of ice cream was considered to be −18°C.

K	thermal conductivity, W/(m.K)
n,n−1 . .	shell number
T	temperature, °C
T_0	initial temperature, °C
T_1	ambient temperature, °C
t	time, h
X	half of the length of the container, m
Y	half the height of the container, m
Z	half of the width of the container, m
x	distance in x-direction, m
y	distance in y-direction, m
z	distance in z-direction, m
α	thermal diffusivity, m^2/h
θ	dimensionless temperature
Δx	incremental length, m
Δy	incremental height, m
Δz	incremental width, m
ρ	density, kg/m^3

REFERENCES

ARPACI, V. 1966. *Conduction Heat Transfer.* Addison-Wesley Publishing Co., Don Mills, Ontario, Canada.

EARLE, R. L. 1983. *Unit Operations in Food Processing*. Pergamon Press, Toronto, Ontario, Canada.

KREITH, F. and BLACK, W. Z. 1980. *Basic Heat Transfer.* Harper and Row Publishers, New York.

F
N
P

PUBLICATIONS IN FOOD SCIENCE AND NUTRITION

Journals

JOURNAL OF SENSORY STUDIES, M.C. Gacula, Jr.
JOURNAL OF FOOD SERVICE SYSTEMS, O.P. Snyder, Jr.
JOURNAL OF FOOD BIOCHEMISTRY, H.O. Hultin, J.R. Whitaker and N.F. Haard
JOURNAL OF FOOD PROCESS ENGINEERING, D.R. Heldman
JOURNAL OF FOOD PROCESSING AND PRESERVATION, D.B. Lund
JOURNAL OF FOOD QUALITY, M.P. De Figueiredo
JOURNAL OF FOOD SAFETY, M. Solberg and J.D. Rosen
JOURNAL OF TEXTURE STUDIES, M.C. Bourne and P. Sherman
JOURNAL OF NUTRITION, GROWTH AND CANCER, G.P. Tryfiates

Books

HANDBOOK OF FOOD COLORANT PATENTS, F.J. Francis
ROLE OF CHEMISTRY IN THE QUALITY OF PROCESSED FOODS, O.R. Fennema, W.H. Chang and C.Y. Lii
NEW DIRECTIONS FOR PRODUCT TESTING AND SENSORY ANALYSIS OF FOODS, H.R. Moskowitz
PRODUCT TESTING AND SENSORY EVALUATION OF FOODS, H.R. Moskowitz
ENVIRONMENTAL ASPECTS OF CANCER: ROLE OF MACRO AND MICRO COMPONENTS OF FOODS, E.L. Wynder *et al.*
FOOD PRODUCT DEVELOPMENT IN IMPLEMENTING DIETARY GUIDELINES, G.E. Livingston, R.J. Moshy, and C.M. Chang
SHELF-LIFE DATING OF FOODS, T.P. Labuza
RECENT ADVANCES IN OBESITY RESEARCH, VOL. IV, J. Hirsch and T.B. Van Itallie
RECENT ADVANCES IN OBESITY RESEARCH, VOL. III, P. Bjorntorp, M. Cairella, and A.N. Howard
RECENT ADVANCES IN OBESITY RESEARCH, VOL. II, G.A. Bray
RECENT ADVANCES IN OBESITY RESEARCH, VOL. I, A.N. Howard
ANTINUTRIENTS AND NATURAL TOXICANTS IN FOOD, R.L. Ory
UTILIZATION OF PROTEIN RESOURCES, D.W. Stanley, E.D. Murray and D.H. Lees
FOOD INDUSTRY ENERGY ALTERNATIVES, R.P. Ouellette, N.W. Lord and P.E. Cheremisinoff
VITAMIN B_6: METABOLISM AND ROLE IN GROWTH, G.P. Tryfiates
HUMAN NUTRITION, 3RD ED , F.R. Mottram
FOOD POISONING AND FOOD HYGIENE, 4TH ED., B.C. Hobbs and R.J. Gilbert
POSTHARVEST BIOLOGY AND BIOTECHNOLOGY, H.O. Hultin and M. Milner
THE SCIENCE OF MEAT AND MEAT PRODUCTS, 2ND ED., J.F. Price and B.S. Schweigert

Newsletters

FOOD INDUSTRY REPORT, G.C. Melson
FOOD, NUTRITION AND HEALTH, P.A. Lachance and M.C. Fisher
FOOD PACKAGING AND LABELING, S. Sacharow

GUIDE FOR AUTHORS

Typewritten manuscripts in triplicate should be submitted to the editorial office. The typing should be double-spaced throughout with one-inch margins on all sides.

Page one should contain: the title, which should be concise and informative; the complete name(s) of the author(s); affiliation of the author(s); a running title of 40 characters or less; and the name and mail address to whom correspondence should be sent.

Page two should contain an abstract of not more than 150 words. This abstract should be intelligible by itself.

The main text should begin on page three and will ordinarily have the following arrangement:

Introduction: This should be brief and state the reason for the work in relation to the field. It should indicate what new contribution is made by the work described.

Materials and Methods: Enough information should be provided to allow other investigators to repeat the work. Avoid repeating the details of procedures which have already been published elsewhere.

Results: The results should be presented as concisely as possible. Do not use tables *and* figures for presentation of the same data.

Discussion: The discussion section should be used for the interpretation of results. The results should not be repeated.

In some cases it might be desirable to combine results and discussion sections.

References: References should be given in the text by the surname of the authors and the year. *Et al.* should be used in the text when there are more than two authors. All authors should be given in the Reference section. In the Reference section the references should be listed alphabetically. See below for style to be used.

DEWALD, B., DULANEY, J.T., and TOUSTER, O. 1974. Solubilization and polyacrylamide gel electrophoresis of membrane enzymes with detergents. In *Methods in Enzymology,* Vol. xxxii, (S. Fleischer and L. Packer, eds.) pp. 82-91, Academic Press, New York.

HASSON, E.P. and LATIES, G.G. 1976. Separation and characterization of potato lipid acylhydrolases. Plant Physiol. *57,*142-147.

ZABORSKY, O. 1973. *Immobilized Enzymes,* pp. 28-46, CRC Press, Cleveland, Ohio.

Journal abbreviations should follow those used in *Chemical Abstracts.* Responsibility for the accuracy of citations rests entirely with the author(s). References to papers in press should indicate the name of the journal and should only be used for papers that have been accepted for publication. Submitted papers should be referred to by such terms as "unpublished observations" or "private communication." However, these last should be used only when absolutely necessary.

Tables should be numbered consecutively with Arabic numerals. The title of the table should appear as below:

Table 1. Activity of potato acyl-hydrolases on neutral lipids, galactolipids, and phospholipids

Description of experimental work or explanation of symbols should go below the table proper. Type tables neatly and correctly as tables are considered art and are not typeset. Single-space tables.

Figures should be listed in order in the text using Arabic numbers. Figure legends should be typed on a separate page. Figures and tables should be intelligible without reference to the text. Authors should indicate where the tables and figures should be placed in the text. Photographs must be supplied as glossy black and white prints. Line diagrams should be drawn with black waterproof ink on white paper or board. The lettering should be of such a size that it is easily legible after reduction. Each diagram and photograph should be clearly labeled on the reverse side with the name(s) of author(s), and title of paper. When not obvious, each photograph and diagram should be labeled on the back to show the top of the photograph or diagram.

Acknowledgments: Acknowledgments should be listed on a separate page.

Short notes will be published where the information is deemed sufficiently important to warrant rapid publication. The format for short papers may be similar to that for regular papers but more concisely written. Short notes may be of a less general nature and written principally for specialists in the particular area with which the manuscript is dealing. Manuscripts which do not meet the requirement of importance and necessity for rapid publication will, after notification of the author(s), be treated as regular papers. Regular papers may be very short.

Standard nomenclature as used in the engineering literature should be followed. Avoid laboratory jargon. If abbreviations or trade names are used, define the material or compound the first time that it is mentioned.

EDITORIAL OFFICES: DR. D.R. HELDMAN, COEDITOR, *Journal of Food Process Engineering,* National Food Processors Association, 1401 New York Avenue, N.W., Washington, D.C. 20005 USA; or DR. R.P. SINGH, COEDITOR, *Journal of Food Process Engineering,* University of California, Davis, Department of Agricultural Engineering, Davis, CA 95616 USA.

CONTENTS